Title

An Efficient and Modular Total Synthesis of Ibogaine and Related Alkaloids

Author

Iyer, Rishab Narsi

Publication Date

2023

Peer reviewed|Thesis/dissertation

An Efficient and Modular Total Synthesis of Ibogaine and Related Alkaloids

By

RISHAB N. IYER
DISSERTATION

Submitted in partial satisfaction of the requirements for the degree of

DOCTOR OF PHILOSOPHY

in

Chemistry

in the

OFFICE OF GRADUATE STUDIES

of the

UNIVERSITY OF CALIFORNIA

DAVIS

Approved:

David E. Olson, Chair

Dean J. Tantillo

Jared T. Shaw

Committee in Charge

2023

Abstract

Few classes of natural products have inspired as many chemists and biologists as have the iboga alkaloids. This family of monoterpenoid indole alkaloids includes the anti-addictive compound ibogaine as well as catharanthine, a precursor to the chemotherapeutic vinblastine. Despite being known for over 120 years, these small molecules continue to challenge our assumptions about biosynthetic pathways, catalyze our creativity for constructing complex architectures, and embolden new approaches for treating mental illness. While significant progress regarding their chemistry and pharmacology has been made since the 1960s, there is an emerging need for the development of an efficient and scalable total synthesis of these alkaloids. Access to iboga alkaloids by means of isolation has been hindered by low yields and environmental challenges. Thus, an efficient and modular total synthesis would enable widespread access for analog development and biological testing. Accordingly, we have developed a facile 5-7 step total synthesis that allows for the preparation of ibogaine and a variety of related alkaloids and analogs. Using substrate-induced radical selectivity, our synthesis offers multiple points for diversification to aid in analog library development. An asymmetric variant has also been developed to provide unprecedented access to both enantiomers of the iboga scaffold.

Acknowledgements

My time in the Olson lab has been an experience that will forever stay close to my heart. I am eternally grateful for the opportunity to grow and develop as both a scientist and person. I deeply value the vibrant discussions and collective triumphs and challenges we have all faced and shared together. I feel incredibly fortunate to have been able to work with such amazing people with diverse backgrounds and perspectives. The lab has truly felt like a family and I will forever cherish all the fun experiences we have shared.

I would like to express my sincerest gratitude to my advisor, David Olson, for his invaluable guidance throughout my PhD. When I first joined UC Davis, I had no intention of working in the Olson lab. After one introductory meeting with David, I was enamored by his intellect and vision. What convinced me to join the Olson lab was David's enthusiasm and passion for the research. He embodied everything I want to be in a scientist and researcher. David, your mentorship has helped me grow as a scientist and individual, thank you for equipping me with the knowledge and skills necessary to embrace the next phase of my life. Additionally, I would like to thank Dean Tantillo, Jared Shaw, and Cody Pitts for your insight, advice and teaching over the past 5 years. I am grateful to have worked in a department with such accomplished and down to earth faculty members.

I would like to thank the iboga pod for the experiences we have shared throughout our PhD journey. Every challenge and triumph was shared with you both and we developed a special bond throughout it all. Special thanks to my colleagues David Favela, Guoliang Zhang, Lee Dunlap, RJ Tombari, Jeremy Tuck, Andy Basargin, David Gutierrez, Lauren Arias, Andy Domokos and Winston Chow for all the fun times and helpful discussions over the years.

To my parents, this PhD is made possible because of you both. There was once a time when my future was in doubt and you were the only people who believed in me. I know I haven't always been the best son, but I am incredibly grateful for the relationship we now have. I value the sacrifices you have made for my education, thank you for your love and guidance along the

way. Nisha and Megha, thank you both for being such amazing sisters and being there for me, especially through the hard times. Thank you to Bharath, Sandhya, Zach, Radhika, Sitaraman, Raghu, Deepa, Patti, Ishaan and Leela for the love and support through the years. I am extremely proud and grateful to call you all my family.

Contents

Chapter 1 – Intro to Ibogaine and Related Alkaloids

1.1 Introduction

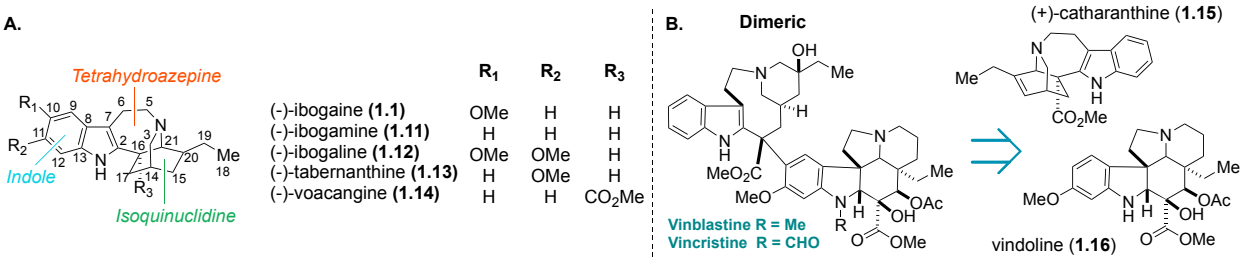

Figure 1.1. (A) Structure of iboga alkaloids **(B)** Dimeric iboga alkaloids vinblastine and vincristine

Ibogaine was first isolated in 1901,[1] and its structure was deduced by Bartlett, Dickel, and Taylor in 1958.[2] In 1960, its absolute stereochemistry was unambiguously assigned by X-ray crystallography.[3] The defining features of the iboga architecture include an indole, a 7-membered tetrahydroazepine, and a bicyclic isoquinuclidine (**Figure 1.1A**). Since ibogaine's initial discovery, hundreds of alkaloids bearing structural and/or biosynthetic similarities to ibogaine have been identified. The chemical structures of some of the more common iboga alkaloids are highlighted in **Figure 1.1A** with the Le Men and Taylor numbering convention indicated.[4] While our work will primarily focus on monomeric iboga alkaloids, dimeric structures containing at least one iboga component are also common and include the notable chemotherapeutics vincristine and vinblastine (**Figure 1.1B**). For information on the chemistry and/or biology of this class of bisindole alkaloids, we point the reader to a recent review.[5]

The unique structures of iboga alkaloids have captured the imagination of chemists for decades, while their unusual effects on the brain have challenged conventional ideas about treating substance use disorder. Though substantial progress has been made concerning the chemistry and neuropharmacology of these alkaloids, many unresolved problems and unanswered questions remain. Ibogaine—the prototypical iboga alkaloid with the most

neurobiological data—still lacks a truly robust, scalable, enantioselective total synthesis. Moreover, its biological mechanism of action is completely opaque, pushing the limits of what traditional neuropharmacology is capable of explaining.

1.2 Isolation of Iboga Alkaloids

Plant Species	Ibogaine	Ibogamine	Voacangine	Coronaridine	Catharanthine
T. iboga[6,7,8,9]	0.27-0.32	0.097-0.40	0.043-0.28	NR	NR
V. africana[10]	0.25	TR	1.67	TR	NR
T. arborea	0.27	0.036	0.96	0.073	NR
C. roseus[11]	NR	NR	NR	NR	0.003-0.099
T. alba	0.046-0.22	0.042-0.30	0.033-0.96	0.075-0.52	NR
T. donnell-smithii	0.069-0.74	0.028-0.032	0.21-0.44	0.046-0.23	NR
T. amygdalifolia	0.047	0.76-0.96	0.19-0.22	1.092-1.38	NR

Table 1.1: Approximate yields of iboga alkaloids isolated from the whole root bark of various sources. Percentages indicate the weight of the alkaloid free base relative to the weight of the plant source. TR = trace (< 0.01%). NR = Not Reported.

Monoterpenoid indole alkaloids (MIA) of the iboga-type are found in a variety of plant species around the world, though historically, isolation of iboga alkaloids has generally been restricted to regions of West Africa.[12] There are hundreds of iboga alkaloids, but the compounds shown in **Figure 1.1A** represent some of the most commonly reported in natural product isolation and total synthesis literature. Of these alkaloids, ibogaine has attracted significant attention due to its therapeutic potential. However, the isolation of ibogaine from natural sources has been plagued by ethical and environmental challenges,[13] as it only accounts for approximately 0.3% of the root bark weight in *Tabernanthe iboga* (**Table 1.1**). In contrast, significantly larger amounts

of voacangine can be extracted from the root bark of *Voacanga africana* (~1.7% of the root bark). As a result, ibogaine is often produced via semi-synthesis starting from voacangine.[13] Conversion of voacangine to ibogaine generally requires a two-step protocol involving saponification of the C16 methyl ester followed by acidification and heating to induce decarboxylation.[13,14] In addition to ibogaine, Table 1 details several other common iboga alkaloids found in the *Tabernanthe* and *Voacanga* genera. Interestingly, catharanthine belongs to the opposite optical series compared to other reported iboga alkaloids and is exclusively found in the *Catharanthus roseus* plant species. The isolated compounds in **Table 1.1** have sparked interest in more recent efforts to determine the alkaloid profiles of plants in the broader Apocynaceae family.

1.3 Biosynthesis of Iboga Alkaloids

Unlike in prokaryotes, the genes encoding metabolic pathways in plants are not typically clustered, making the full elucidation of alkaloid biosynthesis quite challenging. Typically, each individual plant-derived enzyme must be identified, cloned, and isolated to firmly establish a role in the synthesis of a particular alkaloid. Though several enzymes in the production of iboga alkaloids still remain elusive, our knowledge of iboga alkaloid biosynthesis has improved drastically over the past 15 years due in large part to the pioneering work of Sarah O'Connor, Vincenzo De Luca, and others.

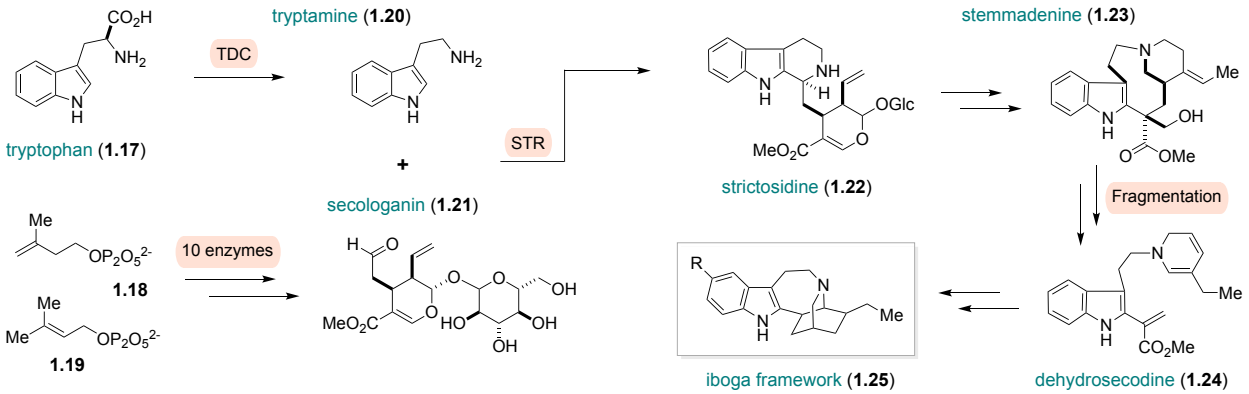

Figure 1.2. Biosynthesis of iboga alkaloids

Like all monoterpenoid indole alkaloids (MIAs), the iboga alkaloids are derived from tryptamine (**1.20**), which is produced from the enzymatic decarboxylation of tryptophan (**1.17**) by tryptophan decarboxylase (TDC) (**Figure 1.2**).[15,16,17] The remainder of the iboga carbon skeleton can trace its origins to secologanin (**1.21**), an iridoid synthesized from isopentenyl pyrophosphate (**1.18**) and dimethylallyl pyrophosphate (**1.19**) via the non-mevalonate pathway.[18] Ten enzymes are required to produce **1.21**,[19,20,21,22,23,24,25] which subsequently reacts with tryptamine to form strictosidine (**1.22**). This critical Pictet-Spengler reaction is catalyzed by strictosidine synthase (STR),[26,27] producing **1.22** as a single enantiomer. Strictosidine (**1.22**) is a key intermediate en route to a number of indole alkaloids including those of the ajmalan, corynanthe, aspidosperma, quinoline, and iboga families.

Many of the enzymes in *T. iboga* and *C. roseus* share a high degree of sequence homology, and thus, the biosynthetic pathways leading to ibogaine and catharanthine are quite similar until their late-stage divergence from dehydrosecodine (**1.24**). Dehydrosecodine is generated from fragmentation of stemmadenine (**1.23**) and isomerization of the resulting iminium. A final intramolecular cycloaddition generates the iboga framework with further functionalization possible through a number of pathways.

1.4 Methods for Synthesizing Isoquinuclidine Ring System

Since Büchi's pioneering synthesis of ibogaine in 1966[27], there have been numerous synthetic approaches to iboga alkaloids. For a comprehensive analysis of strategies prior to 2011, we refer the reader to an excellent review by Sinha and co-workers.[28] Here, we focus on historical strategies for constructing the isoquinuclidine, tetrahydroazepine, and indole ring systems characteristic of this alkaloid family.

The isoquinuclidine ring system represents a structural focal point for the iboga alkaloids.[29] Methods to construct this [2.2.2] bicycle have centered around three fundamental strategies—cycloaddition, transannular cyclization, and radical rearrangement. The cycloaddition strategy

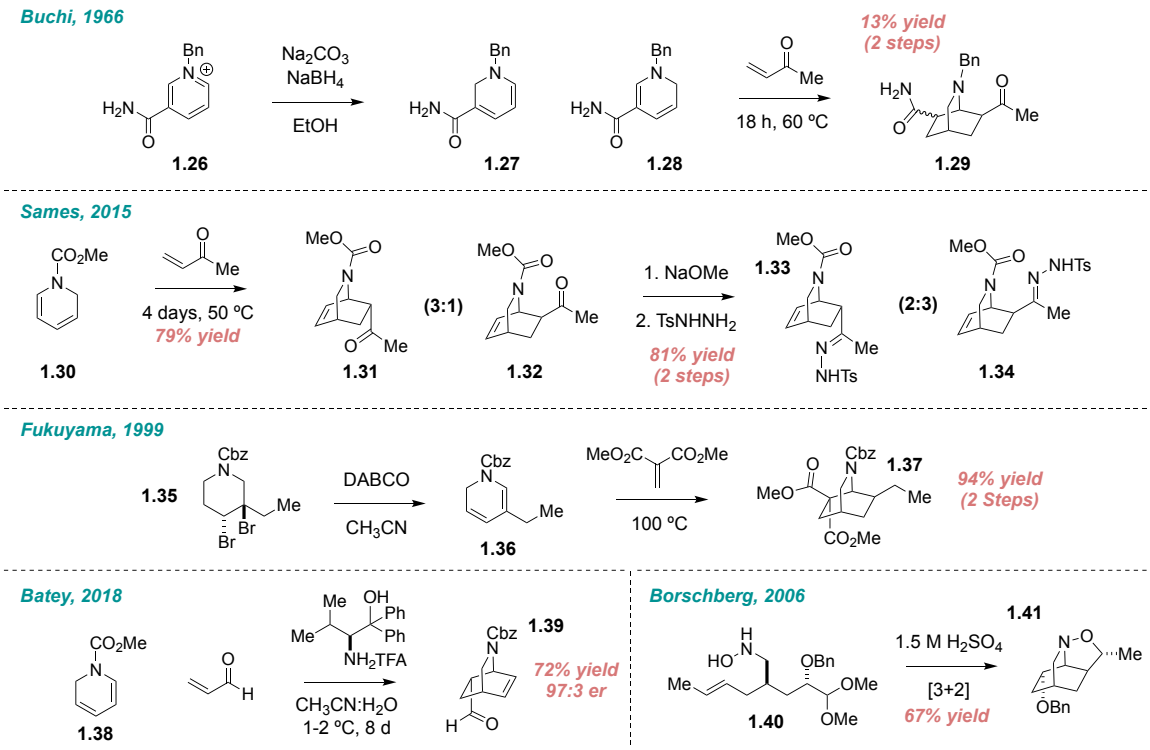

Figure 1.3. Cycloaddition approaches to the isoquinuclidine of iboga alkaloids

was first successfully utilized by Büchi and co-workers (**Figure 1.3**).[30,31] Their approach involved the reduction of nicotinamide pyridinium **1.26** with sodium borohydride to give a regioisomeric mixture of dienes **1.27** and **1.28**. When this mixture was subjected to a Diels-Alder reaction with methyl vinyl ketone (MVK), only dihydropyridine **1.28** underwent cycloaddition, yielding isoquinuclidine **1.29** in 13% yield as a mixture of epimers over two steps. The authors postulated that the greater electron delocalization of **1.27** prevents cycloaddition with MVK.

Most syntheses that have adopted this approach have opted to transform the substituent on the dienophile into the exo C20 ethyl group of the iboga alkaloids.[31,32] This poses an obvious challenge given the inherent endo selectivity of most Diels-Alder reactions. To overcome this issue, Sames and co-workers took advantage of the acidic protons alpha to the carbonyl (**Figure 1.3**). By treating a 3:1 endo:exo mixture of the Diels-Alder adducts with base, they achieved epimerization to a thermodynamic ratio (2:3) of **1.31** and **1.32**. After exo enrichment, conversion

to the tosylhydrazones **1.33** and **1.34** allowed for separation via crystallization. Fukuyama and co-workers sought to avoid endo/exo diastereoselectivity issues altogether by performing the Diels-Alder reaction with a symmetrical dienophile (**Figure 1.3**).[33] Treatment of trans-dibromide **1.35** with DABCO afforded the requisite dihydropyridine **1.36**, which was then reacted with dimethyl methylenemalonate to give isoquinuclidine **1.37** in 94% yield over two steps.

In the approaches described above, the Diels-Alder reactions were uncatalyzed, leading to racemic mixtures of isoquinuclidines. Recently, Batey and co-workers reported an enantioselective Diels-Alder reaction of dihydropyridine **1.38** with acrolein in the presence of a valine-derived organocatalyst (**Figure 1.3**),[34] leading to a formal synthesis of (+)-catharanthine. In 2006, Borschberg and co-workers reported another enantioselective synthesis of an iboga alkaloid, although their approach involved an intramolecular nitrone-olefin [3+2] cycloaddition (**Figure 1.3**).[35,36] Key intermediate **1.40** was synthesized from L-glutamic acid and (2S)-but-3-en-2-ol. A crucial chirality transfer in the Ireland-Claisen rearrangement of a silyl ketene acetal afforded intermediate **1.40** in high diastereoselectivity. The subsequent 1,3-dipolar cycloaddition produced **1.41** in 67% yield.

Another common approach to accessing the isoquinuclidine framework of iboga alkaloids involves the transannular cyclization of an amine derivative. Huffman and co-workers were the first to employ this strategy in 1965.[37,38] Ring opening of cyclic epoxy ester **1.42** followed by transannular amidation produced the isoquinuclidine in a single step. Subsequent tosylation of the C16 alcohol afforded intermediate **1.44** in 57% yield over two steps (**Figure 1.4**). However, when this strategy was applied to the synthesis of ibogamine, the yields were greatly reduced owing to the complex mixture of diastereomeric products obtained during the synthesis of epoxide **1.43**.[39]

Variants of the transannular cyclization strategy have involved the preassembly of the indole and/or tetrahydroazepine rings prior to formation of the isoquinuclidine (**Figure 1.4**). The approach taken by Grieco and co-workers mirrored that of Huffman and produced **1.47** in

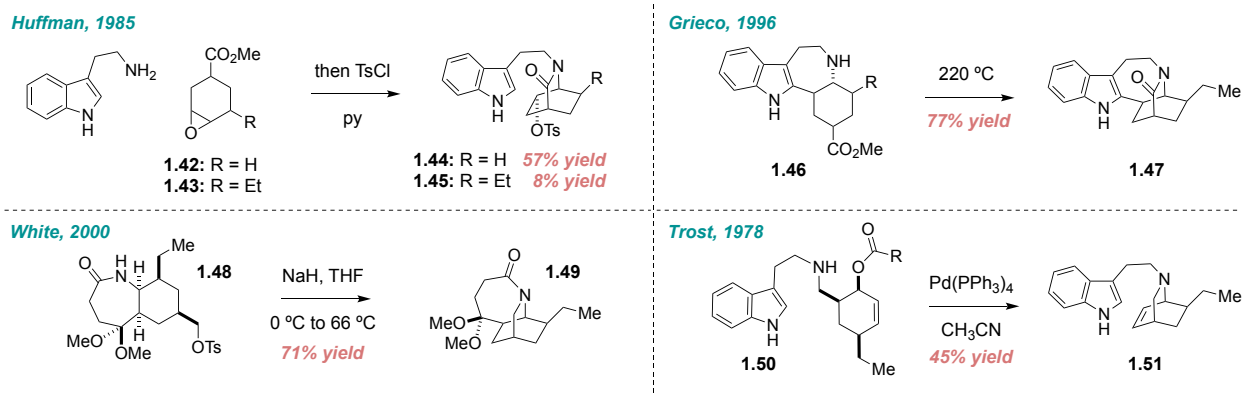

Figure 1.4. Transannular cyclization approaches to the isoquinuclidine of iboga alkaloids

excellent yield.[40] A hallmark of both of the Huffman and Grieco syntheses is the incorporation of an enolizable proton at what will become the bridgehead position, enabling both diastereomers to be converted to the desired isoquinuclidine.

A related approach pioneered by Sallay established what would become the tetrahydroazepine of ibogamine prior to transannular alkylation forming **1.49**.[41] White and co-workers improved upon the racemic Sallay synthesis by constructing **1.48** using an asymmetric Diels-Alder reaction as the key step (**Figure 1.4**). Base-mediated cyclization afforded **105** in high yield, which was converted to (–)-ibogamine.[42]

In addition to classic acylation and alkylation reactions, several other transannular cyclizations have been utilized to access the isoquinuclidine core of iboga alkaloids. For example, Nagata and co-workers favored the use of a transannular aziridination reaction,[43,44,45] while Trost and co-workers relied on Pd-catalyzed allylic alkylation.[46,47] Trost's 1978 synthesis of (+)-ibogamine was a landmark paper for the field (**Figure 1.4**). Use of a chiral auxiliary enabled an asymmetric Diels-Alder reaction (60% ee), and the product was subjected to reductive amination to produce **1.50**. Treatment of **1.50** with Pd^0 led to **1.51**, which was converted to the natural product through a metal-catalyzed olefin arylation. Trost's synthesis was the first to use transition

metal catalysis to access an iboga alkaloid, and it set precedent for many similar strategies to follow.

1.5 Methods for Synthesizing Tetrahydroazepine Ring System

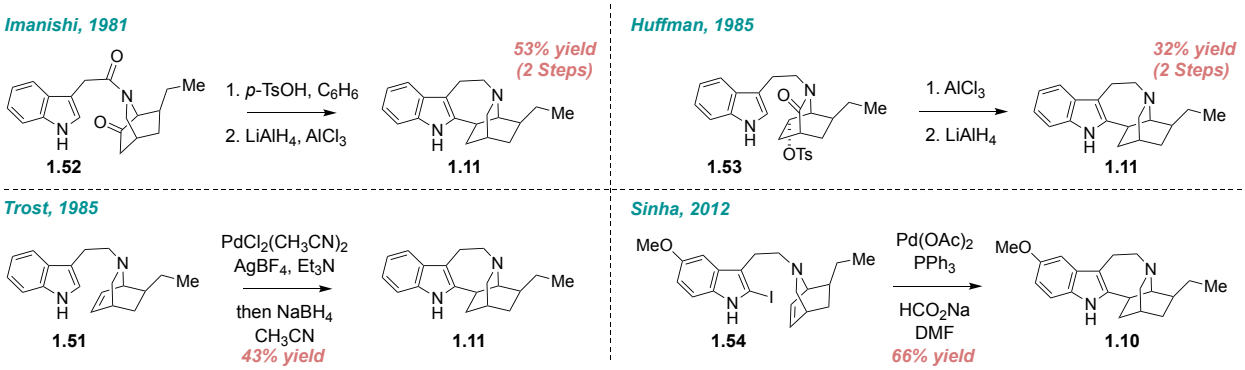

Figure 1.5. Construction of the tetrahydroazepine through C2–C16 bond formation

The 7-membered tetrahydroazepine is a crucial structural element linking the indole and isoquinuclidine rings of the iboga alkaloids. Most syntheses have relied on one of three strategies for its construction—formation of the C2–C16 bond, indole–isoquinuclidine linkage, or ring-expansion. The C2–C16 bond disconnection was first explored by Nagata in 1968 and later exploited by Imanishi.[48] The cyclization of **1.52** was achieved by refluxing in a stoichiometric amount of *p*-TsOH for a short duration. Treatment of the resulting tosylate with *in situ* generated AlH_3 produced ibogamine (**1.11**) in reasonable yields (**Figure 1.5**). In 1985, Huffman employed an alternative strategy using tosylate **1.53**. Lewis acid-mediated cyclization of **1.53** followed by reduction of the lactam gave **1.11** in 32% yield over two steps (**Figure 1.5**).

The C2–C16 bond disconnection was also key feature of Trost's 1978 synthesis. Using a novel Pd-catalyzed olefin arylation, Trost and co-workers were able to forge the C2–C16 bond from **1.51** using a mixture of palladium and silver (**Figure 1.5**). Reduction of the resulting organopalladium species afforded (+)-ibogamine in 43% yield. In 2015, Sames applied a slight modification of this C–H activation strategy by using a preformed palladium tetrafluoroborate

catalyst instead of a combination of $PdCl_2(CH_3CN)_2$ and $AgBF_4$.[32] This result suggests that silver is not directly involved in cyclization and serves merely to facilitate chloride exchange for a noncoordinating tetrafluoroborate, thus generating a more active catalyst. Though interesting, the methods developed by Trost and Sames suffered several drawbacks such as low yields and the need for stoichiometric or supra-stoichiometric amounts of palladium (1–2 eq). In 2012, Sinha employed a modified strategy using only catalytic amounts of palladium catalyst (**Figure 1.5**).[49] Pre-functionalization of the indole C2 position with an iodide (**1.54**) enabled a reductive Heck reaction to be performed using only 10 mol% of $Pd(OAc)_2$. This more economical approach towards the tetrahydroazepine ring system enabled the synthesis of ibogaine (**1.10**) in 66% yield.

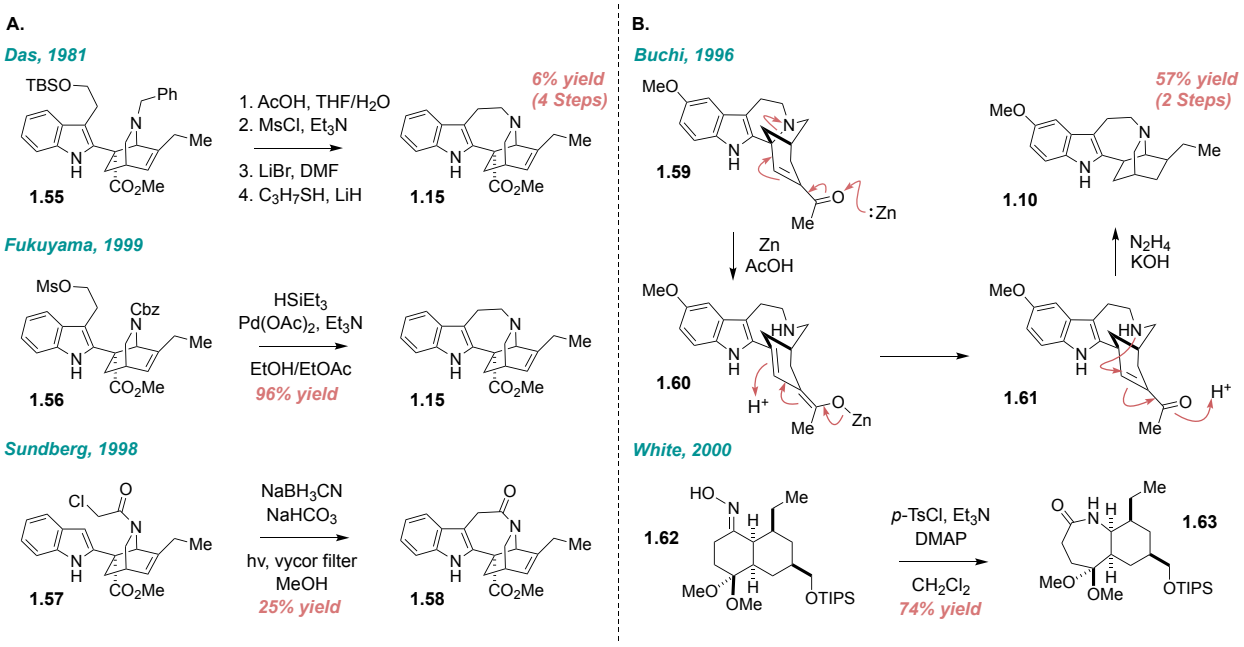

Figure 1.6. (A) Construction of the tetrahydroazepine through indole–isoquinuclidine linkage **(B)** Construction of the tetrahydroazepine through ring expansion

Another popular strategy for constructing the tetrahydroazepine involves the introduction of a linker between the nitrogen of the isoquinuclidine and the C3 position of the indole (C7 based on the Le Men and Taylor numbering). Using a method developed by Kutney,[50] Das and co-

workers performed a debenzylation of a quaternary ammonium salt derived from **1.55** (**Figure 1.6A**).[51] Though they were able to isolate catharanthine, the route was low yielding as formation of the quaternary ammonium salt was challenging. Fukuyama and co-workers took a slightly different approach by deprotecting the isoquinuclidine prior to alkylation. They noticed that hydrogenolysis of **1.56** also resulted in the reduction of the endocyclic olefin. Instead, a mild and chemoselective deprotection using triethylsilane and palladium acetate afforded catharanthine in a single step. Interestingly, the desired intramolecular S_N2 alkylation occurred readily following carbamate deprotection, presumably due to the highly rigidified nature of the intermediate amine. Sundberg and co-workers also chose to construct the tetrahydroazepine after the indole and isoquinuclidine rings had already been established (**Figure 1.6A**).[52] However, their approach involved the generation of a radical through irradiation of chloroacetamide **1.57**. Radical cyclization afforded **1.58** in modest yield.

The final strategy used to construct the tetrahydroazepine involves ring expansion, and this was the method by which Büchi first synthesized ibogaine (**Figure 1.6B**). Treatment of **1.59** with a mixture of Zn and AcOH resulted in reductive opening of the 6-membered ring. Following protonation at the γ-position, conjugate addition of the amine produced ibogaine in 57% yield. White and co-workers also synthesized the tetrahydroazepine through ring expansion. Beckman rearrangement of **1.62** yielded **1.63** in good yield.

1.6 Methods for Synthesizing Indole Ring System

The indole ring system of the iboga alkaloids is biosynthetically derived from tryptophan, and most synthetic efforts toward the iboga alkaloids have started from tryptamine derivatives. For example, Büchi's 1966 synthesis of ibogaine involved the coupling of an isoquinuclidine with indole acetic acid.[30] More recently, alternative approaches to generating the indole have been explored (**Figure 1.7**). In 2000, White and co-workers installed the indole at a late-stage through a Fischer indole cyclization of **1.49** to afford **1.64** in 66% yield over two steps.[42] Fukuyama and

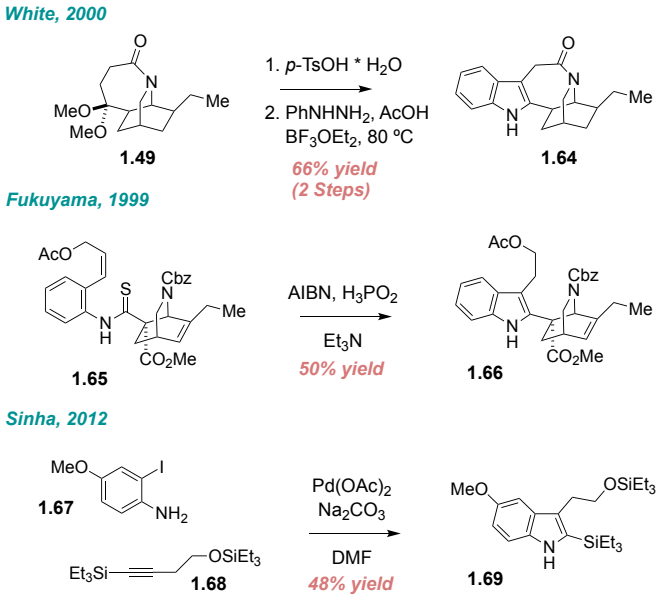

Figure 1.8. Construction of the indole

co-workers built the indole through radical cyclization of thioanilide **1.65**.[33] They noticed that standard tin hydride conditions failed to produce the desired product in acceptable yields. Instead, they found that a phosphorus-based hydrogen atom donor afforded the desired cyclization. Recently, Sinha and co-workers decided to synthesize the indole very early in their synthesis.[28] Larock annulation of aniline **1.67** and alkyne **1.68** provided **1.69** in modest yield. Very few synthetic strategies towards iboga alkaloids have made the construction of the indole a focal point for the synthesis, perhaps because the 7-membered tetrahydroazepine and bicyclic isoquinuclidine ring systems are viewed as being more challenging to access.

In the past decade, numerous syntheses of iboga alkaloids have emerged utilizing the general strategies listed above. A formulated list of all iboga syntheses is listed in **Table 1.2.** For a comprehensive analysis of recent synthetic developments, we point the reader to our recent review.[53]

Year	Group	Alkaloid(s)	Formation Sequence	Step Count	Overall Yield (%)
1965	Buchi	(±)-Ibogamine (**81**)	Q → I → A	14	1.3
1966	Buchi	(±)-Ibogaine (**1**)	Q → I → A	15	0.2
1967	Sallay	(±)-Ibogamine (**81**)	A → Q → I	14	NR
1968	Nagata	(±)-Ibogamine (**81**)	Q → I → A	16	0.8
1978	Trost	(+)-Ibogamine (**81**)	I → Q → A	NR*	NR*
1981	Hanaoka	(±)-Ibogamine (**81**)	Q → I → A	17	3.9
1985	Kuehne	(±)-Ibogamine (**81**)	I/Q → A	10	2.6
1985	Raucher	(±)-Catharanthine (**7**)	Q → I → A	11	9.0
1991	Herdeis	(±)-Ibogamine (**81**)	Q → I → A	8	14
1996	Grieco	(±)-Ibogamine (**81**)	I → Q → A	9	7.0
1999	Fukuyama	(±)-Catharanthine (**7**)	Q → I → A	17	6.0
2000	White	(–)-Ibogamine (**81**)	A → Q → I	15	4.6
2001	Kuehne	(–)-Coronaridine (**4**)	I → Q/A	10	NR
2005	Hodgson	(+)-Ibogamine (**81**)	Q → I → A	11	2.0
2006	Borschberg	(–)-19-hydroxyibogamine	Q → I → A	20	1.9
2012	Sinha	(±)-Ibogaine (**1**) (±)-Ibogamine (**81**)	Q → I → A	9 9	9.4 5.6
2012	Takayama	(–)-Voacangalactone (**169**)	Q → I → A	25	3.2
2014	Oguri	(–)-Catharanthine (**7**)	I → Q/A	10	2.8
2015	Sames	(±)-Ibogamine (**81**)	Q → I → A	9	7.3
2016	Luo	(+)-Ibogamine (**81**)	I → Q/A	12	4.2
2016	She	(±)-Ibogaine (**1**) (±)-Ibogamine (**81**) (±)-Tabertinggine (**25**) (±)-**37** (±)-**51** (±)-Iboluteine (**177**) (±)-Ervaoffines D (**49**)	I → Q/A	12 12 10 13 13 14 14	4.6 6.0 41 3.2 4.3 3.9 2.9
2023	Townsend	(±)-Ibogamine (**81**)	I → A/ Q	9	24

Table 1.2. Total syntheses of iboga alkaloids. The order in which the indole (I), isoquinuclidine (Q), and tetrahydroazepine (A) rings were formed is indicated. A " / " indicates that two ring systems were formed in the same step. NR = not reported (i.e., not enough information was provided to calculate an overall yield or determine step count). *Trost synthesized (+)-ibogamine from an intermediate in 4 steps (17% yield). However, the synthesis of this intermediate from simpler precursors was not detailed, and thus, we cannot provide an overall step count and yield for the Trost synthesis.

1.7 Biological Activity of Ibogaine

The anti-addictive properties of ibogaine have been known since the 1960s, though this initial information was based entirely on anecdotal reports from heroin users. Since that time, several open-label and/or retrospective studies have suggested that ibogaine might be useful for treating substance use disorder (SUD) as it appears to reduce drug cravings, decrease symptoms of withdrawal, and prevent relapse.[54,55,56,57,58] Moreover, rodent studies have confirmed the anti-addictive potential of ibogaine by demonstrating the natural product reduces drug self-administration, prevents drug-induced dopamine release in several brain regions, attenuates drug-induced conditioned place preference, and decreases signs of withdrawal.[59,60,61] However, double-blind, placebo-controlled clinical trials firmly establishing the efficacy of ibogaine are still lacking. It is illegal to possess ibogaine in the United States, as it is classified as a schedule I drug. As a result, many people have sought treatment from informal clinics in countries where ibogaine is not regulated.[62] For information on the history and pharmacology of ibogaine, we point the reader to several excellent reviews on these subjects.[63,64,65,66]

Despite ibogaine's promising therapeutic efficacy, major safety concerns have tempered excitement for its clinical development. First and foremost, ibogaine is known to cause long-lasting hallucinations, and at very high doses it can lead to tremors and Purkinje cell death in rats.[67] However, its cardiotoxicity has been the biggest concern. Ibogaine inhibits hERG potassium channels in the heart,[68,69] with several deaths being linked to its adverse effects on heart function.[70,71] Ibogaine is very nonpolar, as evidenced by the fact that it readily accumulates in adipose tissue,[72] and it is well known that hERG inhibition is a major liability for many non-polar, basic amines.[73] Previously, ibogaine was sold in France as a neurotherapeutic, however its adverse effects led to its removal from the market. Since that time, a major goal for the field has been to identify ibogaine congeners with similar therapeutic efficacies, but improved safety profiles.

1.8 Conclusion

A number of advances have been made in the past 10 years regarding iboga chemistry and biology. We now know how the antipodal series of these alkaloids are generated from a common achiral precursor, and biomimetic approaches are enabling the rapid synthesis of several iboga family members. Furthermore, new clues have emerged regarding how iboga alkaloids might produce long-lasting neurotherapeutic effects. However, there are still a number of chemical and biological challenges that need to be addressed if we are to rationally engineer safe and effective medicines for treating neuropsychiatric disorders based on the iboga core structure.

Acknowledgement

This chapter was adapted from our review titled “The iboga enigma: the chemistry and neuropharmacology of iboga alkaloids and related analogs”. I would like to acknowledge David E. Olson for editing all sections of the manuscript and writing the introduction and biological activity sections. I would like to acknowledge David Favela and Guoliang Zhang for writing the biosynthesis and isolation sections.

REFERENCES

1. Dybowski J, Landrin E. Concerning Iboga, its excitement-producing properties, its composition, and the new alkaloid it contains, ibogaine. *CR Acad. Sci.* **1901**; 133:748.
2. Bartlett MF, Dickel DF, Taylor WI. The alkaloids of Tabernanthe iboga. Part IV. 1 The structures of ibogamine, ibogaine, tabernanthine and voacangine. *J. Am. Chem. Soc*., **1958**, 80, 126–136.
3. Arai, G., Coppola, J., and Jeffrey, G. The Structure of Ibogaine. Acta Crystallogr., 1960, 13, 553–564.
4. Men, J. L.; Taylor, W. I. *Experientia*, **1965**, 21, 508–510.
5. Martino, E.; Casamassima, G.; Castiglione, S.; Cellupica, E.; Pantalone, S.; Papagni, F.; Rui, M.; Siciliano, A. M.; Collina, S. *Bioorg. Med. Chem. Lett.*, **2018**, 28, 2816–2826.
6. Bouso, J. C.; Fornís, I.; Vilamala, M. V.; Loenen, B. D.; Sainz-Cort, A.; Jiménez-Garrido, D. F.; Santos, R. G. D.; Hallak, J. E. C.; Alcázar-Córcoles, M. Á.; Jenks, C. W. An Analytical Study of Iboga Alkaloids Contained in Tabernanthe Iboga-Derived Products Offered by Ibogaine Treatment Providers. Arch. Clin. *Psychiatry*, **2020**, 47, 51–54.
7. Jenks, CW.; Extraction studies of Tabernanthe iboga and Voacanga africana. *Nat. Prod. Lett.*, **2002**, 16, 71–76.
8. Dickel, D.; Holden, C.; Maxfield, R.; Paszek, L.; Taylor, W. The Alkaloids of Tabernanthe iboga. Part III.1 Isolation Studies. *J. Am. Chem. Soc.,* **1958**, *80*, 123–125.
9. Krengel, F.; Chevalier, Q.; Dickinson, J.; Herrera-Santoyo, J.; Reyes-Chilpa, R. Metabolite Profiling of Anti-Addictive Alkaloids from Four Mexican Tabernaemontana Species and the Entheogenic African Shrub Tabernanthe iboga (Apocynaceae). *Chem. Biodiversity*., **2019**, 16, e1800506.
10. Krengel, F.; Dickinson, J.; Reyes-Chilpa, R. Quantitative Evaluation of a Mexican and a Ghanaian Tabernaemontana Species as Alternatives to Voacanga africana for the Production of Antiaddictive Ibogan Type Alkaloids. *Chem. Biodiversity*, **2020**, 17, e2000002.
11. Ferreres, F.; Pereira, D. M.; Valentão, P.; Oliveira, J. M.; Faria, J.; Gaspar, L.; Sottomayor, M.; Andrade, P. B. Simple and Reproducible HPLC–DAD–ESI-MS/MS Analysis of Alkaloids in Catharanthus Roseus Roots. *J. Pharm. Biomed. Anal*., **2010**, 51, 65–69.
12. Pope, H. G. Tabernanthe Iboga: an African Narcotic Plant of Social Importance. *Economic Botany*, **1969**, 23, 174–184.

13. Krengel, F.; Mijangos, M. V.; Reye-Lezama, M.; Reyes-Chilpa, R. Extraction and Conversion Studies of the Antiaddictive Alkaloids Coronaridine, Ibogamine, Voacangine, and Ibogaine from Two Mexican Tabernaemontana Species (Apocynaceae). *Chemistry Biodivers*., **2019**, 16, e1900175.
14. M. Janot, R. Goutarel, US Pat. 2813873A, 1957.
15. Leete, E. Biogenesis of Rauwolfia alkaloids. II. Incorporation of tryptophan into serpentine and reserpine. *Tetrahedron*, **1961**, 14, 35–41.
16. Battersby, A. R.; Burnett, A. R.; Parsons, P. G. Partial synthesis and isolation of vincoside and isovincoside: Biosynthesis of the three major classes of indole alkaloids from the beta carboline system., *Chem. Comm*., **1968**, 1282–1284.
17. De Luca, V.; Marineau, C.; Brisson, N. Molecular cloning and analysis of a cDNA encoding a plant tryptophan decarboxylase. *Proc. Natl. Acad. Sci.*, **1989**, 86, 2582–2586.
18. O'Connor, S. E.; Maresh, J. J. Chemistry and biology of monoterpene indole alkaloid biosynthesis. *Nat. Prod. Rep*. **2006**, 23, 532–472.
19. Miettinen, K.; Dong, L.; Navrot, N. et al. The seco-iridoid pathway from Catharanthus roseus. *Nat Comm.*, **2014**, 5, 3606.
20. Oudin, A.; Courtois, M.; Rideau, M. et al. The iridoid pathway in Catharanthus roseus alkaloid biosynthesis. *Phytochem Rev*., **2007**, 6, 259–276.
21. Rai, A.; Smita, S.; Singh, A.K.; Shanker, K.; Naegegowda, D. A. Heteromeric and Homomeric Geranyl Diphosphate Synthases from Catharanthus roseus and Their Role in Monoterpene Indole Alkaloid *Biosynthesis. Mol. Plant*., **2013**, 6, 1531–1549.
22. Simkin, A. J.; Miettinen, K.; Claudel, P.; Burlat, V.; Guirimand, G.; Courdavault, V.; Papon, N.; Meyer, S.; Godet, S.; St-Pierre, B.; Giglioli-Guivarc'H, N.; Fischer, M. J.; Memelink, J.; Clastre, M. Characterization of the Plastidial Geraniol Synthase from Madagascar Periwinkle Which Initiates the Monoterpenoid Branch of the Alkaloid Pathway in Internal Phloem Associated Parenchyma. *Phytochemistry*, **2013**, 85, 36–43.
23. Geu-Flores, F.; Sherden, N. H.; Courdavault, V.; Burlat, V.; Glenn, W. S.; Wu, C.; Nims, E.; Cui, Y.; O'Connor, S. E. An Alternative Route to Cyclic Terpenes by Reductive Cyclization in Iridoid *Biosynthesis. Nature*, **2012**, 492, 138–142.

24. Murata, J; Roepke, J; Gordon, H; De Luca, V. The Leaf Epidermome of Catharanthus Roseus Reveals its Biochemical Specialization. *Plant Cell*, **2008**, 20, 524–542.

25. Irmler, S.; Schröder, G.; St-Pierre, B.; Crouch, N. P.; Hotze, M.; Schmidt, J.; Strack, D.; Matern, U.; Schröder, J. Indole Alkaloid Biosynthesis in Catharanthus Roseus: New Enzyme Activities and Identification of Cytochrome P450 CYP72A1 as Secologanin Synthase. *The Plant Journal*, **2008**, 24, 797–804.

26. De Waal A.; Meijer A.H.; Verpoorte R. Strictosidine synthase from Catharanthus roseus: Purification and Characterization of Multiple Forms. *Biochem. J.*, **1995**, 306, 571–580.

27. McKnight, T.D.; Roessner, C.A.; Devagupta, R.; Scott, A.I.; Nessler, C.L. Nucleotide Sequence of a cDNA Encoding the Vacuolar Protein Strictosidine Synthase from Catharanthus roseus. *Nucleic Acids Res.,* **1990**, 18, 4939.

28. Jana, G. K.; Paul, S.; Sinha, S. Progress in the Synthesis of Iboga-Alkaloids and Their Congeners. *Organic Preparations and Procedures International*, **2011**, 43, 541–573.

29. Sundberg, R. J.; Smith, S. Q. *The Alkaloids*, **2002**, 59, 281–386.

30. Büchi, G.; Coffen, D. L.; Kocsis, K.; Sonnet, P. E.; Ziegler, F. E. The Total Synthesis of (±)-Ibogamine and of (±)-Epiibogamine. *J. Am. Chem. Soc.*, **1965**, 87, 2073–2075.

31. Jana, G. K.; Sinha, S. Total Synthesis of Ibogaine, Epiibogaine and Their Analogues. *Tetrahedron*, **2012**, 68, 7155–7165.

32. Kruegel, A. C.; Rakshit, S.; Li, X.; Sames, D. Constructing Iboga Alkaloids via C–H Bond Functionalization: Examination of the Direct and Catalytic Union of Heteroarenes and Isoquinuclidine Alkenes. *J. Org. Chem.*, **2015**, 80, 2062–2071.

33. Reding, M. T.; Fukuyama, T. Stereocontrolled Total Synthesis of (±)-Catharanthine via Radical-Mediated Indole Formation. *Org. Lett.*, **1999**, 1, 973–976.

34. Kim, S. J.; Batey, R. A. Enantioselective Isoquinuclidine Synthesis via Sequential Diels–Alder/Visible-Light Photoredox C–C Bond Cleavage: A Formal Synthesis of the Indole Alkaloid Catharanthine. *Org. Chem. Front.*, **2018**, 5, 2934–2939.

35. Höck, S.; Borschberg, H.J. Enantioselective Synthesis of Key Intermediates in a Novel Approach towards the Iboga-Alkaloid Family. *Helvetica Chimica Acta*, **2003**, 86, 1397–1409.

36. Höck, S.; Borschberg, H.J. Enantioselective Synthesis of (−)-(19R)-Ibogamin-19-ol. *Helvetica Chimica Acta*, **2006**, 89, 542–557.

37. Huffman, J. W.; Rao, C. B. S.; Kamiya, T. The Synthesis of Desethylibogamine. *J. Am. Chem. Soc.*, **1965**, 87, 2288–2288.

38. Huffman, J. W.; Rao, C. B. S.; Kamiya, T. The Synthesis of Desethylibogamine. *J. Am. Chem. Soc.*, **1967**, 32, 697–700.

39. Huffman, J. W.; Shanmugasundaram, G.; Sawdaye, R.; Raveendranath, P. C.; Desai, R. C. A Formal Synthesis of (±)-Ibogamine. *J. Org. Chem*., **1985**, 50, 1460–1464.

40. Henry, K. J.; Grieco, P. A.; Dubay, W. J. A Novel Approach to Iboga Alkaloids: Total Synthesis of (±)-Ibogamine and (±)-Epi-Ibogamine. *Tetrahedron Letters*, **1996**, 37, 8289–8292.

41. Sallay, S. I. Total Synthesis of DL-Ibogamine. *J. Am. Chem. Soc*.,**1967**, 89, 6762–6763.

42. White, J. D.; Choi, Y. Catalyzed Asymmetric Diels−Alder Reaction of Benzoquinone. Total Synthesis of (−)-Ibogamine. *Org. Lett.*, **2000**, 2, 2373–2376.

43. Nagata, W.; Hirai, S.; Okumura, T.; Kawata, K. A Stereochemical Controlled Total Synthesis of DL-Ibogamine and DL-Epiibogamine. *J. Am. Chem. Soc.*, **1968**, 90, 1650–1651.

44. Hirai, S.; Kawata, K.; Nagata, W. Total Synthesis of (±)-Coronaridine and an Improved Synthesis of (±)–Ibogamine. Chem. Commun., **1968**, 719, 1016–1017.

45. Nagata, W.; Hirai, S.; Kawata, K.; Aoki, T. One-Step Synthesis of Bridged Aziridines. *J. Am. Chem. Soc.*, **1967**, 89, 5045–5046.

46. Trost, B. M.; Godleski, S. A.; Genet, J. P. A Total Synthesis of Racemic and Optically Active Ibogamine. Utilization and Mechanism of a New Silver Ion Assisted Palladium Catalyzed Cyclization. *J. Am. Chem. Soc.*,**1978**, 100, 3930–3931.

47. Trost, B. M.; Genet, J. P. Palladium Catalyzed Cyclizations to Alkaloid Skeletons. Facile Synthesis of Desethylibogamine. *J. Am. Chem. Soc.*,**1976**, 98, 8516–8517.

48. Imanishi, T.; Yagi, N.; Hanaoka, M. 1,6-Dihydro-3(2H)-Pyridinones. X. 2-Azabicyclo(2.2.2)Octane Ring Formation via Intramolecular Michael Reaction: Total Synthesis of (±)-Ibogamine and (±)-Epiibogamine. *Chem. Pharm. Bull.*, **1985**, 33, 4202–4211.

49. Jana, G. K.; Sinha, S. Reductive Heck Coupling: An Efficient Approach toward the Iboga Alkaloids. Synthesis of Ibogamine, Epiibogamine and Iboga Analogs. *Tetrahedron*, **2012**, 53, 1671–1674.

50. Kutney, J. P.; Fuller, G. B.; Greenhouse, R.; Itoh, I. Selective Debenzylation of Quaternary Salts. The Benzyl Group as an Excellent Protecting Group for Basic Nitrogen Compounds. *Synth. Commun.*, **1974**, 4, 183–187.

51. Marazano, C.; Goff, M.-T. L.; Fourrey, J.L.; Das, B. C. An Unequivocal Synthesis of 1-Benzyl-3-Ethyl-1,6-Dihydropyridine and Its Use for a Biogenetically Modelled Synthesis of (±)-Catharanthine. *J. Chem. Soc.* **1981**, 148, 389–391.

52. Sundberg, R. J.; Hong, J.; Smith, S. Q.; Sabat, M.; Tabakovic, I. Synthesis and Oxidative Fragmentation of Catharanthine Analogs. Comparison to the Fragmentation—Coupling of Catharanthine and Vindoline. *Tetrahedron*, **1998**, 54, 6259–6292.

53. Iyer, R. N.; Favela, D. F.; Zhang, G.; Olson. D. E. The iboga enigma: the chemistry and neuropharmacology of iboga alkaloids and analogs. *Nat. Prod. Rep.* **2020**

54. Sheppard, S. G. A preliminary investigation of ibogaine: case reports and recommendations for further study. J. *Subst. Abuse Treat.*, **1994**, 11, 379–385.

55. Alper, K. R.; Lotsof, H. S.; Frenken, G. M.; Luciano, D. J.; Bastiaans, J. Treatment of acute opioid withdrawal with ibogaine. *Am. J. Addict.*, **1999**, 8, 234–242.

56. Schenberg, E. E.; Comis, M. A. D. C.; Chaves, B. R.; Silveira, D. X. D. Treating Drug Dependence with the Aid of Ibogaine: A Retrospective Study. J. *Psychopharmacol.*, **2014**, 28, 993–1000.

57. Mash, D. C.; Duque, L.; Page, B.; Allen-Ferdinand, K. Ibogaine Detoxification Transitions Opioid and Cocaine Abusers Between Dependence and Abstinence: Clinical Observations and Treatment Outcomes. *Front. Pharmacol.*, **2018**, 9:529.

58. Mash, D. C.; Kovera, C. A.; Pablo, J.; Tyndale, R. F.; Ervin, F. D.; Williams, I. C.; Singleton, E. G.; Mayor, M. Ibogaine: Complex Pharmacokinetics, Concerns for Safety, and Preliminary Efficacy Measures. *Ann N Y Acad. Sci.*, **2000**, 914, 394–401.

59. Cappendijk, S. L.; Dzoljic, M. R. Inhibitory Effects of Ibogaine on Cocaine Self-Administration in Rats. *Eur. J. Pharmacol.*, **1993**, 241(2-3), 261–265.

60. Maisonneuve, I. M.; Keller, R. W.; Glick, S. D. Interactions between Ibogaine, a Potential Anti-Addictive Agent, and Morphine: An in Vivo Microdialysis Study. *Eur. J. Pharmacol*., **1991**, 199, 35−42.

61. Parker, L. A.; Siegel, S. Chapter 11 Modulation of the Effects of Rewarding Drugs by Ibogaine. The Alkaloids: *Chemistry and Biology*, **2001**, 211–225.

62. Brown, T. K. Ibogaine in the treatment of substance dependence. *Current Drug Abuse Reviews*, **2013**, 6, 3–16.

63. Wasko, M. J.; Witt-Enderby, P. A.; Surratt, C. K. DARK Classics in Chemical Neuroscience: Ibogaine. *ACS Chem. Neurosci.*, **2018**, 9, 2475–2483.

64. Maciulaitis, R.; Kontrimaviciute, V.; Bressolle, F. M.; Briedis, V. Ibogaine, an anti-addictive drug: pharmacology and time to go further in development. A narrative review. *Hum. Exp. Toxicol*., **2008**, 27, 181–94.

65. Alper, K. R. Ibogaine: a review. *Alkaloids Chem Biol*., **2001**, 56, 1–38.

66. Popik, P.; Layer, R. T.; Skolnick, P. 100 Years of Ibogaine: Neurochemical and Pharmacological Actions of a Putative Anti-Addictive Drug. *Pharmacol. Rev*., **1995**, 47, 235−253.

67. Ohearn, E.; Molliver, M. Degeneration of Purkinje Cells in Parasagittal Zones of the Cerebellar Vermis after Treatment with Ibogaine or Harmaline. *Neuroscience*, **1993**, 55, 303–310.

68. Koenig, X.; Kovar, M.; Boehm, S.; Sandtner, W.; Hilber, K. Anti-Addiction Drug Ibogaine Inhibits HERG Channels: A Cardiac Arrhythmia Risk. *Addict. Biol.*, **2014**, 19, 237−239.

69. Thurner, P.; Stary-Weinzinger, A.; Gafar, H.; Gawali, V. S.; Kudlacek, O.; Zezula, J.; Hilber, K.; Boehm, S.; Sandtner, W.; Koenig, X. Mechanism of HERG Channel Block by the Psychoactive Indole Alkaloid Ibogaine. *J. Pharmacol. Exp. Ther.*, **2014**, 348, 346−358.

70. Alper, K. R.; Stajić, M.; Gill, J. R. Fatalities Temporally Associated with the Ingestion of Ibogaine. *J. Forensic Sci.*, **2012**, 57, 398−412.

71. Koenig, X.; Hilber, K. The Anti-Addiction Drug Ibogaine and the Heart: A Delicate Relation. *Molecules*, **2015**, 20, 2208− 2228.

72. Hough, L. B.; Pearl, S. M.; Glick, S. D. Tissue Distribution of Ibogaine after Intraperitoneal and Subcutaneous Administration. *Life Sci.*, **1996**, 58, 119−122.

73. Jamieson, C.; Moir, E. M.; Rankovic, Z.; Wishart, G. Medicinal chemistry of hERG optimizations: Highlights and hang-ups. *J. Med. Chem.*, **2006**, 49, 5029–5046.

Chapter 2 – Synthesis of Des-ethylibogaine

2.1 Retrosynthetic Analysis of Ibogaine and Initial Preparation of Isoquinuclidine

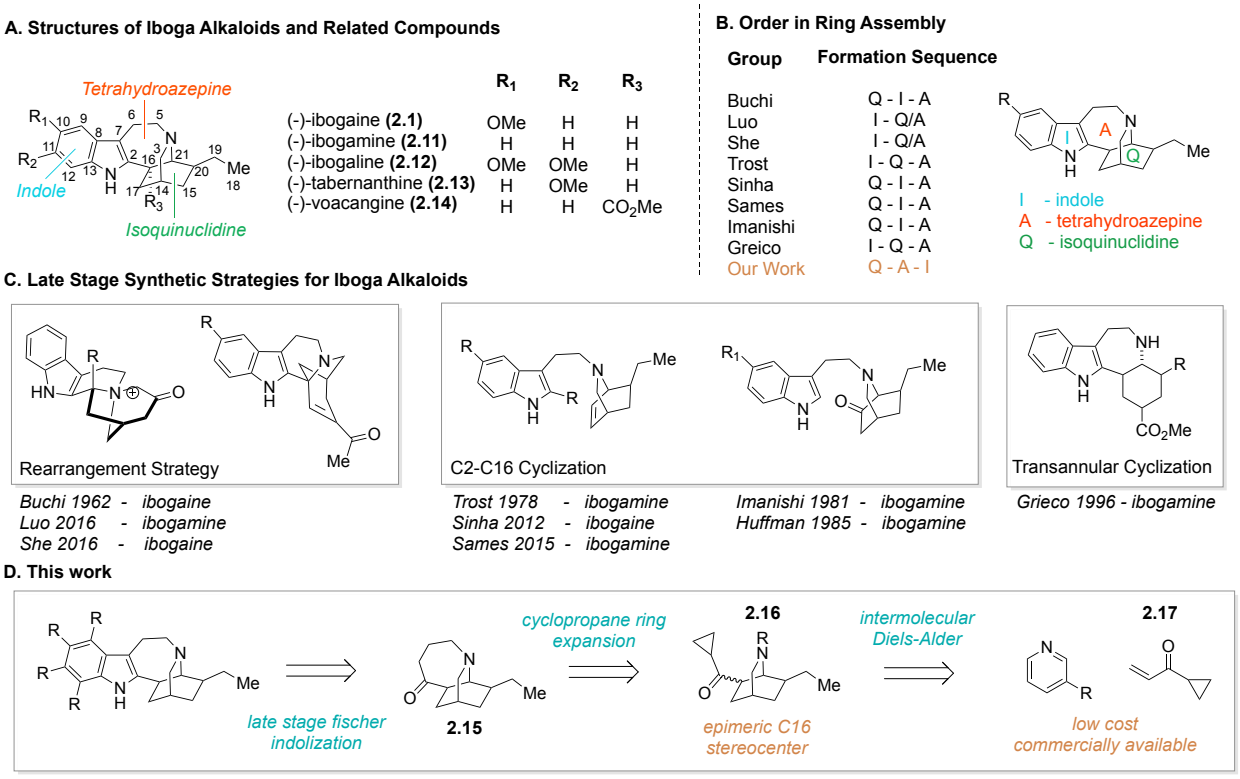

Figure 2.1. (A) Structures of iboga alkaloids **(B)** Order in ring assembly in various synthetic routes towards iboga alkaloids **(C)** Late-stage synthetic strategies towards iboga alkaloids **(D)** Our retrosynthetic analysis of ibogaine.

The vast majority of iboga alkaloid syntheses can be grouped into three main late-stage strategies:[74] rearrangement to generate the isoquinuclidine, indole C2 to C16 cyclization, and transannular cyclization (**Figure 2.1C**). Unfortunately, these late-stage strategies are variable in yields and necessitate pre-functionalization of the indole; a strategy that is not ideal for the generation of analogs containing various indole substitution patterns. Therefore, we envisioned a synthesis that would deviate significantly from traditional routes by constructing the indole ring system last though a Fischer indole cyclization of tricyclic ketone **2.15 (Figure 2.1D)**. Late-stage

diversification using substituted phenylhydrazines or various other reactions of the carbonyl gives access to a large number of analogs from a single late-stage intermediate. We envisioned that tricyclic ketone **2.15** could be constructed through exploitation of strained cyclopropyl ketone **2.16** to generate the 7-membered ring. Finally, the isoquinuclidine ring system would be prepared from an intermolecular Diels-Alder reaction between a commercially available pyridine derivative and cyclopropyl enone. A significant challenge associated with constructing the isoquinuclidine core is the inherent endo selectivity of the Diels-Alder reaction. In our retrosynthetic model, it is imperative that the cyclopropyl ketone of intermediate **2.16** is in the exo orientation for ring expansion with the basic amine. Thus, strategic placement of a ketone in intermediate **2.16** allows for epimerization of the C16 carbon to ultimately conduct a dynamic resolution in our ring closure.

In order to establish a proof of concept for synthesizing the core iboga scaffold, we shifted our focus towards the preparation of desethylibogaine (**2.18**) as a model system for the eventual construction of ibogaine (**2.1**) (**Figure 2.2A**). This allowed us to establish a general route to the iboga framework without the regioselectivity challenges associated with forming a substituted dihydropyridine.

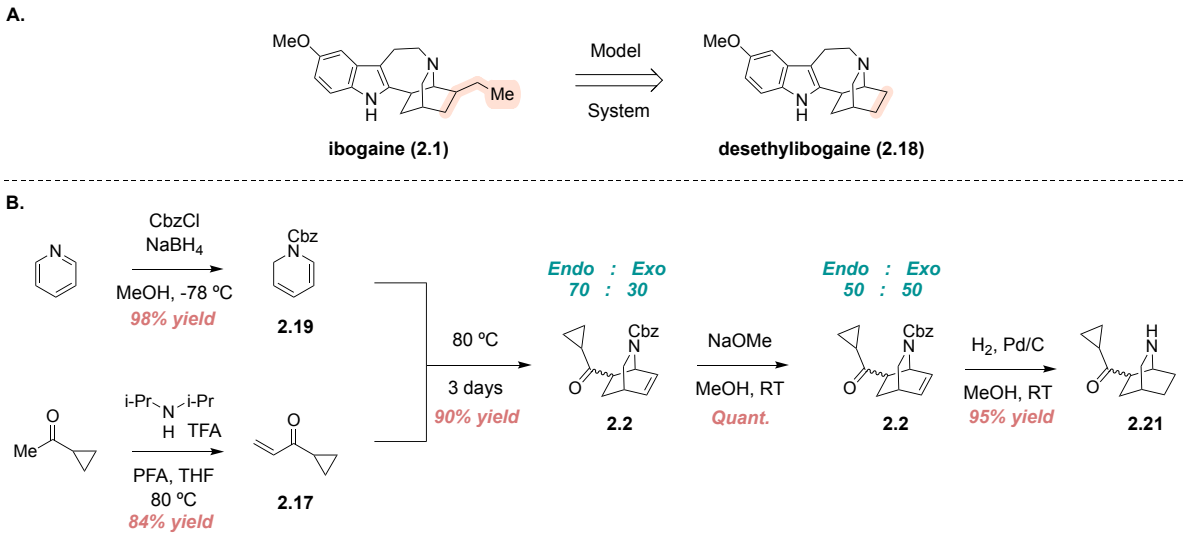

Figure 2.2. (A) Desethylbogaine as a model system for the construction of ibogaine **(B)** Initial synthetic efforts towards free amine **2.21**

Initial synthetic efforts commenced with preparation of the requisite diene and dienophile for our Diels-Alder reaction (**Figure 2.2B**). Pyridine was reduced using sodium borohydride and benzyl chloroformate to afford dihydropyridine **2.19** in high yield.[75] Dihydropyridine **2.19** is prone to oxidation and must be used immediately upon isolation. We observed that samples of **2.19** showed immediate discoloration after just 30 minutes of air exposure. Cyclopropyl enone **2.17** was prepared from an enamine assisted aldol reaction with cyclopropyl methyl ketone and paraformaldehyde (PFA). We found that diisopropylammonium trifluoroacetate performed best in the aldol condensation and was needed in stoichiometric quantity. With intermediates **2.19** and **2.17** in hand, a Diels-Alder reaction was conducted in a sealed microwave tube to afford a 70:30 (endo:exo) epimeric mixture of isoquinuclidine **2.2** in 90% yield. Due to the high instability of dihydropyridine **2.19**, it is critical that the reaction is degassed at -78 °C prior to heating. Reactions that were not degassed showed a reduction in yield and significant pyridinium byproduct. Isoquinuclidine **2.2** was then subjected to a base-mediated epimerization using sodium methoxide to produce a 50:50 (endo:exo) ratio of epimers at the C16 carbon. Concomitant carbamate deprotection and olefin saturation was accomplished by hydrogenation using Pd/C to give free amine **2.21** in good yield. Having devised an efficient and convergent 4 step route to **2.21**, focus shifted towards ring expansion of the cyclopropane to our desired tetrahydroazepinone.

2.2 Tetrahydroazapinone Synthesis by Lewis Acid and Photoredox Catalysis Strategy

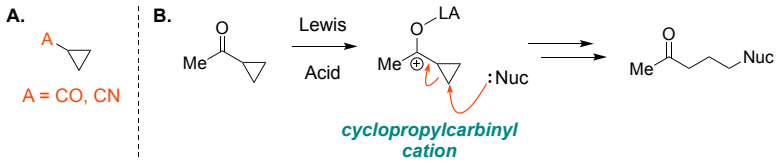

Figure 2.3. (A) Acceptor stabilized cyclopropanes **(B)** Cyclopropylcarbinyl cation stabilization and nucleophilic attack

Cyclopropanes are incredibly valuable synthetic intermediates generally utilized for their inherent ring strain.[76,77] Often times a cyclopropane is activated by an acceptor with significant p orbital character such as a carbonyl or nitrile[78] (**Figure 2.3A**). Formation of a cation adjacent to the cyclopropane is stabilized by the bent nature of the cyclopropane C-C bonds through electron donation of the cyclopropyl σ orbital to the neighboring vacant p orbital (**Figure 2.3B**). This stabilized cyclopropylcarbinyl cation allows for a myriad of transformations including nucleophilic attack at the distal carbon of the cyclopropane.[79]

We envisioned a similar pathway for ring expansion of cyclopropyl ketone **2.21** to tetrahydroazepinone **2.22** (**Figure 2.4A**). Though this is a 7-endo-tet cyclization that is disfavored by Baldwin's rules, we thought we could exploit an exception through the formation of the cyclopropylcarbinyl cation in **2.21a**. Furthermore, we hoped Lewis acidic conditions would induce epimerization of endo **2.21** to achieve a kinetic resolution in our reaction.

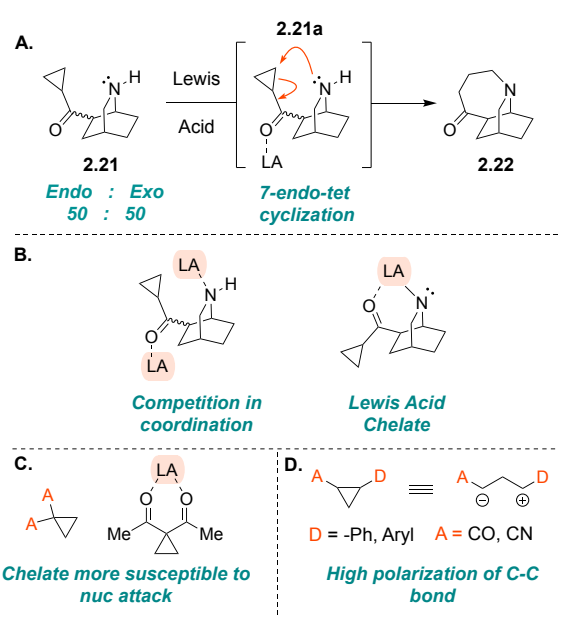

Table 2.1

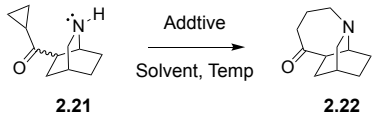

Entry	Additive	Solvent	Temp	**2.22**
1[a]	$AlCl_3$ (0.1 – 0.5)	CH_3CN	RT to 90 °C	-
2[a]	$Yb(OTf)_3$ (0.1 – 0.5)	CH_3CN	RT to 90 °C	-
3[a]	$Sc(OTf)_3$ (0.1 – 0.5)	CH_3CN	RT to 90 °C	-
4	TFA (0.1), MgI_2 (0.6)	HFIP	80 °C	Trace
5	TFA (0.1)	HFIP	RT to 90 °C	-
6	MgI_2 (0.1)	HFIP	RT to 90 °C	-
7	$RuCl_3$ (0.1 – 0.5)	CH_3CN	90 °C	Trace
8	$Ti(O\text{-}iPr)_4$ (0.1)	CH_3CN	90 °C	-
9[a]	$AlMe_3$	CH_3CN	RT to 90 °C	Trace

[a]DCE, DCM, DMF, DMSO, DMA also screened as solvents. All reactions run at 0.1M solvent.

Figure 2.4. (A) Proposed 7-endo-tet pathway to product **2.22** **(B)** Lewis acid coordination competition between carbonyl and basic amine **(C)** Geminal Acceptor-Acceptor di-activation of cyclopropane, chelate pathway **(D)** Vicinal Donor-Acceptor di-activation of cyclopropane

A total of 45 different Lewis Acid, solvent and temperature combinations were screened with intermediate **2.21** to produce the desired ring expansion. Unfortunately, nearly all conditions screened were unsuccessful and primarily starting material was recovered. It became clear that there is likely a competition in coordination between the carbonyl and basic amine (**Figure 2.4B**). Lewis acid coordination to the nitrogen would effectively diminish the nucleophilicity of the amine and prevent ring opening of the cyclopropane. Oxophilic Lewis acids[80] such as $Yb(OTf)_3$ and $Sc(OTf)_3$ (**Table 2.1, 2—3**) gave similar results owing to the possibility of a Lewis acid chelate between the basic amine and carbonyl (**Figure 2.4B**).

A thorough examination of the literature reveals a limitation in adding hard nucleophiles to mono-activated cyclopropanes. Generally hard nucleophiles such as an amine or alkoxide can only be added to a di-activated system using an acceptor-acceptor or a donor-acceptor activator[81,82]. A geminal acceptor-acceptor system can produce a Lewis acid chelate making the cyclopropane very prone for attack (**Figure 2.4C**). In a vicinal donor-acceptor system, the synergistic "push-pull" effect of vicinal charge stabilizing groups boosts the high polarization of the cyclopropane C-C bond, allowing for rupture under mild conditions (**Figure 2.4D**). [83]

Final attempts for optimization included the use of MgI_2 to induce ring opening of the cyclopropane (Table 2.1, **4—6**).[84] LCMS analysis indicated that in the presence of trifluoroacetic acid (TFA), the cyclopropane undergoes ring opening with MgI_2 to produce to the corresponding alkyl iodide. Through this pathway we hoped that the basic amine would undergo S_n2 ring closure to furnish the desired product. Unfortunately, only a trace amount of product was detected, and this strategy was deemed unsuccessful.

We next investigated if inversing the polarity of our ring closure via photoredox catalysis would give the desired cyclization. In this strategy, an excited photocatalyst (PC) would oxidize basic amine **2.21** to the corresponding radical cation[85] and induce subsequent ring opening of the exo- cyclopropyl ketone (**Figure 2.5A**). Cyclization through this pathway would produce an alpha stabilized radical that can be reduced to the corresponding enolate to ultimately furnish

tetrahydroazepinone **2.22**. We postulated that kinetic resolution of the endo **2.21** could occur through a fragmentation of radical cation **2.21b**. Fragmentation of the isoquinuclidine would effectively racemize the C16 epimeric center (**2.21c**) and subsequent recombination could allow for a resolution in our reaction mixture.

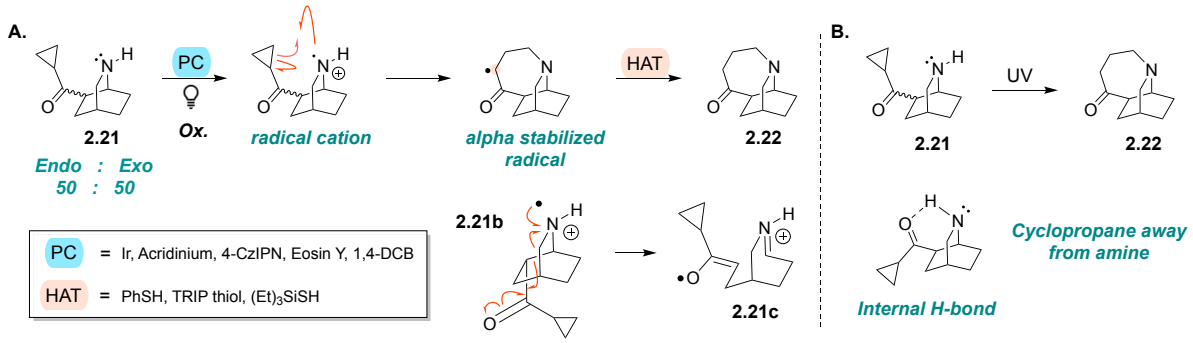

Figure 2.5. (A) Mechanism for photoredox catalyzed ring expansion of **2.21**, Pathway for kinetic resolution of **2.21b (B)** UV light catalyzed ring expansion of **2.21**, internal H bond in **2.21**

A variety of photocatalyst, thiol and solvent combinations were screened, and none proved successful. In most reactions, starting material was recovered in appreciable amounts. Prolonged irradiation with 1,4-dicyanobenzene (1,4-DCB) and thiophenol (PhSH) in acetonitrile led to significant decomposition and possible fragmentation of the isoquinuclidine ring. Irradiation with UV light was unsuccessful as starting material was also recovered. We surmise that an internal hydrogen bond between the carbonyl and basic amine forces the cyclopropane away from the amine and prevents any tetrahydroazepinone formation (**Figure 2.5B**).

2.3 Tetrahydroazapinone Synthesis by Cyclopropyl Hydrazone Cascade Strategy

Review of our Lewis acid catalyzed experiments revealed that the Lewis basicity of the amine was too much to overcome for ring closure with the cyclopropane. The clear difference in Lewis basicity can be seen by the large pKa difference between the protonated states of the amine and carbonyl in **2.21d** (**Figure 2.6A**). We surmised that we could minimize the large pKa

difference by substituting the carbonyl for a hydrazone. In this scenario, there would be a significantly smaller difference in acidity for the ammonium and iminium in intermediate **2.21e**. We envisioned a strategy in which upon formation of cyclopropyl phenyl hydrazone **2.21f**, ring opening of the cyclopropane would produce an intermediate (**2.21g**) perfectly templated for a Fischer indole cyclization (**Figure 2.6B**). Assuming that this would be an acid-catalyzed process, we hoped that the reduced difference in basicity between the amine and imine would increase the likelihood of cyclopropyl ring opening by the quinuclidine nitrogen. Finally, a [3 + 3] sigmatropic rearrangement of **2.21g** would furnish the iboga framework in a "one-pot" sequence from intermediate **2.21**.

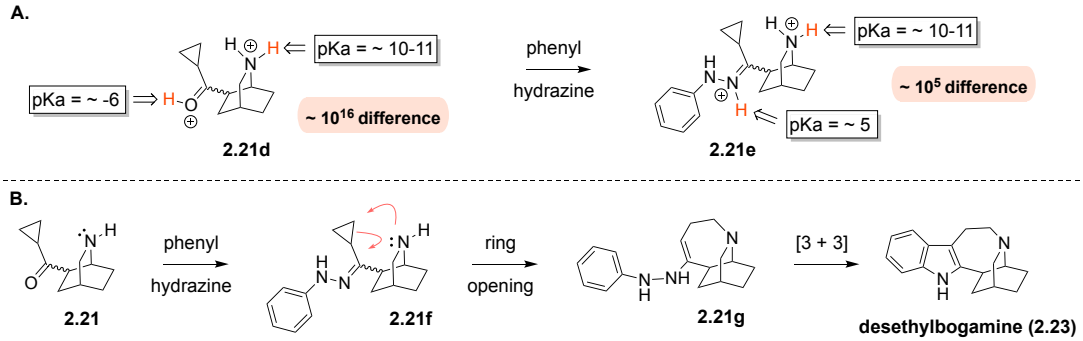

Figure 2.6. (A) pKa differences between **2.21d** and **2.21e (B)** Cyclopropyl hydrazone strategy for "one-pot" sequence from **2.21** to **2.23**

LCMS analysis revealed that our cascade cyclization stalled at cyclopropyl hydrazone **2.21f** when using acetic acid, hydrochloric acid, or sulfuric acid in both protic and aprotic solvents. Inspired by the work of Garg and co-workers,[86] we reacted free amine **2.21** with phenylhydrazine in the presence of stoichiometric trifluoroacetic acid (TFA) in 1,2-dichloroethane (DCE) and noticed a large LCMS peak corresponding to the mass (m/z 253) of desethylibogamine **2.23**. However, ^{1}H-NMR analysis of the major product revealed a structure with 5 aromatic hydrogen peaks and the cyclopropane moiety still in place (**Figure 2.7A**). A strong ^{1}H-^{1}H coupling between

the aromatic singlet at δ 6.95 ppm and the indole N-H indicated that the isolated product was a C3 substituted indole analog **(Figure 2.7B**). Structure elucidation via 1D and 2D NMR experiments led to the determination that the isoquinuclidine ring system had been deconstructed to yield compound **2.24** (**Figure 2.8A**)

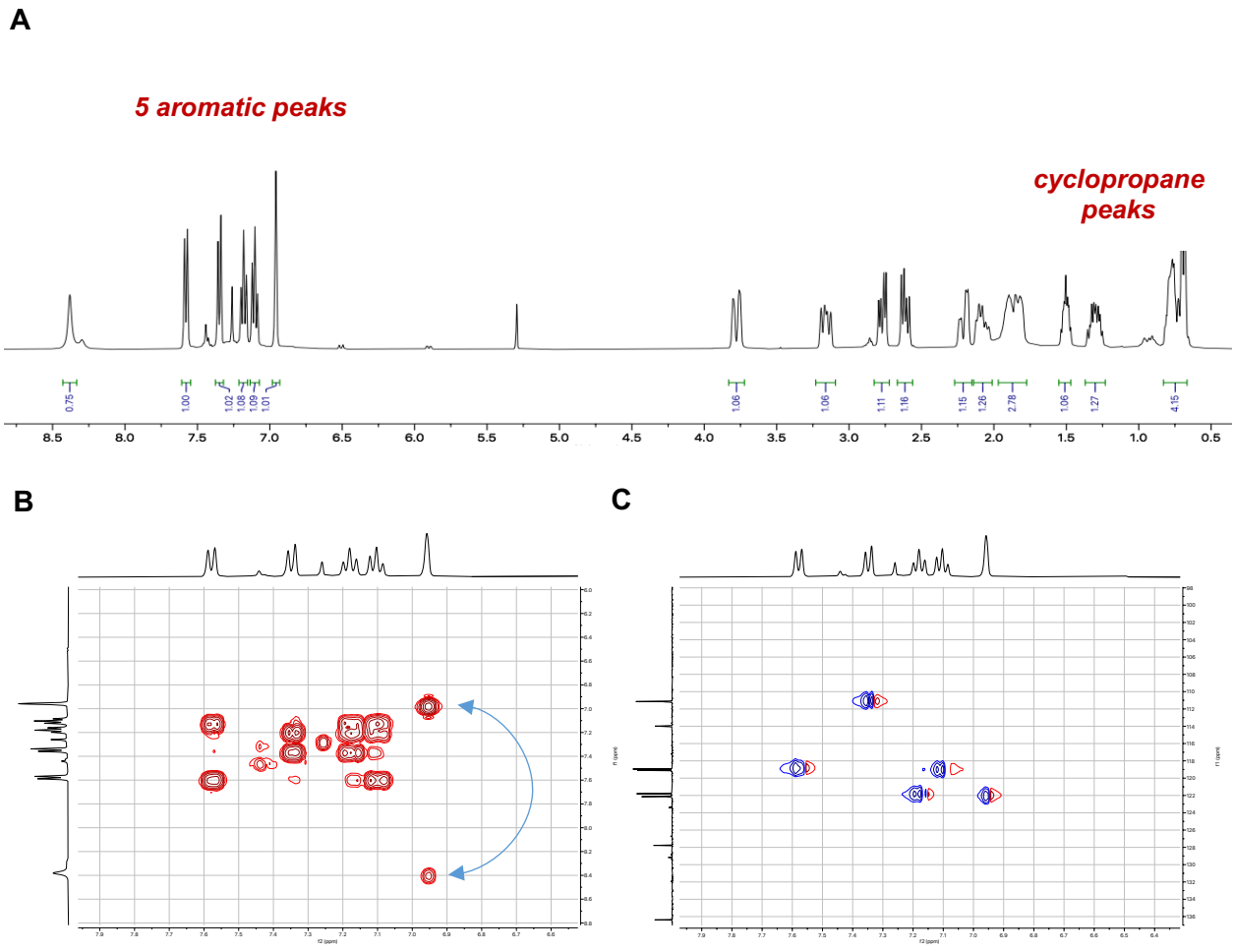

Figure 2.7. (A) ^{1}H-NMR spectra of unexpected product from cyclopropyl cascade route **(B)** ^{1}H-^{1}H COSY NMR of unexpected product **(C)** ^{1}H -^{13}C HSQC NMR of unexpected product

Having ruled out the possibility of a cyclopropane migration, we propose a mechanism involving a Grob like fragmentation of hydrazone **2.25** (**Figure 2.28C**). Fragmentation of the isoquinuclidine ring produces imine **2.26** which can undergo addition and subsequent ring fragmentation to yield linear intermediate **2.28.** Finally, amine condensation to the cyclopropyl hydrazone followed by elimination and Fischer indolization produces rearranged scaffold **2.25**. To probe this mechanism further, we altered the substituents on the *para*- position of the phenylhydrazine (**Figure 2.28B**) and noticed that with *para*-methoxyphenylhydrazine there was a significant reduction in yield and an appreciable amount of starting material was recovered. In contrast, the rearrangement proceeded smoothly with *para*-nitrophenylhydrazine and was complete in roughly half the amount of time as our pilot experiment. We believe this lends evidence to the notion that the Grob fragmentation of intermediate **2.25** is the rate determining step in the mechanism and the presence of a *para*- electron withdrawing group significantly enhances the rate of fragmentation. When subjecting pure epimers of intermediate **2.21** to the

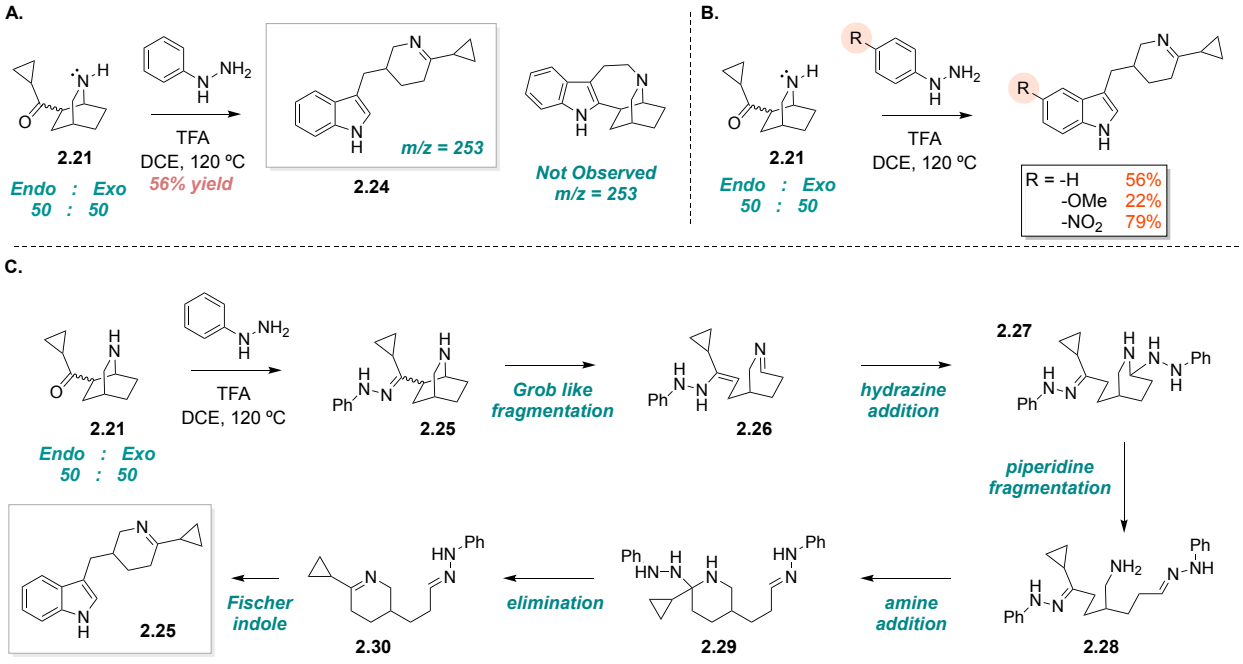

Figure 2.8. (A) Unexpected product from cascade cyclization reaction **(B)** Substituent effects on reaction efficiency **(C)** Proposed mechanism for rearrangement

reaction conditions, the endo epimer outperformed the exo epimer likely due to the anti-periplanar geometry of the fragmentation. We do observe epimerization in the reaction mixture, owing to the possibility of some kinetic resolution of the exo epimer.

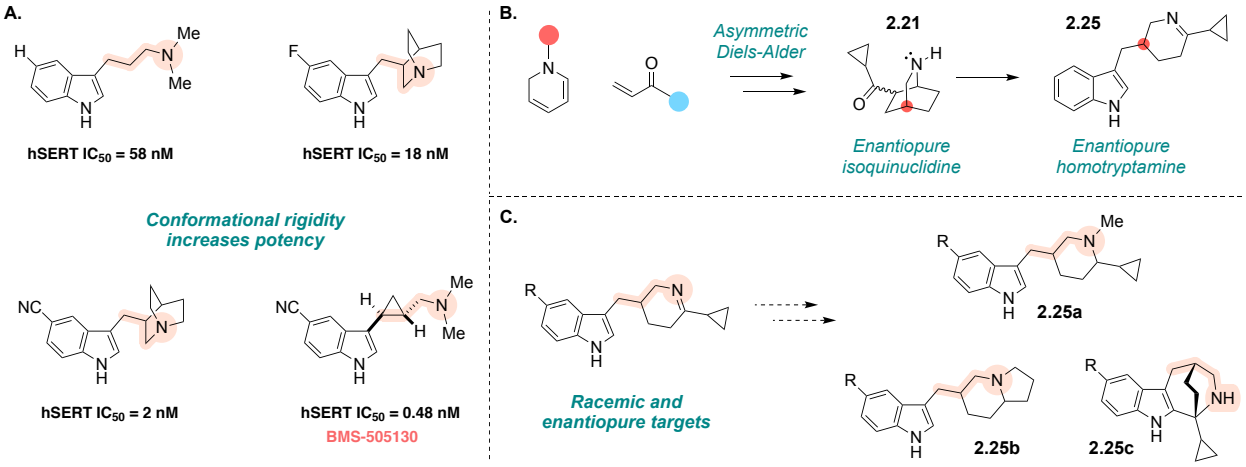

Figure 2.9. (A) Conformationally restricted homotryptamine and SERT inhibition potency **(B)** Preparation of enantiopure homotryptamine **(C)** Racemic and enantiopure homotryptamine targets

Though we had not intended to synthesize product **2.25,** our rearrangement does offer new chemical space for the development of novel homotryptamine therapeutics. Several reports have assessed the anti-depressant like properties of the homotryptamine scaffold in serotonin transporter (SERT) inhibition assays.[87,88] The serotonin transporter (SERT) is a monoamine transporter protein responsible for the reuptake of serotonin from the synaptic cleft back to the presynaptic neuron. Many selective serotonin reuptake inhibitor (SSRI) and tricyclic antidepressants work by binding to SERT thus reducing serotonin reuptake and increasing the amount of serotonin available in the synapse.[89] It was found that a more conformationally rigid propylamine chain increased potency in SERT inhibition (**Figure 2.9A**). With this in mind, we envisioned that we could synthesize a library of both racemic and enantiopure homotryptamine targets using our methodology (**Figure 2.9C**). Enantiopure homotryptamine targets would be

accessed from enantiopure isoquinuclidine **2.21** which could be derived from an asymmetric Diels-Alder reaction (**Figure 2.9B**). Current work is underway to synthesize and assess the therapeutic potential of these analogs in both SERT inhibition and SERT efflux assays.

2.4 Alkyl Halide Ring Closure and Completion of Desethylibogaine

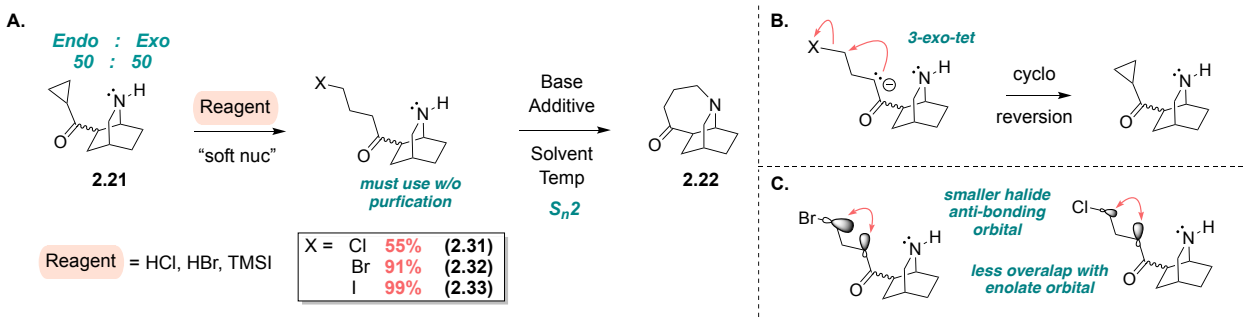

Figure 2.11. (A) Two-step process for preparation of 2.22 **(B)** Cycloreversion by-product from Sn2 ring closure **(C)** Alkyl halide anti-bonding orbital overlap hypothesis

Our previous attempts to synthesize **2.22** indicate the relative difficulty for obtaining a 7-endo-tet cyclization of free amine **2.21** Encouraged by our Lewis acid catalyzed results with MgI_2/TFA, we elected to ring open the cyclopropane to the corresponding alkyl halide and then perform an intramolecular S_n2 alkylation to furnish tetrahydroazapinone **2.22** in a two-step process (**Figure 2.11A**). It has been demonstrated that Bronsted or Lewis acid activation of a cyclopropyl ketone can induce nucleophilic attack with a polarizable, "soft" nucleophile.[90,91] Ring opening of intermediate **2.21** with either hydrogen bromide (HBr) or trimethylsilyl iodide (TMSI) enables facile access to alkyl halides **2.32** and **2.33**, respectively.

Numerous combinations of base, additive, solvent, and temperature were screened to achieve formation of intermediate **2.22** (**Table 2.2**). We noticed that base mediated ring closure of alkyl iodide **2.33** had undergone cycloreversion to intermediate **2.21** rather than forming the desired tricycle (**Table 2.2, Entry 15—17**). Though this appears to be a thermodynamically

disfavored pathway, we rationalized that this product is kinetically favored due to significant overlap between the enolate pi orbital and the halide antibonding orbital. When using alkyl bromide **2.32**, we were able to obtain our desired product in 45% yield using cesium carbonate and sodium sulfate in acetonitrile. This reaction was especially sensitive to water (**Entry 5**) and nearly all of endo **2.32** had undergone cycloreversion to intermediate **2.21**.

We hypothesized that the antibonding orbital of a chloride leaving group would have less orbital overlap with the enolate pi orbital (**Figure 2.11C**) and minimize the likelihood of cycloreversion. Formation of alkyl chloride **2.31** was sluggish when using hydrogen chloride (HCl)

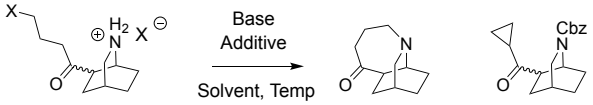

2.31-2.33 **2.22** **2.21**

Entry	X =	Base	Additive	Solvent	Temp	**2.22**	**2.21**
1	Br	Cs_2CO_3 (1.5 equiv)	Na_2SO_4 (3 equiv.)	CH_3CN	60 °C	45%	38%
2	Br	Cs_2CO_3 (1.5 equiv)	-	CH_3CN	60 °C	40%	41%
3	Br	Cs_2CO_3 (1.0 equiv)	-	CH_3CN	60 °C	22%	64%
4	Br	Cs_2CO_3 (1.5 equiv)	LiI	CH_3CN	60 °C	38%	48%
5	Br	Cs_2CO_3 (1.5 equiv)	H_2O (3 equiv.)	CH_3CN	60 °C	8%	78%
6	Br	Cs_2CO_3 (1.5 equiv)	Na_2SO_4 (3 equiv.)	CH_3CN	80 °C	28%	41%
7	Br	K_2CO_3 (1.5 equiv)	Na_2SO_4 (3 equiv.)	CH_3CN	60 °C	-	65%
8	Br	2,6-lutidine (1.5 equiv)	-	CH_3CN	60 °C	-	18%
9	Br	DIPEA (1.5 equiv.)	-	CH_3CN	60 °C	-	34%
10	Br	Cs_2CO_3 (1.5 equiv)	Na_2SO_4 (3 equiv.)	DMF	60 °C	trace	66%
11	Br	Cs_2CO_3 (1.5 equiv)	Na_2SO_4 (3 equiv.)	DME	60 °C	trace	trace
12	Br	Cs_2CO_3 (1.5 equiv)	Na_2SO_4 (3 equiv.)	t-BuCN	60 °C	22%	44%
13[a]	Cl	Cs_2CO_3 (1.5 equiv)	Na_2SO_4 (3 equiv.)	CH_3CN	60 °C	-	-
14[a]	Cl	Cs_2CO_3 (1.5 equiv)	Na_2SO_4 (3 equiv.)	DMF	60 °C	-	-
15	I	Cs_2CO_3 (1.5 equiv)	Na_2SO_4 (3 equiv.)	CH_3CN	60 °C	trace	88%
16	I	Cs_2CO_3 (1.5 equiv)	Na_2SO_4 (3 equiv.)	DMF	60 °C	trace	78%
17	I	K_2CO_3 (1.5 equiv)	Na_2SO_4 (3 equiv.)	CH_3CN	60 °C	trace	77%

Table 2.2. Isolated yields shown. All reactions run at 0.1M solvent and chromatographed using gradient elution 20:1→10:1 DCM/MeOH. Product **S-3** was isolated as a mixture of endo and exo epimers. [a] Reaction run at 60 °C to 120 °C

or trimethylsilyl chloride (TMSCl) due to the poor nucleophilicity of the chloride anion (**Figure 2.11A**). Alkyl chloride **2.31** was unreactive in our ring closure conditions and elevated temperature, longer reaction times or additional base led to decomposition (**Table 2.2, Entry 13 and 14**). Other leaving groups such as the dimethylsulfonium salt, tosylate, and mesylate gave similar results and minimal product was detected.

We elected to progress forward in the synthesis albeit our sub-par yields for the preparation of intermediate **2.22**. We noticed that hydrazone formation of **2.22** did not go to completion in protic solvents with mineral acids. However, heating a mixture of **2.22** with *para*-methoxyphenylhydrazine in acetic acid and DCE enabled full hydrazone formation and subsequent cyclization to produce desethylibogaine (**2.18**) in 84% yield (**Figure 2.12**). Fischer indolization with phenylhydrazine stalled at the hydrazone stage and needed stoichiometric BF_3OEt_2 to induce cyclization to desethylibogamine **2.23.** Taken together, these strategic decisions have led to the development of a scalable and efficient 6-step synthesis to the iboga framework. Our route allows for late-stage diversification of the indole ring system and enables the production of des-ethyl iboga compounds in roughly 26-28% overall yield from commercially available pyridine.

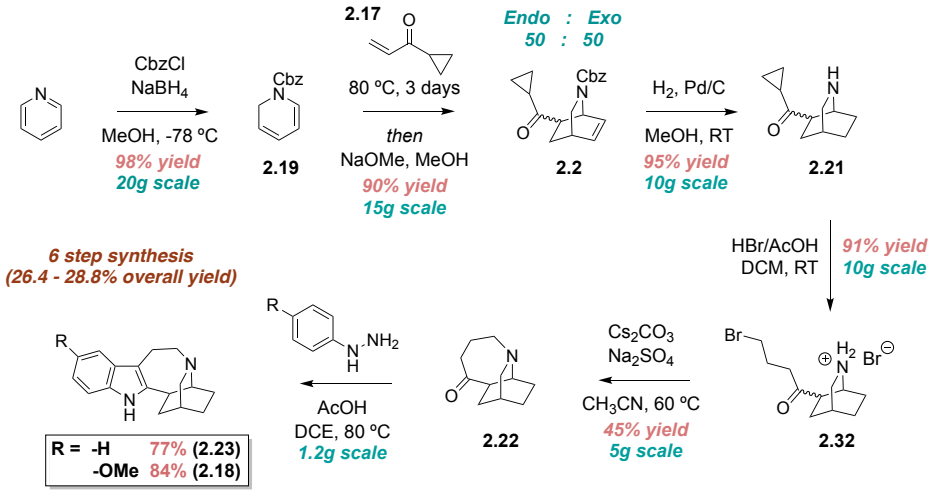

Figure 2.12. 6 step synthesis of desethylibogaine (**2.18**) and desethylibogamine (**2.23**)

REFERENCES

74. Iyer, R. N.; Favela, D.; Zhang, G.; Olson, D. E. The Iboga Enigma: The Chemistry and Neuropharmacology of Iboga Alkaloids and Related Analogs. *Nat. Prod. Rep.* **2021**, 38, 307—329
75. Fowler, F. W. Synthesis of 1,2- ad 1,4-Dihydropyridines. *J. Org. Chem.* 1972, 37, 1321—1323
76. De Meijere, A. Bonding properties of cyclopropane and their chemical consequences. *Angew. Chem. Int. Ed.* **1979**, *18*, 809–826
77. Gordon, M. S. Ring strain in cyclopropane, cyclopropene, silacyclopropane, and silacyclopropene. *J Am. Chem. Soc.* **1980**, 102, 7419—7422
78. Danishefsky, S. Electrophilic cyclopropanes in organic synthesis. *Acc. Chem. Res.* **1979**, 12, 66—72
79. Ghosh, K.; Das, S. Recent advances in ring-opening of donor acceptor cyclopropanes using C-nucleophiles. *Org. Biomol. Chem.* **2021**, 19 , 965—982
80. Sagawa, T.; Kobayashi, H.; Fukuoka, A. Effect of Lewis acid on catalytic dehydration of a chitin-derived sugar alcohol. *Molecular Catalysis*. **2020**, 498
81. Cavitt, M. A.; Phun, L. H.; France, S. Intramolecular donor–acceptor cyclopropane ring-opening cyclizations. *Chem. Soc. Rev.,* **2014**, 43, 804—818
82. Schneider, T. F.; Kaschel, J.; Werz, D. B. A New Golden Age for Donor–Acceptor Cyclopropanes. *Angew. Chem. Int. Ed.* **2014**, 53, 5504—5523
83. Bisag, G. D.; Viola, P.; Bernardi, L.; Fochi, M. Divergent Reactivity of D-A Cyclopropanes under PTC Conditions, Ring-Opening vs. Decyanation Reaction. *Catalysts.* **2023**, 13, 760
84. Tang, P.; Wei, Y.; Wen, L.; Ma, H.; Yang, Y.; Jiang, Y. MgI2-Catalyzed Nucleophilic Ring-Opening Reactions of Donor–Acceptor Cyclopropanes with Indoline-2-thiones. *J. Org. Chem.* **2022**, 87, 10890—10901
85. Hu, J.; Wang, J.; Nguyen, T. H.; Zheng, N. The chemistry of amine radical cations produced by visible light photoredox catalysis. *Beilstein J. Org. Chem.* **2013**, 9, 1977—2001
86. Picazo, E.; Morrill, L. A.; Susick, R. A.; Moreno, J.; Smith, J. M.; Garg, N. K. Enantioselective Total Syntheses of Methanoquinolizidine Containing Akuammiline Alkaloids and Related Studies. *J Am. Chem. Soc.* **2018**, 140, 6483—6492

87. Schmitz, W. D.; Denhart, D. J.; Brenner, A. B.; Ditta, J. L.; Mattson, R. J.; Mattson, G. K.; Molski, T. F.; Macor, J. E. Homotryptamines as potent and selective serotonin reuptake inhibitors (SSRIs). *Bioorg Med Chem Lett.* **2005,** 15, 1619—1621

88. King, D. H.; Meng, Z.; Mattson, R. J. Macor, J. E. Conformationally Restricted Homotryptamines. Part 7: 3-cis-(3-Aminocyclopentyl)indoles As Potent Selective Serotonin Reuptake Inhibitors. *J. Med. Chem.* **2010**, 53, 7564—7572

89. Yang, D.; Gouaux, E. Illumination of serotonin transporter mechanism and role of the allosteric site. *Science Advances.* **2021**, 7

90. Keinan, E.; Perez, D.; Sahai, M; Shivly, R. Diiodosilane. 2. A multipurpose reagent for hydrolysis and reductive iodination of ketals, acetals, ketones, and aldehydes. *J. Org. Chem.* **1990**, 55, 2927—2938

91. Xu, W.; Dolbier, W. R.; Salazar, J. Ionic Liquid, Surrogate Hydrogen Bromide Reagent for Ring Opening of Cyclopropyl Ketones. *J. Org. Chem.* **2008**, 73, 3535—3538

2.5. Methods

General Information for Chemical Synthesis

All reagents were obtained from commercial sources and reactions were performed using oven-dried glassware (120°C) under an inert N_2 atmosphere unless otherwise noted. Air- and moisture-sensitive liquids and solutions were transferred via syringe or stainless-steel cannula. Organic solutions were concentrated under reduced pressure (~5 Torr) by rotary evaporation. Solvents were purified by passage under 12 psi N_2 through activated alumina columns. Chromatography was performed using Fisher Chemical™ Silica Gel Sorbent (230–400 Mesh, Grade 60). Compounds purified by chromatography were typically applied to the adsorbent bed using the indicated solvent conditions with a minimum amount of added dichloromethane as needed for solubility. Thin layer chromatography (TLC) was performed on Merck silica gel 60 F254 plates (250 μm). Visualization of the developed chromatogram was accomplished by fluorescence quenching or by staining with iodine, butanolic ninhydrin, aqueous potassium permanganate, or aqueous ceric ammonium molybdate (CAM). Irradiation of photochemical reactions was carried out using 2 HIGROW LED Aquarium Light Blub, Wolezek 30W LED Plant Grow Light Bulb with 18x2W 450-460nm.

Nuclear magnetic resonance (NMR) spectra were acquired on either a Bruker 400 operating at 400 and 100 MHz, a Varian 600 operating at 600 and 150 MHz, or a Bruker 600 operating at 600 and 150 MHz for ^{1}H and ^{13}C, respectively, and are referenced internally according to residual solvent signals. Data for ^{1}H NMR are recorded as follows: chemical shift (δ, ppm), multiplicity (s, singlet; d, doublet; t, triplet; q, quartet; quint, quintet; m, multiplet), coupling constant (Hz), and integration. Data for ^{13}C NMR are reported in terms of chemical shift (δ, ppm). High-resolution mass spectra were obtained using a Thermo Fisher Scientific Q-Exactive HF Orbitrap.

Detailed Synthesis Procedures and Experimental Data

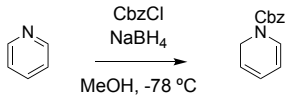

benzyl pyridine-1(2*H*)-carboxylate

A flask was charged with methanol (500 mL, ~0.5M) and pyridine (20.36 mL, 252.84 mmol, 1 equiv.) and cooled to -78 °C after which sodium borohydride (11.47 g, 303.41 mmol, 1.2 equiv.) was added in one portion. Benzyl chloroformate (43.13 mL, 303.41 mmol, 1.2 equiv.) was added dropwise over 1 h to the reaction mixture. The reaction mixture was stirred at -78°C for an additional 3 h after which it was diluted in Et_2O (200 mL), poured into 1M HCl (400 mL) and the layers were separated. The aqueous layer was extracted with Et_2O (2 x 200 mL) and the combined organic extracts were washed with 1M NaOH (100 mL) followed by brine (100 mL). The organic extracts were dried over sodium sulfate, filtered and concentrated under reduced pressure. The residue (54.31 g, 98%) was immediately used without further purification.

Note: Dihydropyridine is prone to oxidation and must be used immediately upon isolation

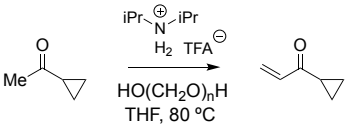

1-cyclopropylprop-2-en-1-one

A Schlenk tube was sequentially charged with THF (100 mL, 0.70M), cyclopropyl methyl ketone (7 mL, 70.65 mmol, 1 equiv.), diisopropylammonium trifluoroacetate (17 g, 78.99, 1.12 equiv.) and paraformaldehyde (5 g, 166.50 mmol, 2.35 equiv.) under a stream of nitrogen. The mixture was stirred and heated at 80 °C for 48 h, after which it was cooled to ambient temperature, diluted with DCM (200 mL) and filtered. The reaction vessel and filter cake were washed with additional

DCM. The filtrate was poured into water (200 mL) and the layers were separated. The aqueous layer was further extracted with DCM (2 x 100 mL) and the combined organic fractions were dried over sodium sulfate, filtered and concentrated under reduced pressure. Purification via chromatography on silica gel (3:2 hexanes/DCM) afforded cyclopropyl enone (5.50 g, 81%) as a light-yellow oil.

Note: Enone **11** is volatile (60°C at 60 torr) and very pungent. Extreme caution should be used when handling.

R_f = 0.35 (2:1 hexanes/DCM)

^{1}H NMR (400 MHz, $CDCl_3$) δ (ppm) = 6.43 (dd, *J* = 17.6, 10.5 Hz, 1H), 6.24 (dd, *J* = 17.6, 1.2 Hz, 1H), 5.77 (dd, *J* = 10.5, 1.2 Hz, 1H), 2.20 – 2.11 (m, 1H), 1.05 (td, *J* = 3.7, 1.0 Hz, 2H), 0.94 – 0.86 (m, 2H)

^{13}C NMR (101 MHz, $CDCl_3$) δ (ppm) = 200.39, 136.57, 127.44, 18.14, 11.12

HRMS (ESI) = *m/z* $[M + H]^+$ calcd. For $C_6H_9O^+$, 97.0658; found, 97.0655

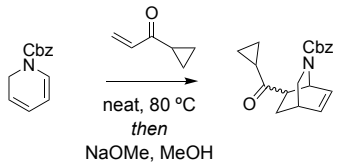

benzyl (1*S*,4*S*)-7-(cyclopropanecarbonyl)-2-azabicyclo[2.2.2]oct-5-ene-2-carboxylate (17)

A Schlenk flask was sequentially charged with compound dihydropyridine (15.50 g, 72.00 mmol, 1 equiv.) and cyclopropyl enone (13.84 g, 144.01 mmol, 2 equiv.). The mixture was cooled to -78 °C after which it was evacuated and refilled with nitrogen 3 times. The mixture was stirred and heated at 80 °C for 72 h. The reaction vessel was cooled to ambient temperature, diluted with methanol (240 mL, 0.3M) and solid sodium methoxide (1.16 g, 21.60 mmol, 0.3 equiv.) was added

in small portions over 5 min. The resulting solution was stirred at ambient temperature for an additional 12 h after which it was concentrated under reduced pressure to remove methanol and any volatiles. The crude residue was diluted in DCM (200 mL), poured into water (100mL) and the layers were separated. The aqueous layer was further extracted with DCM (2 x 100 mL) and the combined organic fractions were dried over sodium sulfate, filtered and concentrated under reduced pressure. The residue was purified via chromatography on silica gel (7:3 hexanes/EtOAc) to afford the product (20.17 g, 90%) as a clear yellow oil. The product was isolated as a 50:50 mixture of exo:endo epimers.

Note: Separation of endo and exo epimers can be achieved by chromatography on silica gel using 10:1 DCM/EtOAc

R_f = 0.42 (7:3 hexanes:EtOAc)

^{1}H NMR (400 MHz, $CDCl_3$) δ (ppm) (rotamers observed) **=** 7.38 – 7.30 (m, 10H), 6.58 – 6.44 (m, 2H), 6.43 – 6.34 (m, 1H), 6.30 – 6.24 (m, 1H), 5.23 (d, *J* = 6.1 Hz, 1H), 5.18 – 5.02 (m, 4H), 4.70 (d, *J* = 5.7 Hz, 1H), 3.38 – 3.25 (m, 3H), 3.05 – 2.71 (m, 5H), 2.27 – 2.16 (m, 1H), 2.14 – 2.02 (m, 1H), 2.03 – 1.81 (m, 2H), 1.77 – 1.67 (1H), 1.48 – 1.41 (m, 1H), 1.06 – 0.81 (m, 8H)

^{13}C NMR (101 MHz, $CDCl_3$) δ (ppm) = 209.36, 208.75, 208.49, 155.26, 154.76, 137.04, 136.85, 136.78, 135.52, 135.35, 134.90, 134.72, 132.28, 131.88, 130.42, 130.15, 128.53, 128.50, 128.43, 128.36, 128.18, 128.09, 127.99,127.84, 127.72, 127.57, 127.49, 66.93, 66.59, 52.49, 52.32, 52.29, 47.91, 47.62, 47.50, 47.19, 47.00, 30.78, 30.55, 30.31, 30.13, 24.28, 23.62, 23.50, 20.05, 19.73, 19.43, 19.27, 12.50, 11.82, 11.50, 11.36, 11.21, 10.86, 10.64

HRMS (ESI) = *m/z* $[M + H]^+$ calcd. For $C_{19}H_{22}NO_3^+$, 312.1598; found, 312.1599

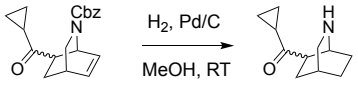

((1*S*,4*R*)-2-azabicyclo[2.2.2]octan-6-yl)(cyclopropyl)methanone

A flask was charged with starting material (10.3 g, 33.07 mmol, 1 equiv.) and unreduced Pd/C (1.03 g, 10 wt%). The flask was evacuated and refilled with nitrogen 3 times. MeOH (330 mL, 0.1M) was added in one portion and hydrogen gas was bubbled through the resulting solution for 1 min. The reaction mixture was stirred at ambient temperature for 1 h after which it was filtered through a pad of celite. The reaction vessel and filter cake were washed with DCM (3 x 50 mL). The filtrate was concentrated under reduced pressure to afford compound the free amine (5.63 g, 95%) as a yellow oil. The epimers were not separated nor characterized individually.

Note: It was observed that prolonged reaction times (>1.5 h) gave an over reduced product with a m/z of 182. We surmise that the cyclopropyl ketone is prone to reduction to the corresponding alcohol.

R_f = 0.10 (10:1 DCM/MeOH, 1% NH_4OH)

^{1}H NMR (400 MHz, $CDCl_3$) δ (ppm) = 3.38 (br. s, 1H), 3.29 – 3.23 (m, 1H), 3.14 (br. s, 1H), 3.08 – 3.01 (m, 2H), 2.99 – 2.96 (m, 2H), 2.95 – 2.84 (m, 3H), 2.26 – 2.20 (m, 1H), 2.12 – 2.08 (m, 1H), 2.05 – 1.95 (m, 3H), 1.93 (ddd, *J* = 7.7, 3.6, 1.7 Hz, 1H), 1.79–1.66 (m, 8H), 1.63 – 1.57 (m, 3H), 1.57 – 1.47 (m, 1H), 1.09 – 0.98 (m, 3H), 0.95 (dd, *J* = 7.4, 4.2 Hz, 1H), 0.92 – 0.82 (m, 4H)

^{13}C NMR (101 MHz, $CDCl_3$) δ (ppm) = 212.75, 210.44, 52.36, 51.28, 47.04, 46.74, 45.70, 45.41, 27.58, 26.71, 25.41, 24.49, 24.44, 24.23, 24.04, 23.52, 19.89, 19.73, 11.23, 10.86, 10.81, 10.67

HRMS (ESI) = *m/z* $[M + H]^+$ calcd. For $C_{11}H_{18}NO^+$, 180.1388; found, 180.1381

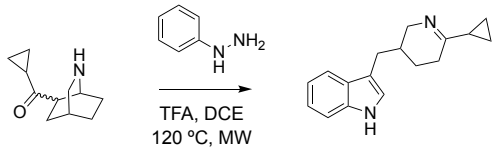

3-((6-cyclopropyl-2,3,4,5-tetrahydropyridin-3-yl)methyl)-1*H*-indole

A microwave vial was charged with a 50:50 ratio of endo:exo epimers of the free amine (200 mg, 1.1 mmol, 1 equiv.) and phenylhydrazine HCl (241 mg, 1.65 mmol, 1 equiv.) and evacuated and refilled with nitrogen 3 times. 1,2-dichloroethane (11 mL, 0.1M) was added in one portion followed by trifluoroacetic acid (0.841 mL, 11 mmol, 10 equiv.) and the resulting solution was heated in a microwave reactor at 120 °C for 12 h. The mixture was quenched with 4M NaOH and the layers were separated. The aqueous layer was further extracted with DCM (2 x 50 mL) and the combined organic fractions were dried over sodium sulfate, filtered and concentrated under reduced pressure. Purification via chromatography on silica gel (10:1 DCM/MeOH) afforded the product (155 mg, 56%) as an orange oil.

R_f = 0.25 (10:1 DCM/MeOH, 1% NH_4OH)

^{1}H NMR (400 MHz, $CDCl_3$) δ (ppm) = 8.28 (s, 1H), 7.57 (dq, *J* = 7.9, 0.9 Hz, 1H), 7.35 (dd, *J* = 8.0, 0.9 Hz, 1H), 7.18 (ddd, *J* = 8.1, 7.0, 1.2 Hz, 1H), 7.10 (ddd, *J* = 8.0, 7.0, 1.1 Hz, 1H), 6.96 (d, *J* = 2.3 Hz, 1H), 3.77 (ddt, *J* = 16.8, 4.4, 2.0 Hz, 1H), 3.15 (ddt, *J* = 16.8, 9.9, 2.5 Hz, 1H), 2.77 (dd, *J* = 14.4, 6.3 Hz, 1H), 2.61 (dd, *J* = 14.4, 7.6 Hz, 1H), 2.26 – 2.15 (m, 1H), 2.15 – 2.00 (m, 1H), 1.96 – 1.77 (m, 1H), 1.55 (ddd, *J* = 13.4, 8.2, 5.0 Hz, 1H), 1.37 – 1.22 (m, 1H), 0.84 – 0.67 (m, 4H)

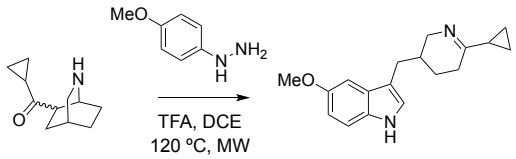

3-((6-cyclopropyl-2,3,4,5-tetrahydropyridin-3-yl)methyl)-5-methoxy-1*H*-indole

A microwave vial was charged with a 50:50 ratio of endo:exo epimers of the free amine (200 mg, 1.1 mmol, 1 equiv.) and phenylhydrazine HCl (290 mg, 1.65 mmol, 1 equiv.) and evacuated and refilled with nitrogen 3 times. 1,2-dichloroethane (11 mL, 0.1M) was added in one portion followed by trifluoroacetic acid (0.841 mL, 11 mmol, 10 equiv.) and the resulting solution was heated in a microwave reactor at 120 °C for 12 h. The mixture was quenched with 4M NaOH and the layers were separated. The aqueous layer was further extracted with DCM (2 x 50 mL) and the combined organic fractions were dried over sodium sulfate, filtered and concentrated under reduced pressure. Purification via chromatography on silica gel (10:1 DCM/MeOH) afforded the product (68 mg, 22%) as an orange oil.

R_f = 0.30 (10:1 DCM/MeOH, 1% NH_4OH)

^{1}H NMR (400 MHz, $CDCl_3$) δ (ppm) = 7.81 (s, 1H), 7.28 (s, 1H), 7.15 (dt, *J* = 1.68, 0.58 Hz, 1H), 7.01(dt, *J* = 8.55, 0.51, 1H), 6.77 (dd, *J* = 8.2, 1.45 Hz, 1H), 3.77 (ddt, *J* = 16.8, 4.4, 2.0 Hz, 1H), 3.65 (s, 3H), 3.15 (ddt, *J* = 16.8, 9.9, 2.5 Hz, 1H), 2.77 (dd, *J* = 14.4, 6.3 Hz, 1H), 2.61 (dd, *J* = 14.4, 7.6 Hz, 1H), 2.26 – 2.15 (m, 1H), 2.15 – 2.00 (m, 1H), 1.96 – 1.77 (m, 1H), 1.55 (ddd, *J* = 13.4, 8.2, 5.0 Hz, 1H), 1.37 – 1.22 (m, 1H), 0.84 – 0.67 (m, 4H)

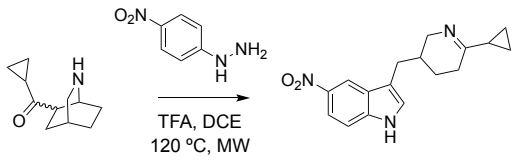

3-((6-cyclopropyl-2,3,4,5-tetrahydropyridin-3-yl)methyl)-5-nitro-1*H*-indole

A microwave vial was charged with a 50:50 ratio of endo:exo epimers of the free amine (200 mg, 1.1 mmol, 1 equiv.) and *para*-nitrophenylhydrazine HCl (315 mg, 1.65 mmol, 1 equiv.) and evacuated and refilled with nitrogen 3 times. 1,2-dichloroethane (11 mL, 0.1M) was added in one portion followed by trifluoroacetic acid (0.841 mL, 11 mmol, 10 equiv.) and the resulting solution was heated in a microwave reactor at 120 °C for 12 h. The mixture was quenched with 4M NaOH and the layers were separated. The aqueous layer was further extracted with DCM (2 x 50 mL) and the combined organic fractions were dried over sodium sulfate, filtered and concentrated under reduced pressure. Purification via chromatography on silica gel (10:1 DCM/MeOH) afforded the product (258 mg, 56%) as a red oil.

R_f = 0.20 (10:1 DCM/MeOH, 1% NH_4OH)

^{1}H NMR (400 MHz, $CDCl_3$) δ (ppm) = 8.66 (s, 1H), 7.91 (s, 1H), 7.69 (dt, *J* = 1.68, 0.51 Hz, 1H), 7.54 (dt, *J* = 8.55, 0.44, 1H), 6.77 (dd, *J* = 8.2, 1.45 Hz, 1H), 3.77 (ddt, *J* = 16.8, 4.4, 2.0 Hz, 1H), 3.15 (ddt, *J* = 16.8, 9.9, 2.5 Hz, 1H), 2.77 (dd, *J* = 14.4, 6.3 Hz, 1H), 2.61 (dd, *J* = 14.4, 7.6 Hz, 1H), 2.26 – 2.15 (m, 1H), 2.15 – 2.00 (m, 1H), 1.96 – 1.77 (m, 1H), 1.55 (ddd, *J* = 13.4, 8.2, 5.0 Hz, 1H), 1.37 – 1.22 (m, 1H), 0.84 – 0.67 (m, 4H)

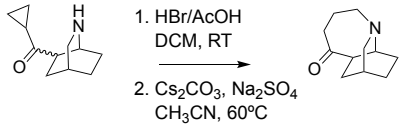

octahydro-3,10-methanopyrido[1,2-*a*]azepin-9(6*H*)-one

To a stirring solution of the free amine (5.63 g, 31.42 mmol, 1 equiv.) in DCM (31 mL, 1.0M) was added 33 wt% HBr/AcOH (16.27 mL, 94.27 mmol, 3 equiv.) in one portion. The solution was stirred at ambient temperature for 2 h after which it was concentrated under reduced pressure. The residue was dried under high vacuum for 1 h and then stirred vigorously in diethyl ether (50 mL). The diethyl ether was decanted and the residue was dried under high vacuum. The alkyl bromide was used isolated as an orange foam and was used in the next reaction without any further purification or characterization.

A flask was charged with compound alkyl bromide (10.71 g, 31.41 mmol, 1 equiv.), anhydrous Cs_2CO_3 (15.35 g, 47.13 mmol, 1.5 equiv.), and anhydrous Na_2SO_3 (13.38 g, 94.26 mmol, 3 equiv.). The flask was evacuated and refilled with nitrogen 3 times after which anhydrous CH_3CN (314 mL, 0.1M) was added in one portion. The reaction mixture was heated to 60 °C and stirred for 6 h. The heterogeneous mixture was cooled to ambient temperature and filtered. The reaction vessel and filter cake were washed with DCM. The filtrate was concentrated under reduced pressure and the residue was purified via chromatography on silica gel (20:1 DCM/MeOH) to afford the product (2.31 g, 41% over 2 steps) as a light brown oil.

R_f = 0.40 (10:1 DCM/MeOH)

^{1}H NMR (400 MHz, $CDCl_3$) δ (ppm) = 3.20 – 3.17 (m, 1H), 3.10 – 2.98 (m, 2H), 2.92 (dd, J = 9.6, 4.1 Hz, 1H), 2.88 – 2.81 (m, 1H), 2.59 (d, J = 9.7 Hz, 1H), 2.54 (dd, J = 12.5, 6.8 Hz, 1H), 2.49 (d, J = 12.5 Hz, 1H), 2.07 – 1.93 (m, 3H), 1.93 – 1.84 (m, 1H), 1.80 – 1.76 (m, 1H), 1.74 – 1.65 (m, 1H), 1.61 – 1.47 (m, 3H).

^{13}C NMR (101 MHz, $CDCl_3$) δ (ppm) = 216.49, 54.40, 51.61, 50.56, 50.37, 43.50, 29.56, 28.47, 25.82, 23.74, 20.80

HRMS (ESI) = *m/z* $[M + H]^+$ calcd. For $C_{11}H_{18}NO^+$, 180.1388; found, 180.1384

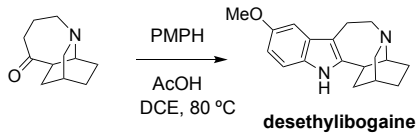

desethylibogaine

Desethylibogaine

A flask was charged with tetrahydroazepinone (1.25 g, 6.97 mmol, 1 equiv.) and para-methoxyphenylhydrazine HCl (1.82 g, 10.45 mmol, 1.5 equiv.). The flask was evacuated and refilled with nitrogen 3 times after which anhydrous DCE (69.70 mL, 0.1M) and AcOH (5.98 mL, 104.59 mmol, 15 equiv.) was added. The resulting mixture was degassed by bubbling nitrogen through the solution for 10 mins. The flask was heated to 80 °C and stirred for 12 h after which it was cooled to ambient temperature and diluted with DCM (30 mL). Saturated aq. $NaHCO_3$ was added to the reaction mixture until the pH was adjusted to 7-8. The organic layer was separated, and the aqueous layer was further extracted with DCM (2 x 50 mL). The combined organic fractions were dried over sodium sulfate, filtered and concentrated under reduced pressure. Purification via chromatography on silica gel (gradient elution 20:1→10:1 DCM/MeOH, 0.25% NH_4OH) afforded **desethylibogaine** (1.65 g, 84%) as a yellow foam.

R_f = 0.38 (10:1 DCM/MeOH)

^{1}H NMR (400 MHz, $CDCl_3$) δ (ppm) = 7.61 (s, 1H), 7.14 (d, *J* = 8.6 Hz, 1H), 6.93 (s, 1H), 6.77 (d, *J* = 9.9 Hz, 1H), 3.86 (s, 3H), 3.42 – 3.33 (m, 1H), 3.32 – 3.19 (m, 3H), 3.17–3.09 (m, 2H), 2.98 (dd, *J* = 11.8, 4.7 Hz, 1H), 2.73–2.65 (m, 1H), 2.19 – 2.08 (m, 2H), 1.95 – 1.88 (m, 1H), 1.82 – 1.57 (m, 4H)

^{13}C NMR (101 MHz, $CDCl_3$) δ (ppm) = 154.22, 142.34, 129.90, 129.75, 111.17, 111.13, 109.05, 100.33, 56.15, 54.48, 54.25, 50.18, 39.23, 34.58, 29.16, 25.32, 23.41, 20.05

HRMS (ESI) = *m/z* $[M + H]^+$ calcd. For $C_{18}H_{23}N_2O^+$, 283.1808; found, 283.1815

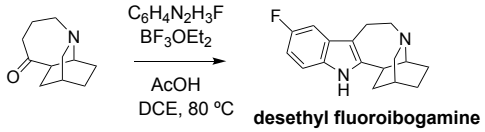

desethyl fluoroibogamine

Desethyl-fluoroibogamine

A flask was charged with tetrahydroazepinone (1.25 g, 6.97 mmol, 1 equiv.) and para-fluorophenylhydrazine HCl (1.69 g, 10.45 mmol, 1.5 equiv.). The flask was evacuated and refilled with nitrogen 3 times after which anhydrous DCE (69.70 mL, 0.1M) and AcOH (5.98 mL, 104.59 mmol, 15 equiv.) was added. The resulting mixture was degassed by bubbling nitrogen through the solution for 10 mins. The flask was heated to 80 °C and stirred for 12 h after which it was cooled to ambient temperature and diluted with DCM (30 mL). Saturated aq. $NaHCO_3$ was added to the reaction mixture until the pH was adjusted to 7-8. The organic layer was separated, and the aqueous layer was further extracted with DCM (2 x 50 mL). The combined organic fractions were dried over sodium sulfate, filtered and concentrated under reduced pressure. Purification via chromatography on silica gel (gradient elution 20:1→10:1 DCM/MeOH, 0.25% NH_4OH) afforded **desethyl-fluoroibogamine** (1.65 g, 88%) as an orange foam.

R_f = 0.11 (10:1 DCM/MeOH)

^{1}H NMR (400 MHz, $CDCl_3$) δ (ppm) = 7.87 (s, 1H), 7.14 (ddd, *J* = 14.3, 9.3, 3.4 Hz, 3H), 6.86 (ddd, *J* = 9.3, 8.7, 2.5 Hz, 1H), 3.41 – 2.89 (m, 10H), 2.66 – 2.48 (m, 1H), 2.21 – 1.98 (m, 3H), 1.91 (p, *J* = 2.9 Hz, 1H)

^{13}C NMR (101 MHz, $CDCl_3$) δ (ppm) = 159.43, 156.34, 143.87, 143.72, 130.96, 130.16, 130.03, 110.74, 110.61, 109.73, 109.67, 109.11, 108.76, 103.06, 102.75, 54.04, 53.76, 50.03, 40.07, 40.02, 34.70, 29.88, 29.72, 25.54, 23.64, 20.18

Chapter 3 – Synthesis of Epiibogaine

3.1 Challenges with Translating Model System Towards Construction of Ibogaine

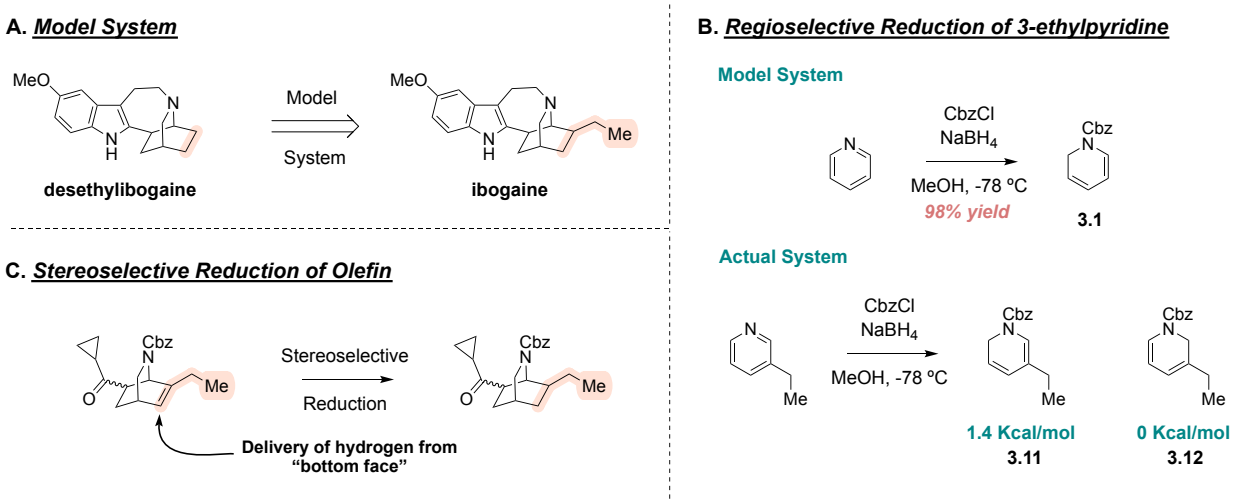

Figure 3.1. (A) Desethylibogaine as a model system for construction of ibogaine **(B)** Reduction of 3-ethylpyridine to 1,3-dihydropyridine **(C)** Stereoselective reduction of ethylated isoquinuclidine

Having devised an efficient synthetic strategy to the iboga framework, we were tasked with translating our model system to the construction of ibogaine (**Figure 3.1A**). Two considerable challenges were faced when developing a route to ibogaine: a regioselective reduction of 3-ethylpyridine to dihydropyridine **3.11** (**Figure 3.1B**) and a stereoselective reduction of the Diels-Alder adduct to afford the ethyl group in the exo orientation (**Figure 3.1C**).

Unlike our model system, the actual system employs an unsymmetrical pyridine to yield two 1,3-dhydropyridine regioisomers (**Figure 3.1B**).[92] Evaluation of the ground state thermodynamic energies of the two isomers reveals that undesired dihydropyridine **3.12** is 1.4 kcal/mol lower in energy than dihydropyridine **3.11**. We hypothesize that this may be due to the slightly increased "push-pull" interactions between the ethyl group and nitrogen in **3.11**. Reduction using the conditions developed in our model system afforded undesired dihydropyridine **3.12** as the predominant regioisomer (**Entry 3, Table 3.1**). Other sodium-based hydride reductants

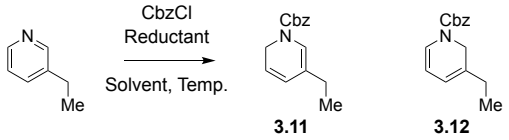

3.11 **3.12**

Entry	Reductant	Solvent	Temp	**3.11**	**3.12**
1	$NaBH_4$ (0.9 equiv.)	ROH[a]	-78 °C to RT	<10%	>90%
2	$NaBH_4$ (1.1 equiv.)	ROH[a]	-78 °C to RT	<10%	>90%
3	$NaBH_4$ (1.5 equiv.)	ROH[a]	-78 °C to RT	<10%	>90%
4	$NaBH_4$ (2.0 equiv.)	ROH[a]	-78 °C to RT	<10%	>90%
5	$NaBH_4$ (1.5 equiv.)	THF	-78 °C to RT	<10%	>90%
6	$NaBH(Et)_3$ (1.5 equiv.)	THF	-78 °C to RT	N.R	N.R
7	$NaBH(OAc)_3$ (1.5 equiv.)	THF	-78 °C	10%	90%
8	$LiBH_4$ (0.9 equiv.)	THF	-78 °C	35%	65%
9	$LiBH_4$ (1.1 equiv.)	THF	-78 °C	50%	50%
10	$LiBH_4$ (1.5 equiv.)	THF	-78 °C	60%	40%
11	$LiBH_4$ (1.5 equiv.)	ROH[a]	-78 °C	25%	75%
12	DIBAL- H (1.1 equiv.)	THF	-78 °C to RT	N.R	N.R

Table 3.1. Product distribution determined by LCMS. All reactions run at 0.1M.

[a] Both methanol and ethanol were screened

such as sodium triethylborohydride and sodium triacetoxyborohydride produced similar results irrespective of solvent or temperature (**Entry 6 and 7, Table 3.1**). It was hypothesized that substituting the sodium counterion may favor a kinetic pathway for the pyridine reduction.[93,94] Reduction with 1.5 equivalents of lithium borohydride ($LiBH_4$) in THF produced the most favorable ratio for dihydropyridine formation (**Entry 10, Table 3.1**). As expected, a sub-stoichiometric amount of $LiBH_4$ led to a more thermodynamic product distribution with dihydropyridine **3.12** being favored (**Entry 8, Table 3.1**). Alcoholic solvents negatively affected product distribution likely due to the reduced lithium counterion influence in polar protic solvents (**Entry 11, Table 3.1**).

Unsatisfied with only 60% conversion to dihydropyridine **3.11**, we sought to circumvent regioselectivity issues by preparing our diene from an elimination of dihalide **3.14 (Figure 3.2A)**. In this scenario, our elimination would produce only the desired diene needed for our Diels-Alder

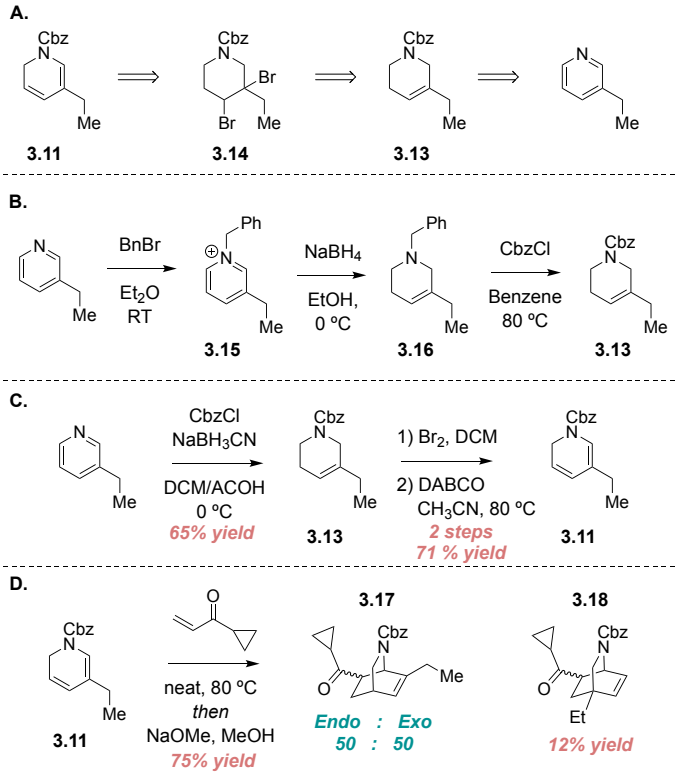

Figure 3.2. (A) Alternative approach to preparing dihydropyridine **3.11 (B)** Previous methods to prepare tetrahydropyridine **3.13 (C)** Efforts towards **3.11 (D)** Synthesis of isoquinuclidine **3.17**

cycloaddition. Dihalide **3.14** can be synthesized from a standard bromination of tetrahydropyridine **3.13**, which could be obtained from a direct reduction of 3-ethylpyridine.

Previously utilized methods to prepare tetrahydropyridine **3.13** have involved a three-step protocol[95] via formation of alkyl pyridinium **3.15** and alkyl tetrahydropyridine **3.16** (**Figure 3.2B**). An intermediary alkyl pyridinium is used because an acylated pyridinium is generally too withdrawn to tautomerize at the dihydropyridine stage for further reduction.[96] We hypothesized that an acidic medium would facilitate tautomerization of a Cbz- acylated pyridinium to generate tetrahydropyridine **3.13** in one step from 3-ethylpyridine (**Figure 3.2C**). To our delight, reduction of 3-ethylpyridine with sodium cyanoborohydride ($NaBH_3CN$) in DCM and acetic acid proceeded smoothly to furnish **3.13** in 65% yield. Subsequent bromination and dehydrohalogenation afforded dihydropyridine **3.11** in 71% yield over two steps. Dihydropyridine **3.11** was susceptible to

isomerization with excess base or prolonged reaction times. Mixing dihydropyridine **3.11** with cyclopropyl enone in a sealed vessel followed by treatment with sodium methoxide produced isoquinuclidine **3.17** in a 50:50 ratio of endo- and exo- epimers (**Figure 3.2D**). We did notice minimal dihydropyridine isomerization in the reaction mixture and isomerized Diels-Alder adduct **3.18** was isolated in 12% yield.[97]

3.3 Olefin Reduction Approach to Epiibogaine

Having prepared isoquinuclidine **3.17**, we were now tasked with the challenge of developing a stereoselective reduction to afford our C20 ethyl group in the exo- orientation. Taking inspiration from our model system, we conducted a standard hydrogenation of intermediate **3.17** and observed full endo selectivity to free amine **3.19** (**Figure 3.3A**). Unfortunately, addition of palladium hydride proceeded from the "top-face" of our isoquinuclidine to orient the C20 ethyl group in the endo position. It was clear that our Pd-H mediated hydrogenation proceeded via kinetic pathway[98] and we sought to reduce our olefin using thermodynamic conditions. A cationic reduction[99,100] using triethylsilane (Et_3SiH) and trifluoroacetic acid (TFA) was performed to give a

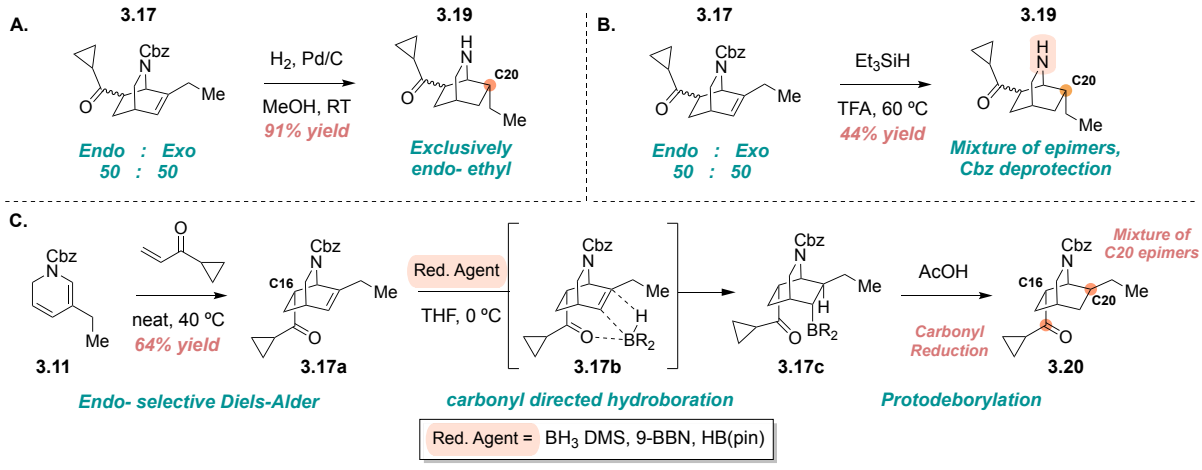

Figure 3.3. (A) Hydrogenation of **3.17 (B)** Cationic reduction of **3.17 (C)** Carbonyl directed hydroboration-protodeborylation strategy

mixture of C20 epimers and concomitant carbamate deprotection in 44% yield (**Figure 3.3B**). Unfortunately, even a reduction involving the generation of a cation intermediate produced the same selectivity as our Pd/C hydrogenation.

It was hypothesized that we could use the C16 cyclopropyl ketone as a directing group for endo- functionalization of our olefin. We envisioned a carbonyl directed hydroboration[101,102] of intermediate **3.17a** to afford alkyl boronate **3.17c** (**Figure 3.3C**). Carbonyl directed syn addition of B-H across our alkene would force the C20 ethyl group into the exo- orientation and a subsequent protodeborylation[103] using acetic acid (AcOH) should furnish product **3.20** in 2 steps from **3.17a**. We sought to take advantage of the inherent endo selectivity in our Diels-Alder reaction by avoiding epimerization of **3.17a.** When subjecting endo- **3.17a** to hydroboration-protodeborylation conditions, we noticed yet again a mixture of epimers for the C20 ethyl group. Furthermore, we also observed significant carbonyl reduction to the corresponding cyclopropyl alcohol and it was clear that this strategy was not useful for our total synthesis.

We elected to continue with intermediate **3.19** (**Figure 3.4**) albeit the incorrect stereochemistry at C20. Ring opening was conducted with HBr/AcOH to furnish the corresponding alkyl bromide which was then subjected to a base mediated ring closure with cesium carbonate

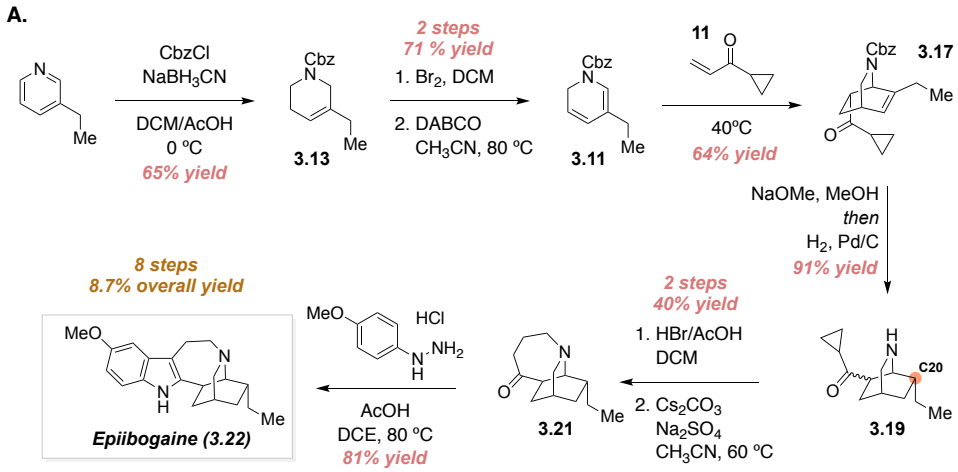

Figure 3.4. Synthesis of epiibogaine (**3.22**)

in acetonitrile to afford tetrahydroazapinone **3.21** in 40% yield over two steps. A Fischer indole cyclization with *para*-methoxyphenylhydrazine produced epiibogaine in 81% yield. Though this is one the most efficient syntheses of epiibogaine to date[104], a route towards the construction of ibogaine still remained.

REFERENCES

92. Büchi, G.; Coffen, D. L.; Kocsis, K.; Sonnet, P. E.; Ziegler, F. E. The Total Synthesis of Iboga Alkaloids. *J. Am. Chem. Soc.* **1966**, 88, 3099—3109
93. Zhang, W.; Zhang, X.; Huang, Z.; Li, H.; Gao, M.; Pan, H.; Liu, Y. Recent Development of Lithium Borohydride-Based Materials for Hydrogen Storage. *Adv. Energy Sustainability Res.* **2021**, 2, 2100073
94. Brown, H. C.; Choi, Y. M.; Narasimham, S. Addition Compounds of Alkali Metal Hydrides. 22. Convenient Procedures for the Preparation of Lithium Borohydride from Sodium Borohydride and Borane-Dimethyl Sulfide in Simple Ether Solvents. *Inorg. Chem.* **1982**, 21, 3657—3661
95. Redding, M. T.; Fukuyama, T. Stereocontrolled Total Synthesis of (±)-Catharanthine via Radical-Mediated Indole Formation. *Org. Lett.* **1999**, 1, 973—976
96. Comins, D. L.; Abdullah, A. H. Synthesis of 1- Acyl-1,4-dihydropyridines via Copper Hydride Reduction of 1-Acylpyridinium Salts. *J. Org. Chem.* **1984**, 49, 3392—3394
97. Hatano, M.; Goto, Y.; Izumiseki, A.; Akakura, M.; Ishihara, K. Boron Tribromide-Assisted Chiral Phosphoric Acid Catalyst for a Highly Enantioselective Diels–Alder Reaction of 1,2-Dihydropyridines. *J. Am. Chem. Soc.* **2015**, 137, 13472—13475
98. Barton, D. H. R.; Robinson, C. H. The Stereospecificity of Carbanion Reduction Processes. *J. Chem. Soc.*, **1954**, 3045—3051
99. Kursanov, D. N.; Parnes, Z. N.; Bolestova, G. I. Dokl. Akad. Nauk. *USSR Chem. (Engl. Transl.)* **1968**, 181, 726
100. Takano, S.; Moriya, M.; Ogasawara, K. *Tetrahedron Lett.* **1992**, 33, 1909.
101. Evans, D. A.; Fu, G. C.; Hoveyda, A. H. Rhodium(I)- and Iridium(I)-Catalyzed Hydroboration Reactions: Scope and Synthetic Applications. *J. Am. Chem. Soc.* **1992**, 114, 6671—6679
102. Hoang, G. L.; Yang, Z.; Smith, S. M.; Pal, R.; Miska, J. L.; Takacs, J. M. Enantioselective Desymmetrization via Carbonyl-Directed Catalytic Asymmetric Hydroboration and Suzuki–Miyaura Cross-Coupling. *Org. Lett.* **2015**, 17, 940—943
103. Zhang, G.; Li, Y.; Liu, J. Acid-promoted metal-free protodeboronation of arylboronic acids. *RSC Adv.* **2017**, 7, 34959—34962

104. Yu, P.; Karmakar, A.; Sabbers, W. A.; Shajan, F.; Andrade, R. B. Asymmetric Total Synthesis of (+)-Epiibogamine Enabled by Three-Component Domino Michael/Michael/Mannich Annulation of N-Sulfinyl Metallosilylenamines. *Org. Lett.* **2023**, 25, 956—960

3.4 Methods

General Information for Chemical Synthesis

All reagents were obtained from commercial sources and reactions were performed using oven-dried glassware (120°C) under an inert N_2 atmosphere unless otherwise noted. Air- and moisture-sensitive liquids and solutions were transferred via syringe or stainless-steel cannula. Organic solutions were concentrated under reduced pressure (~5 Torr) by rotary evaporation. Solvents were purified by passage under 12 psi N_2 through activated alumina columns. Chromatography was performed using Fisher Chemical™ Silica Gel Sorbent (230–400 Mesh, Grade 60). Compounds purified by chromatography were typically applied to the adsorbent bed using the indicated solvent conditions with a minimum amount of added dichloromethane as needed for solubility. Thin layer chromatography (TLC) was performed on Merck silica gel 60 F254 plates (250 μm). Visualization of the developed chromatogram was accomplished by fluorescence quenching or by staining with iodine, butanolic ninhydrin, aqueous potassium permanganate, or aqueous ceric ammonium molybdate (CAM). Irradiation of photochemical reactions was carried out using 2 HIGROW LED Aquarium Light Blub, Wolezek 30W LED Plant Grow Light Bulb with 18x2W 450-460nm.

Nuclear magnetic resonance (NMR) spectra were acquired on either a Bruker 400 operating at 400 and 100 MHz, a Varian 600 operating at 600 and 150 MHz, or a Bruker 600 operating at 600 and 150 MHz for ^{1}H and ^{13}C, respectively, and are referenced internally according to residual solvent signals. Data for ^{1}H NMR are recorded as follows: chemical shift (δ, ppm), multiplicity (s, singlet; d, doublet; t, triplet; q, quartet; quint, quintet; m, multiplet), coupling constant (Hz), and integration. Data for ^{13}C NMR are reported in terms of chemical shift (δ, ppm). High-resolution mass spectra were obtained using a Thermo Fisher Scientific Q-Exactive HF Orbitrap.

Detailed Synthesis Procedures and Experimental Data

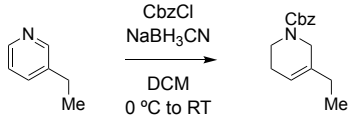

benzyl 5-ethyl-3,6-dihydropyridine-1(2*H*)-carboxylate

A stirred solution of 3-ethylpyridine (10.48 mL, 93.40 mmol, 1 equiv.) in DCM/AcOH (374 mL/187 mL, 0.166M) was cooled to 0 °C and solid sodium cyanoborohydride (14.67 g, 233 mmol, 2.5 equiv.) was added in one portion. Benzyl chloroformate (17.26 mL, 121 mmol, 1.3 equiv.) was added dropwise over 15 mins and the reaction mixture was slowly warmed to ambient temperature over the course of 16 h. The reaction mixture was quenched by the addition of aqueous saturated $NaHCO_3$ (150 mL) and the organic layers were separated. The aqueous layer was extracted further with DCM (2 x 200 mL) and the combined organic fractions were dried over sodium sulfate, filtered and concentrated under reduced pressure. Purification via chromatography on silica gel (20:1 hexanes/ethyl acetate) afforded the product (14.89 g, 65%) as a colorless oil.

R_f = 0.65 (7:3 hexanes/EtOAc)

^{1}H NMR (400 MHz, $CDCl_3$) δ (ppm) (rotamers observed) **=** 7.40 – 7.28 (m, 5H), 5.53 (s, 1H), 5.16 (s, 2H), 3.89 – 3.81 (m, 2H), 3.52 (t, *J* = 5.74 Hz, 2H), 2.12 (s, 2H), 1.98 (s, 2H), 1.03 (t, *J* = 7.4 Hz, 3H)

^{13}C NMR (101 MHz, $CDCl_3$) δ (ppm) = 136.97, 128.49, 128.46, 127.95, 127.90, 118.11, 117.68, 66.97, 49.75, 46.00, 44.76, 40.74, 40.47, 30.59, 27.38, 24.99, 24.65, 12.19, 11.29

HRMS (ESI) = *m/z* $[M + H]^+$ calcd. for $C_{15}H_{20}NO_2^+$, 246.1498; found, 246.1490

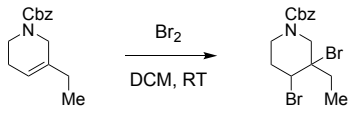

benzyl 3,4-dibromo-3-ethylpiperidine-1-carboxylate

Dibromo compound was synthesized using a referenced procedure. Compound S-1 (9.85 g, 96%) was isolated as a clear oil that crystallized into a white solid upon standing. Spectral data matches that reported in the literature.

R_f = 0.45 (7:3 hexanes/EtOAc)

^{1}H NMR (400 MHz, $CDCl_3$) δ (ppm) (rotamers observed) **=** 7.41 – 7.28 (m, 5H), 5.20 – 5.08 (m, 2H), 4.63 – 4.59 (s, 1H), 4.31 – 3.97 (m, 2H) 3.52 – 3.25 (m, 2H), 2.85 – 2.70 (m, 1H), 2.08 – 1.80 (m, 3H), 1.19 – 1.07 (m, 3H)

^{13}C NMR (101 MHz, $CDCl_3$) δ (ppm) = 155.42, 155.28, 137.19, 136.67, 128.58, 128.54, 128.15, 128.05, 127.95, 127.85, 71.54, 67.53, 66.96, 55.99, 50.96, 50.59, 49.83, 44.84, 39.52, 39.37, 33.83, 31.52, 31.19, 30.67, 11.38, 8.67

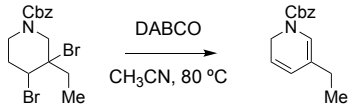

benzyl 5-ethylpyridine-1(2*H*)-carboxylate

A 2-neck flask was charged with dibromo starting material (8.50 g, 20.98 mmol, 1 equiv.) and anhydrous DABCO (8.14 g, 72.59 mmol, 3.46 equiv.). The flask was evacuated and refilled with nitrogen 3 times after which anhydrous acetonitrile (159 mL, 0.132M) was added. The resulting solution was stirred and heated at reflux for 3 h after which the reaction was allowed to cool to ambient temperature and filtered. The reaction vessel and filter cake were washed with DCM (2 x 50 mL) and the filtrate was concentrated under reduced pressure to remove excess acetonitrile.

The resulting residue was diluted in DCM (75 mL) and extracted with brine (3 x 50 mL). The organic fractions were dried over sodium sulfate, filtered and concentrated under reduced pressure. The residue (3.77 g, 74%) was used immediately in the Diels-Alder reaction without further purification.

Note: DABCO was recrystallized and dried prior to use. The dihydropyridine is prone to isomerization and the rigorous omission of water is critical to maintaining reproducibility. Prolonged reaction times can also result in isomerization to the undesired diene. It is advised to monitor the reaction via TLC and LCMS.

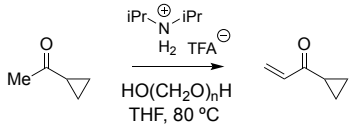

1-cyclopropylprop-2-en-1-one

A Schlenk tube was sequentially charged with THF (100 mL, 0.70M), cyclopropyl methyl ketone (7 mL, 70.65 mmol, 1 equiv.), diisopropylammonium trifluoroacetate (17 g, 78.99, 1.12 equiv.) and paraformaldehyde (5 g, 166.50 mmol, 2.35 equiv.) under a stream of nitrogen. The mixture was stirred and heated at 80 °C for 48 h, after which it was cooled to ambient temperature, diluted with DCM (200 mL) and filtered. The reaction vessel and filter cake were washed with additional DCM. The filtrate was poured into water (200 mL) and the layers were separated. The aqueous layer was further extracted with DCM (2 x 100 mL) and the combined organic fractions were dried over sodium sulfate, filtered and concentrated under reduced pressure. Purification via chromatography on silica gel (3:2 hexanes/DCM) afforded cyclopropyl enone (5.50 g, 81%) as a light yellow oil.

Note: Enone **11** is volatile (60°C at 60 torr) and very pungent. Extreme caution should be used when handling.

R_f = 0.35 (2:1 hexanes/DCM)

^{1}H NMR (400 MHz, $CDCl_3$) δ (ppm) = 6.43 (dd, *J* = 17.6, 10.5 Hz, 1H), 6.24 (dd, *J* = 17.6, 1.2 Hz, 1H), 5.77 (dd, *J* = 10.5, 1.2 Hz, 1H), 2.20 – 2.11 (m, 1H), 1.05 (td, *J* = 3.7, 1.0 Hz, 2H), 0.94 – 0.86 (m, 2H)

^{13}C NMR (101 MHz, $CDCl_3$) δ (ppm) = 200.39, 136.57, 127.44, 18.14, 11.12

HRMS (ESI) = *m/z* $[M + H]^+$ calcd. For $C_6H_9O^+$, 97.0658; found, 97.0655

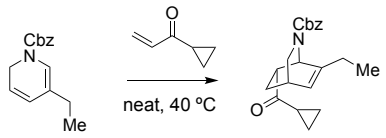

Benzyl(1*R*,4*S*,7*R*)-7-(cyclopropanecarbonyl)-6-ethyl-2-azabicyclo[2.2.2]oct-5-ene-2-carboxylate

A Schlenk flask was sequentially charged with dihydropyridine (3.77 g, 15.51 mmol, 1 equiv.) and cyclopropyl enone (2.98 g, 31.02 mmol, 2 equiv.). The mixture was cooled to -78 C after which it was evacuated and refilled with nitrogen 3 times. The mixture was stirred and heated at 40 °C for 72 h. The reaction mixture was directly loaded onto silica gel and purified via flash column chromatography (gradient elution 10:1→7:3 hexanes/EtOAc) to afford the product (3.03 g, 64%) as clear yellow oil.

Note: Purification is easiest when performed using “dry-load” method.

R_f = 0.40 (7:3 hexanes/ethyl acetate)

^{1}H NMR (400 MHz, $CDCl_3$) δ (ppm) (rotamers observed) **=** 7.40 – 7.27 (m, 11H), 6.00 – 5.96 (m, 1H), 5.96 – 5.91 (m, 1H), 5.20 – 4.99 (m, 6H), 4.95 – 4.88 (d, *J* = 9.05 Hz, 1H), 3.41 – 3.20 (m, 3H), 3.02 – 2.90 (m, 2H), 2.88 – 2.65 (m, 3H), 2.32 – 2.01 (m, 7H), 1.98 – 1.79 (m, 3H), 1.71 – 1.59 (m, 2H), 1.46 – 1.32 (m, 1H), 1.14 – 1.02 (m, 4H), 1.01 – 0.79 (m, 11H)

^{13}C NMR (101 MHz, $CDCl_3$) δ (ppm) = 209.63, 209.09, 208.95, 208.58, 155.30, 147.44, 146.92, 144.93, 137.24, 137.02, 128.68, 128.62, 128.59, 128.54, 128.45, 128.11, 128.05, 127.98, 127.94, 127.80, 127.76, 127.64, 127.10, 125.75, 125.55, 125.20, 125.14, 67.05, 67.00, 66.97, 66.66, 52.60, 52.51, 52.40, 51.87, 51.45, 51.20, 51.17, 48.36, 48.02, 47.91, 47.77, 30.77, 30.51, 30.00, 26.74, 26.48, 26.39, 25.05, 24.96, 24.85, 20.15, 19.76, 19.60, 19.32, 12.56, 11.89, 11.88, 11.72, 11.61, 11.50, 11.41, 11.33, 11.23

HRMS (ESI) = *m/z* $[M + Na]^+$ calcd. for $C_{21}H_{25}NO_3Na^+$, 362.1728; found, 362.1722

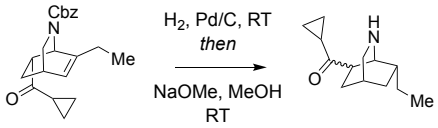

cyclopropyl((1*S*,4*R*,7*R*)-7-ethyl-2-azabicyclo[2.2.2]octan-6-yl)methanone

A flask was charged with the starting material (2.95 g, 8.69 mmol, 1 equiv.) and solid sodium methoxide (141 mg, 2.60 mmol, 0.3 equiv.). The flask was evacuated and refilled with nitrogen 3 times after which MeOH (87 mL, 0.1M) was added in one portion. The resulting solution was stirred at ambient temperature for 12 h after which it was uncapped and unreduced Pd/C (295 mg, 10 wt%) was added under a stream of nitrogen. Hydrogen gas was bubbled through the resulting solution for 1 min and the reaction mixture was stirred at ambient temperature for 6 h. The heterogeneous reaction mixture was filtered through a pad of celite and the reaction vessel and filter cake were washed with DCM (2 x 50 mL). The filtrate was concentrated under reduced pressure and purified via chromatography on silica gel (10:1 DCM:MeOH, 1% NH_4OH) to afford

compound **13** (1.64 g, 91%) as a yellow oil. The epimers were not separated nor characterized individually.

Note: It was noticed that using reduced Pd/C gave irreproducible results for carbamate removal.

R_f = 0.1(10:1 DCM/MeOH)

^{1}H NMR (400 MHz, $CDCl_3$) δ (ppm) = 3.09 – 3.01 (m, 1H), 2.97 (s, 1H), 2.88 – 2.77 (m, 2H), 2.05 – 2.00 (m, 1H), 1.99 – 1.82 (m, 2H), 1.70 (s, 1H), 1.66 – 1.53 (m, 2H), 1.40 (tt, *J* = 13.5, 6.7 Hz, 3H), 1.06 – 0.99 (m, 3H), 0.99 – 0.91 (m, 3H), 0.91 – 0.78 (m, 3H)

^{13}C NMR (101 MHz, $CDCl_3$) δ (ppm) = 212.53, 201.21, 49.20, 47.06, 46.99, 45.98, 45.79, 40.31, 38.53, 36.06, 32.10, 30.02, 27.98, 27.71, 26.65, 24.88, 19.69, 19.62, 15.55, 12.11, 11.79, 11.04, 10.86, 10.82, 10.75, 10.68

HRMS (ESI) = *m/z* $[M + H]^+$ calcd. for $C_{13}H_{22}NO^+$, 208.1698; found, 208.1699

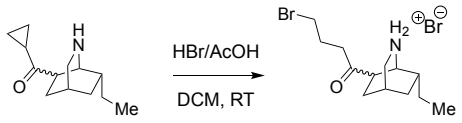

(1*S*,4*R*,7*R*)-6-(4-bromobutanoyl)-7-ethyl-2-azabicyclo[2.2.2]octan-2-ium bromide

To a stirring solution of the starting material (1.25 g, 6.03 mmol, 1 equiv.) in DCM (6.03 mL, 1.0M) was added 33 wt% HBr/AcOH (3.12 mL, 18.08 mmol, 3 equiv.) in one portion. The solution was stirred at ambient temperature for 2 h after which it was concentrated under reduced pressure. The residue was dried under high vacuum for 1 h and then stirred vigorously in diethyl ether (30 mL). The diethyl ether was decanted and the residue was dried under high vacuum. The product (2.18 g, 98%) was used isolated as an orange foam and was used in the next reaction without any further purification or characterization.

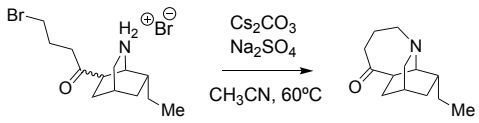

1-ethyloctahydro-3,10-methanopyrido[1,2-*a*]azepin-9(6*H*)-one

A flask was charged with the alkyl bromide (2.18 g, 5.90 mmol, 1 equiv.), anhydrous Cs_2CO_3 (2.88 g, 8.85 mmol, 1.5 equiv.), and anhydrous Na_2SO_3 (2.52 g, 17.71 mmol, 3 equiv.). The flask was evacuated and refilled with nitrogen 3 times after which anhydrous CH_3CN (59 mL, 0.1M) was added in one portion. The reaction mixture was heated to 60 °C and stirred for 6 h. The heterogeneous mixture was cooled to ambient temperature and filtered. The reaction vessel and filter cake were washed with DCM (2 x 30 mL). The filtrate was concentrated under reduced pressure and the residue was purified via chromatography on silica gel (20:1 DCM/MeOH) to afford the product (499 mg, 41%) as a light brown oil.

R_f = 0.43 (20:1 DCM/MeOH)

^{1}H NMR (400 MHz, $CDCl_3$) δ (ppm) = 3.18 – 2.92 (m, 3H), 2.80 (dd, *J* = 13.2, 2.7 Hz, 1H), 2.66 – 2.51 (m, 3H), 2.06 – 1.75 (m, 7H), 1.61 – 1.49 (m, 1H), 1.39 – 1.19 (m, 2H), 1.08 (dd, *J* = 12.7, 2.6 Hz, 1H), 0.90 (t, *J* = 7.4 Hz, 3H)

^{13}C NMR (101 MHz, $CDCl_3$) δ (ppm) = 216.98, 54.88, 53.83, 50.10, 46.87, 43.79, 41.70, 31.40, 30.54, 27.92, 26.77, 21.24, 12.31

HRMS (ESI) = *m/z* $[M + H]^+$ calcd. For $C_{14}H_{26}NO^+$, 208.1698; found, 208.1694

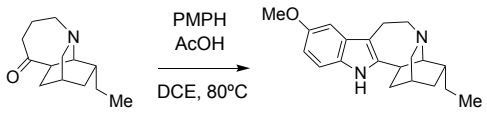

Epiibogaine

epiibogaine

A flask was charged with the starting material (200 mg, 0.964 mmol, 1 equiv.) and para-methoxy phenylhydrazine (252 mg, 1.44 mmol, 1.5 equiv.). The flask was evacuated and refilled with nitrogen 3 times after which anhydrous DCE (9.64 mL, 0.1M) and AcOH (0.827 mL, 14.47 mmol, 15 equiv.) was added. The resulting mixture was degassed by bubbling nitrogen through the solution for 10 mins. The flask was heated to 80 °C and stirred for 12 h after which it was cooled to ambient temperature and diluted with DCM (20 mL). Saturated aq. $NaHCO_3$ was added to the reaction mixture until the pH was adjusted to 7-8. The organic layer was separated, and the aqueous layer was further extracted with DCM (2 x 50 mL). The combined organic fractions were dried over sodium sulfate, filtered and concentrated under reduced pressure. Purification via chromatography on silica gel (gradient elution 20:1→10:1 DCM/MeOH, 0.25% NH_4OH) afforded **epiibogaine** (242 mg, 81%) as a colorless oil.

R_f = 0.33 (10:1 DCM/MeOH)

^{1}H NMR (400 MHz, MeOD) δ (ppm) = 7.16 (d, *J* = 8.7 Hz, 1H), 6.95 (d, *J* = 2.4 Hz, 1H), 6.73 (dd, *J* = 8.8, 2.4 Hz, 1H), 3.81 (s, 3H), 3.62–3.51 (m, 2H), 3.55 – 3.33 (m, 4H), 3.33 – 3.20 (m, 2H), 3.16 – 3.06 (m, 1H), 2.28 (d, *J* = 2.6 Hz, 1H), 2.22 – 2.01 (m, 3H), 1.75 – 1.63 (m, 1H), 1.56 (td, *J* = 7.3, 3.1 Hz, 2H), 1.38 – 1.19 (m, 1H), 1.01 (t, *J* = 7.4 Hz, 3H)

^{13}C NMR (101 MHz, MeOD) δ (ppm) = 154.01, 139.67, 130.07, 128.55, 111.18, 111.01, 107.34, 99.39, 59.08, 56.25, 54.92, 50.37, 48.27, 48.05, 47.91, 47.84, 47.70, 47.63, 47.41, 47.20, 46.99, 37.60, 32.16, 29.14, 28.18, 26.49, 24.11, 17.90, 10.58

HRMS (ESI) = *m/z* $[M + H]^+$ calcd. For $C_{20}H_{27}N_2O^+$, 311.2128; found, 311.2126

Chapter 4 – Strategies Towards Ethyl Piece Installation and Synthesis of Ibogaine

4.1 MHAT Hydrogenation Approach

Analysis of our route to epiibogaine reveals that a Pd-H mediated hydrogenation of intermediate **4.1** produced exclusively the endo- epimer for the C20 ethyl group (**Figure 4.1A**). We also observed that hydrogenation of pure endo- cyclopropyl ketone **4.1a** afforded the endo- epimer of the C20 ethyl group in high stereocontrol (**Figure 4.1B**). Intrigued by these observations, we sought to examine the relative thermodynamic ground state energies for the four possible stereoisomers formed from hydrogenation of **4.1** (**Figure 4.1C**). Computational studies revealed that when the C16 cyclopropyl ketone is in the endo orientation, there is a 2.3 kcal/mol difference in ground state energy between the exo- (**4.12c**) and endo- (**4.12d**) C20 ethyl group conformers. This result was expected as we postulated that the 1,3-diaxial strain in **4.12d** would be a destabilizing interaction. It was clear that our hydrogenation proceeded via kinetic pathway to selectively position the C20 ethyl group in the endo- orientation.

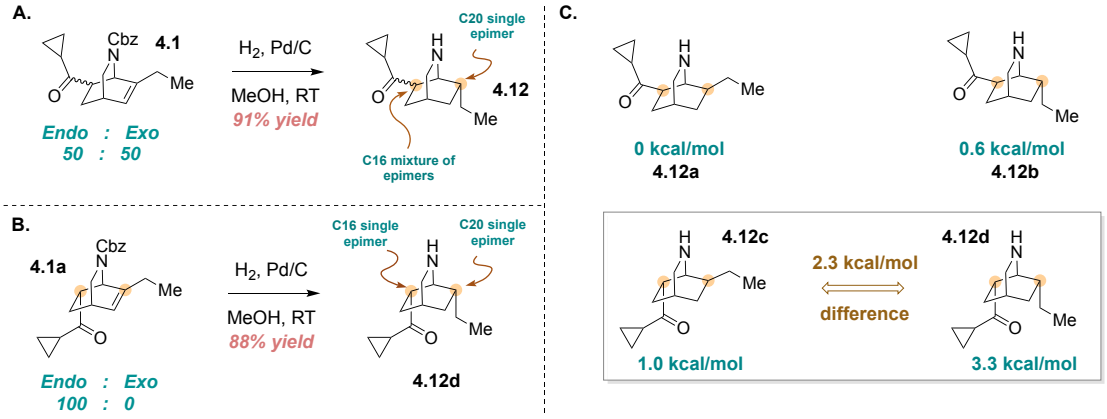

Figure 4.1. (A) Hydrogenation of 50:50 epimeric ratio of **4.1 (B)** Hydrogenation of pure endo **4.1a (C)** Computational evaluation of thermodynamic ground state energy, M06-2X/6-31+G(d,p)

A long-standing challenge in complex molecule synthesis is the hydrogenation of alkenes to a thermodynamically favored configuration when steric constraints of the substrate favor hydrogenation to a kinetic alkane product.[105] Dissolving metal reductions provides a means to thermodynamic control but is seldom used due to poor chemoselectivity and the need for elevated temperatures when reducing electron-neutral alkenes.[106] The origin of this poor chemoselectivity can be attributed to the low reduction potential of an electron-neutral alkene, thus resulting in the formation of a high energy radical anion (**Figure 4.2A**). Recent methodology developed by Shenvi and co-workers[107] circumvents the formation of a radical anion via direct metal-hydride hydrogen atom transfer (MHAT) while producing the same stereochemical outcome as a dissolving metal reduction (**Figure 4.2A**). Thermodynamic selectivity is achieved through the formation of tertiary radical intermediate **4.13b** which has lifetime and can adopt the most stable conformation upon hydrogen addition. Review of our previous computations indicate that the biggest difference in thermodynamic ground state energy is between the C16 endo- cyclopropyl ketone stereoisomers

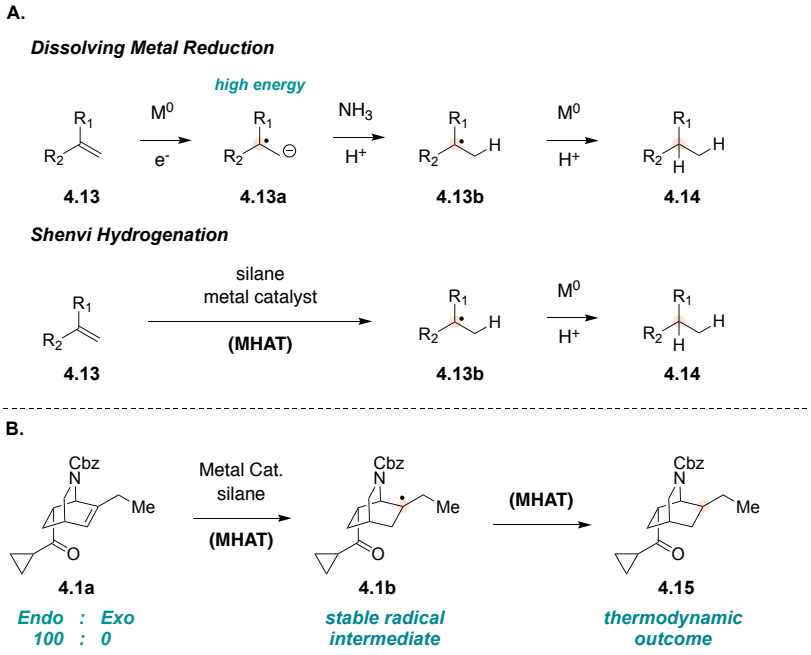

Figure 4.2. (A) Mechanism for dissolving metal reduction and Shenvi hydrogenation **(B)** Proposed thermodynamic hydrogenation of alkene **4.1a**

(**4.12c and 4.12d, Figure 4.1c**). We sought to utilize this pronounced difference to guide a thermodynamic HAT hydrogenation to our desired C20 stereoisomer. Subjecting pure endo **4.1a** to a Shenvi hydrogenation using a metal catalyst and silane would produce a tertiary radical intermediate that could ultimately undergo stereoselective hydrogen atom transfer (HAT) to afford product **4.15**. Because this reaction is governed by the thermodynamic stability of radical **4.1b**, the second HAT process should give the more stable conformer **4.15** in high selectivity.

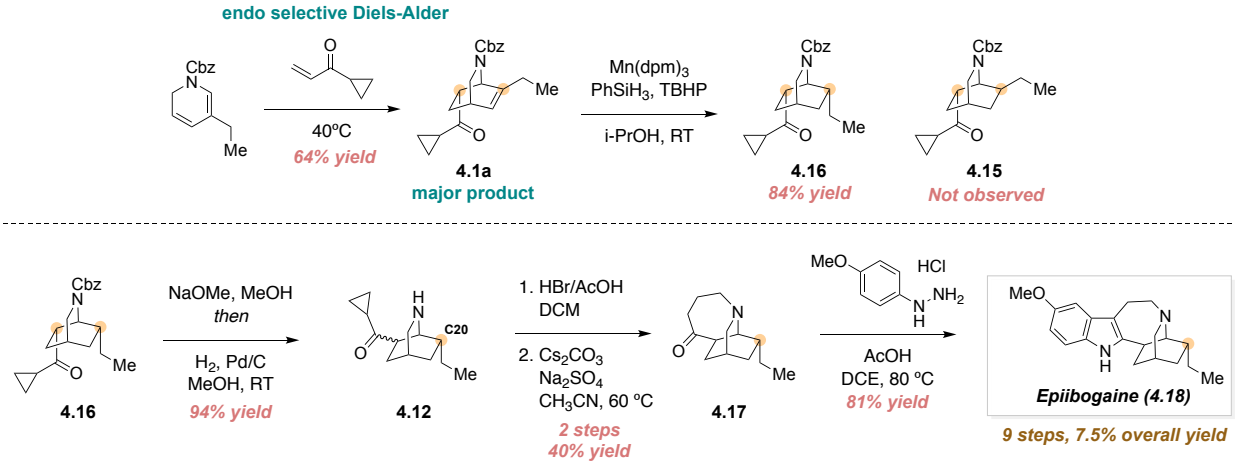

Figure 4.3. (A) Endo-selective Diels-Alder and MHAT hydrogenation of **4.1a (B)** Synthesis of epiibogaine from intermediate **4.16**

We sought to take advantage of the endo selectivity in our Diels-Alder reaction by conducting the cycloaddition at lower temperatures to kinetically favor endo- cyclopropyl ketone **4.1a** (**Figure 4.3A**). A subsequent MHAT hydrogenation was performed on intermediate **4.1a** using $Mn(dpm)_3$ and $PhSiH_3$ to afford product **4.16** with the C20 ethyl group in the endo orientation, similar to that of our Pd-H mediated hydrogenations. To our surprise, product **4.15** was not observed and thermodynamically unfavored isomer **4.16** was isolated in high diastereoselectivity. Compound **4.16** was taken through the rest of the synthesis to afford epiibogaine in 9 steps and 7.5% overall yield. Though this is one of the most efficient syntheses

of epiibogaine to date[108], it was clear that we needed to reevaluate the mechanism of our HAT reduction and further examine the reactivity of our substrate.

4.2 Investigation of MHAT Olefin Reduction Pathway

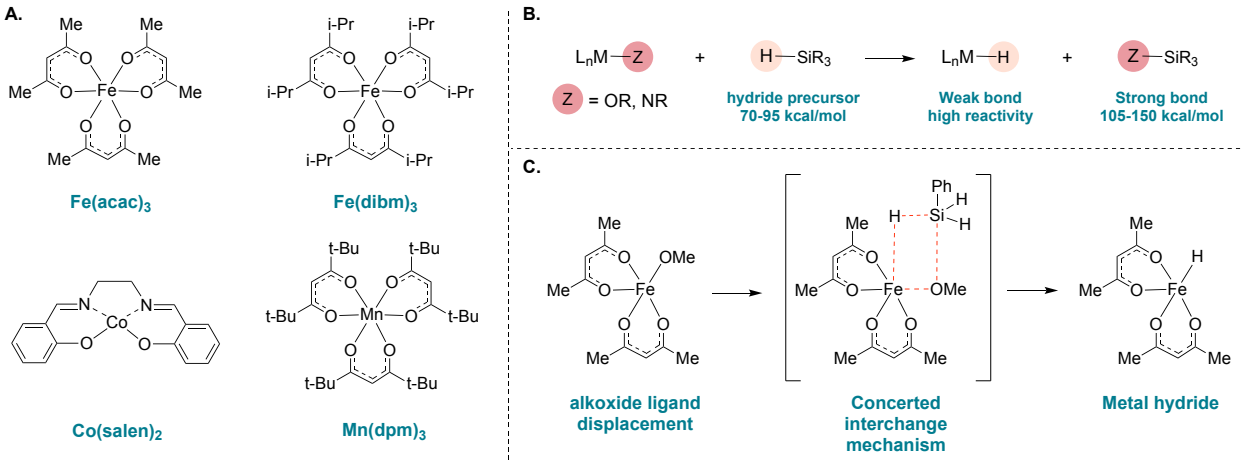

Figure 4.4. (A) Transition metal catalysts containing weak field supporting ligands **(B)** Use of -OR, -NR groups provide strong Si-Z bond for uphill M-H bond formation **(C)** Concerted mechanism for metal-hydride formation

A variety of synthetic advances have originated from the development of organometallic reagents that contain strong-field ligands (i.e cyclopentadienyl, carbonyl, phosphine) and are governed by the 18-electron rule.[109] However, a new generation of organometallic reagents have surfaced in which weak field ligands are utilized and the availability of multiple oxidation sates facilitate homolysis to form radical intermediates (**Figure 4.4A**).[110] Drago and Mukaiyama initially studied Fe, Mn, and Co catalysts containing weak field supporting ligands based on N or O donors.[111,112] In these systems, a reductant is added to generate a transition metal-hydride (M-H) complex. In weak field systems, the M-H bond is thought to be relatively weak and must be accompanied by the formation of a strong bond in another product (**Figure 4.4B**). Thus, reductants in weak field systems are generally silanes or borohydrides, which have Si-H or B-H

bonds that can be broken to form much stronger Si-O or B-O bonds. Seminal reports of metal-hydride hydrogen atom transfer (MHAT) hydrofunctionalizations noted the importance of an alcoholic solvent or co-solvent.[113] An important role of the alcohol may be to provide the alkoxide that supplies the driving force for Si-O or B-O bond formation. DFT calculations have revealed a concerted mechanism for the exchange of a hydride for an alkoxide between $(acac)_2$Fe-OMe and phenylsilane (**Figure 4.4C**).[114]

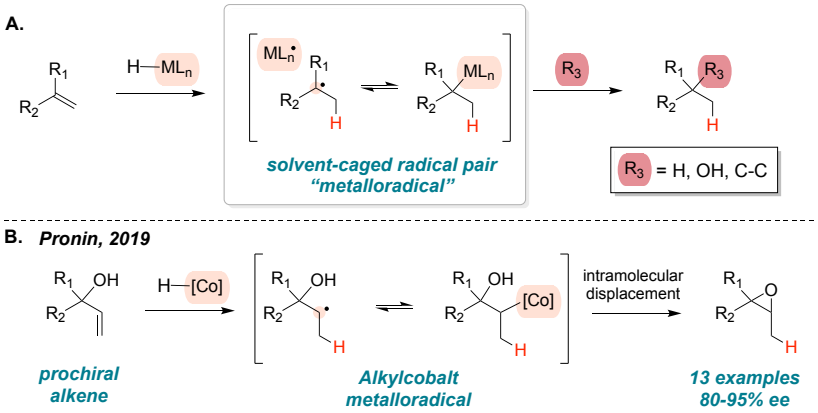

Figure 4.5. (A) Solvent-caged radical pair formed from addition of metal-hydride to alkene; hydrofunctionalizations from resulting metalloradical **(B)** Asymmetric MHAT epoxidation developed by Pronin and co-workers

Upon formation of the metal-hydride, the next step in the MHAT cycle involves the collision between the metal-hydride and an alkene, whereby a hydrogen atom is transferred to generate a carbon-centered radical and a metal complex that is formally reduced by one electron (**Figure 4.5A**). The resulting metal species is commonly described as a metal-centered radical or metalloradical.[115] It is likely that the radical and metal behave together as a "radical pair" through solvent caged pairing. The original conception of solvent-caged radical pairs was introduced by Franck and Rabinowitsch[116] in 1934, and explains the rate-viscosity correlations, isotope scrambling, and stereochemistry of certain radical based reactions. In 2019, the Pronin group reported the first example of an asymmetric MHAT reaction by influence of a solvent caged radical

pair (**Figure 4.5B**).[117,118] Enantioenriched epoxides (80-95% ee) were accessed from dialkyl(vinyl)carbinols using a modified cobalt salen catalyst. The authors propose an enantiodetermining organocobalt intermediate supported by an Erying analysis of enantioselectivity, which showed that enantioselectivity was enthalpically controlled and that electron-rich and polarizable salen ligands of similar steric bulk exhibited higher levels of asymmetry.

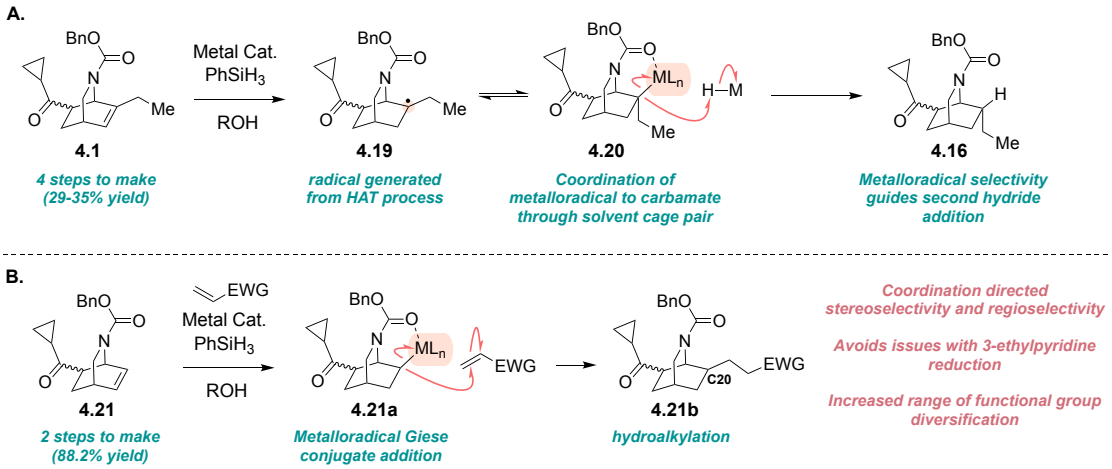

Figure 4.6. (A) Mechanistic proposal for MHAT hydrogenation selectivity; coordination stabilized metalloradical **(B)** Alternative proposal for hydroethylation using coordination directed selectivity

We suggest that the selectivity observed in our MHAT hydrogenation is also influenced by a solvent caged radical pair after initial hydrogen atom transfer to alkene **4.1** (**Figure 4.6A**). The resulting metalloradical (**4.20**) may be stabilized in the exo-orientation by the neighboring carbamate protecting group, consequently forcing the C20 ethyl group into the endo- position. Subsequent addition of a second metal-hydride is influenced by the exo- metalloradical to ultimately afford hydrogenation from the "top-face" of the isoquinuclidine. Using this mechanistic knowledge, we hypothesized that we could use the exo-stabilized metalloradical to our advantage by guiding addition into an electron-deficient alkene (**Figure 4.6B**). A MHAT catalyzed Giese conjugate addition of **4.21** with an acceptor alkene would provide the necessary carbons needed

for our C20 ethyl group. We propose that metalloradical coordination to the carbamate in **4.21b** would dictate the regioselectivity and stereoselectivity in the coupling. This strategy would circumvent the issues with reducing 3-ethylpyridine and allow us to use a reactant (**4.21**) that was previously accessed in our model system. Furthermore, the development of a stereoselective and regioselective hydrofunctionalization of **4.21** would enable another point of modularity in our synthesis for the preparation of iboga analogs bearing a C20 substituent.

4.3 Phenyl Vinyl Sulfone MHAT Olefin-Olefin Coupling Strategy

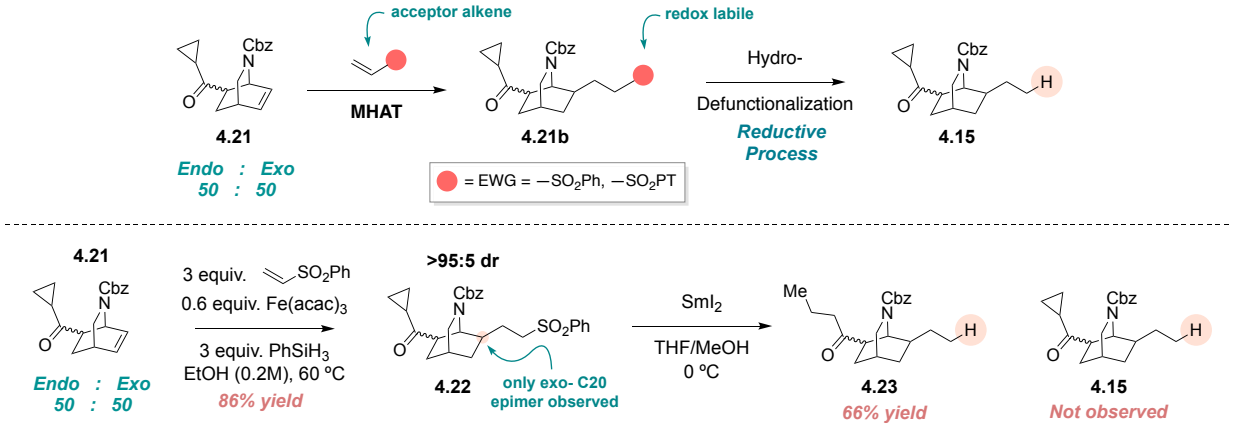

Figure 4.7. (A) Two-step (MHAT coupling, hydrodefunctionalization) sequence to afford C20 ethyl group **(B)** Olefin-Olefin coupling with phenyl vinyl sulfone and subsequent desulfonylation

We envisioned that we could install our C20 ethyl group in a two-step sequence involving a selective MHAT olefin-olefin coupling followed by a subsequent hydrodefunctionalization (**Figure 4.7A**). In order to ensure a facile hydrodefunctionalization, we must use a reductively labile electron withdrawing group (EWG) in our acceptor alkene for MHAT coupling. We envisioned that a vinyl sulfone would be an ideal coupling partner due to its well-documented redox activity. Inspired by the work of Baran and co-workers[119], a MHAT coupling between **4.21** and phenyl vinyl sulfone was conducted using $Fe(acac)_3$ and phenylsilane in ethanol to afford product **4.22** with high regioselectivity and stereoselectivity at the C20 carbon (**Figure 4.7B**). To

our delight, the exo-stabilized metalloradical had influenced the regiochemical and stereochemical outcome of this reaction to generate only one out of four possible products. Next, we were tasked with reductively eliminating the phenyl sulfone to un-mask our desired C20 ethyl group. A standard reductive desulfonylation with SmI_2 was performed on intermediate **4.22** to yield **4.23** as the major product. Unfortunately, the hydrodefunctionalization with SmI_2 was not chemoselective and a reductive ring opening of the cyclopropyl ketone was also observed.[120] Optimization proved futile as product **4.15** was not detected in a variety of desulfonylation conditions (**Table 4.1**)

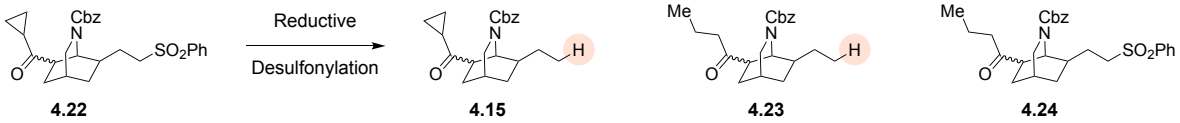

4.22 **4.15** **4.23** **4.24**

Entry	Condition	**4.15**	**4.23**	**4.24**
1	SmI_2, THF/MeOH, 0 ºC	-	66%	12%
2	SmI_2, THF/MeOH, -78ºC	-	31%	44%
3	SmI_2, THF, -78 - 0 ºC	-	12%	18%
4	Raney Ni., MeOH	-	-	10%
5	Raney Ni., THF	-	12%	Trace

Table 4.1: Isolated yields shown. All reactions run at 0.1M. All reactions chromatographed using gradient elution 10:1→7:3 hexanes/EtOAc.

We speculated that altering the aryl attachment to the sulfone could improve redox activity and allow for milder desulfonylation conditions (**Figure 4.8A**). Redox active phenyl tetrazole (PT) sulfone can undergo single electron transfer (SET) to ultimately form a sulfinic acid by-product and carbon-centered radical.[121] We noticed that coupling **4.21** with PT vinyl sulfone was sluggish and **4.25** was isolated in 34% yield (**Figure 4.8B**). Optimization of this reaction was unsuccessful as it appeared that the steric constraints of the phenyl tetrazole attachment negatively affected the MHAT coupling. We elected to forgo the phenyl tetrazole strategy and return back to our phenyl sulfone for a late-stage desulfonylation. It was clear that desulfonylation was not

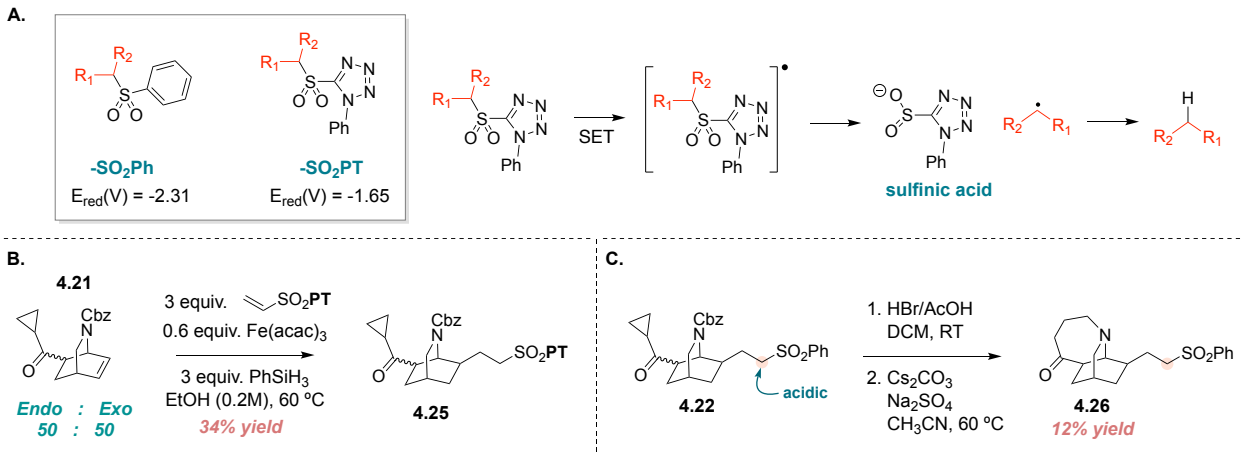

Figure 4.8. (A) Redox activity of -SO_2Ph vs -SO_2PT; SET desulfonylation pathway to sulfinic acid **(B)** MHAT coupling with PT vinyl sulfone **(C)** Subjecting **4.22** through iboga synthesis for late-stage desulfonylation

compatible with a cyclopropyl ketone in place; thus, we proposed constructing the iboga framework first and performing the desulfonylation at the end of the synthesis (**Figure 4.8C**). Ring opening and closing of **4.22** afforded tetrahydroazapinone **4.26** in 12% yield over two steps. This dramatic decrease in yield compared to the defunctionalized congener can be attributed to the acidic protons adjacent to the sulfone.[122] We suspect that a variety of side reactions take place in the base mediated ring closure to diminish the yield of **4.26**. It was clear that the sulfone strategy was unsuccessful and a different withdrawing group with better redox activity was needed instead.

4.4 Methyl Acrylate MHAT Olefin-Olefin Coupling Strategy

Having realized that the desulfonylation strategy was not viable due to issues with chemoselectivity, we elected to search for an alternative electron-withdrawing group with better redox capability. Inspired by recent developments in decarboxylative cross couplings via redox-active esters,[123,124] we envisioned that we could synthesize product **4.15** from a radical mediated

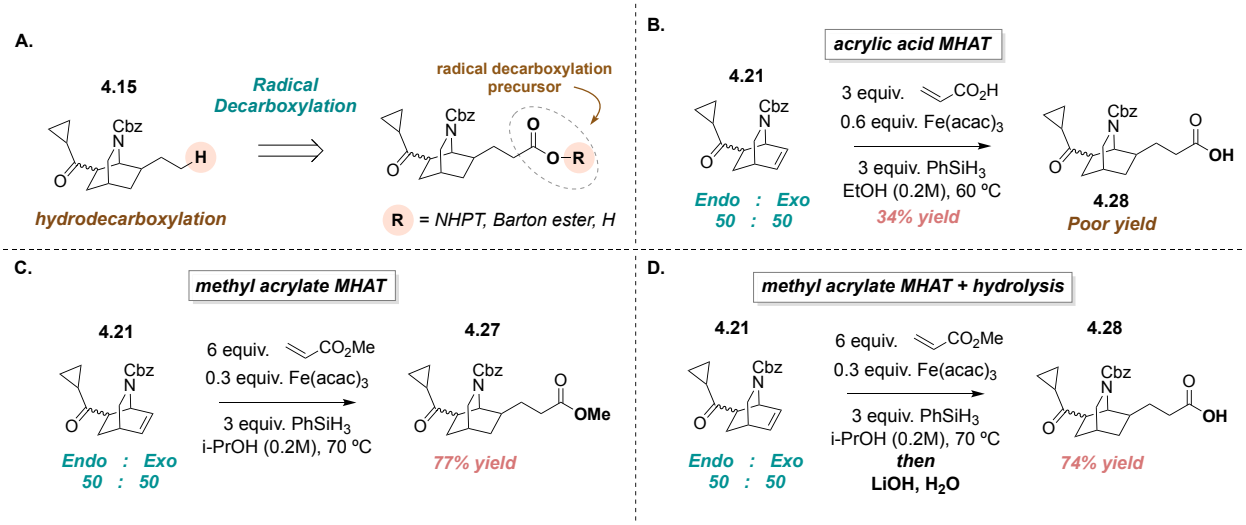

Figure 4.9. (A) Radical decarboxylation strategy to prepare **4.15 (B)** MHAT coupling of **4.21** and acrylic acid **(B)** Optimized MHAT coupling of 4.21 and methyl acrylate **(C)** "One-pot" MHAT coupling of **4.21** and methyl acrylate followed by ester hydrolysis

hydrodecarboxylation of a carbonyl derived precursor (**Figure 4.9A**). Preparation of our decarboxylation precursor would come from the corresponding carboxylic acid generated from our MHAT coupling. MHAT olefin-olefin coupling of 4.21 with acrylic acid was sluggish and carboxylic acid **4.28** was isolated in only 34% yield (**Figure 4.9B**). Further attempts at optimization were unsuccessful and it was evident that acrylic acid was not a suitable substrate for this reaction. We noticed that masking the free acid in the form of an ester dramatically improved the MHAT coupling to afford product **4.28** in 77% yield after optimization (**Figure 4.9C**). This reaction was sensitive to the relative equivalences of catalyst, silane and acceptor alkene (**Entry 3, 15 and 16, Table 4.2**) and found to perform best at 70 ºC in isopropanol. When subjecting pure epimers of **4.21** to the coupling, the exo epimer outperformed the endo epimer by a dramatic margin (**Entry 4—5, Table 4.2**). We hypothesize that there is significant orbital overlap between the cyclopropane and alkene in endo- **4.21**, thus stalling initiation of the MHAT cycle. Epimerization was not observed in this reaction; however, endo- **4.21** can be recovered,

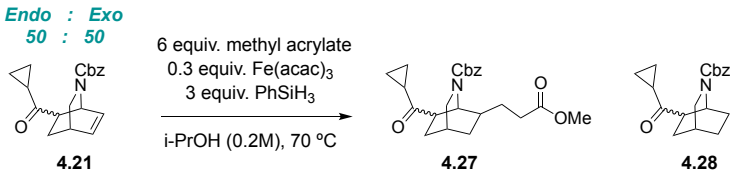

Entry	Deviation	4.27	4.28	4.21
1	none	77%	4%	17%
2	EtOH (0.2M)	69%	18%	8%
3	1 equiv. $Fe(acac)_3$	28%	56%	8%
4	Pure Exo SM	90%	5%	5%
5	Pure Endo SM	23%	12%	58%
6	i-PrOH (0.1M)	62%	21%	11%
7	$Ph(i\text{-}PrO)SiH_2$ (1 equiv.)	58%	34%	-
8	0.3 equiv. $Fe(dibm)_3$	22%	46%	25%
9	1:1 DCE/$(CH_2OH)_2$	8%	15%	71%
10	60 °C	61%	8%	20%
11	80 °C	58%	21%	14%
12	10 mol% Na_2HPO_4 as additive	55%	24%	18%
13	1 equiv. Na_2HPO_4 as additive	31%	31%	15%
14	0.6 equiv. $Fe(acac)_3$	71%	24%	-
15	1.5 equiv. $PhSiH_3$	43%	18%	35%
16	3 equiv. methyl acrylate	41%	45%	trace

Table 4.2: Isolated yields shown. All reactions run on 1.0 mmol scale for **17** (312 mg). All reactions chromatographed using gradient elution 10:1→7:3 hexanes/EtOAc.

epimerized and re-subjected to a subsequent MHAT coupling. In an effort to reduce overall step count, we postulated that we could “un-mask” our carboxylic acid by performing ester hydrolysis in the same reaction vessel. Upon completion of the MHAT coupling with methyl acrylate, the reaction mixture was diluted with water and lithium hydroxide was added to generate carboxylic acid **4.28** in 74% yield after isolation (**Figure 4.9D**). We noticed that in situ hydrolysis assisted chromatography of **4.28** by converting residual $Fe(acac)_3$ to more polar $Fe(H_2O)_6$.[125] We were now tasked with developing a chemoselective hydrodecarboxylation of **4.28** to obtain our desired C20 ethyl group.

4.5 Photoredox Hydrodecarboxylation

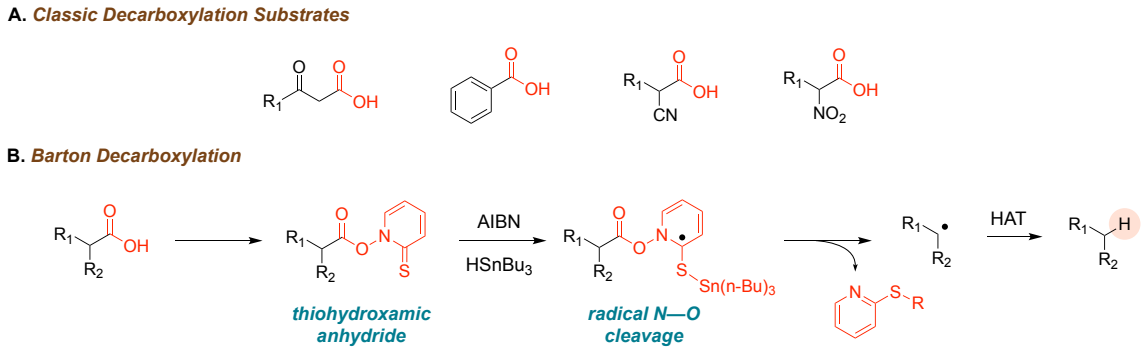

Figure 4.11. (A) Classic substrates for decarboxylation reactions **(B)** Barton radical mediated decarboxylation using thiohydroxamic anhydride

Decarboxylation reactions are amongst the oldest known organic transformations and are pervasive in numerous industrial and biological processes. Traditional reports of decarboxylations have involved a β-keto, α-aryl, α-nitro or α-cyano acids and are accelerated due to the formation of a zwitterionic tautomer or stabilized anion (**Figure 4.11A**).[126] In 1983, Sir Derek Barton rapidly expanded the paradigm of decarboxylation reactions by enlisting radical reactivity to selectively remove carboxylic acids on unfunctionalized alkyl systems (**Figure 4.11B**).[127] The invention of the Barton ester utilizes a thiohydroxamic anhydride and the presence of a weak N—O bond (BDE = ~45 kcal/mol) that can undergo visible light-induced fragmentation to liberate carbon dioxide while furnishing alkyl radicals that can be converted to a myriad of functional groups.[128] Though pioneering, chemists have transitioned away from Barton esters due to their limited thermal stability and the need for toxic and odorous reductants for decarboxylation. In recent years, *N*-hydroxyphthalimide redox active esters (RAE) have been used for their ability to undergo facile single electron transfer (SET) reduction with inexpensive metal catalysts while obviating the need for toxic reductants or elaborate specialized equipment.[129]

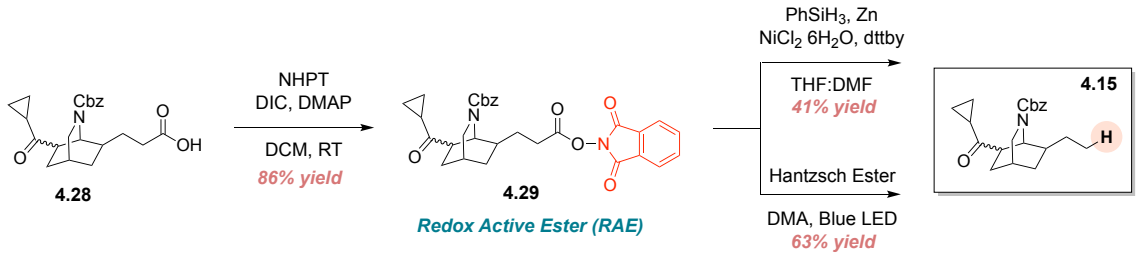

Figure 4.12. Hydrodecarboxylation of **4.28** using N-hydroxypthalimide redox active ester

We envisioned that converting carboxylic acid **4.28** to the corresponding N-hydroxyphthalimide derived RAE would allow for a facile hydrodecarboxylation to intermediate **4.15** (**Figure 4.12**). Redox active ester **4.29** was prepared in 86% yield from a coupling reaction using *N',N"*-diisopropylcarbodiimide (DIC) and catalytic *N,N*-dimethylaminopyridine (DMAP). Subjecting **4.29** to Baran's reductive decarboxylation[24] conditions afforded product **4.15** in 41% yield. Intrigued by the possibility of using photochemical single electron transfer to **4.29**, we noticed a significant increase in conversion and yield when conducting the reductive decarboxylation with Hantzsch ester in DMA with blue LED light irradiation.[130] We suspect that the Hantzsch ester serves as a potent photoreductant by generating an electron donor-acceptor (EDA) complex with the phthalimide to enable radical cleavage.

Though we had completed an efficient two-step protocol for hydrodecarboxylation, we postulated whether we could avoid the phthalimide RAE altogether and directly decarboxylate **4.28** to its saturated alkyl congener. In 2015, Nicewicz[131] and co-workers developed a pioneering photochemical hydrodecarboxylation of homobenzylic carboxylic acids using an organic acridinium photocatalyst and blue LED irradiation (**Figure 4.13A**). This method involves Hunig's base for generation of the carboxylate salt and a disulfide for hydrogen atom transfer (HAT) upon radical generation. Hydrodecarboxylation of **4.28** using Nicewicz's conditions proved challenging as product **4.15** was isolated in only 22% yield and significant starting material was recovered.

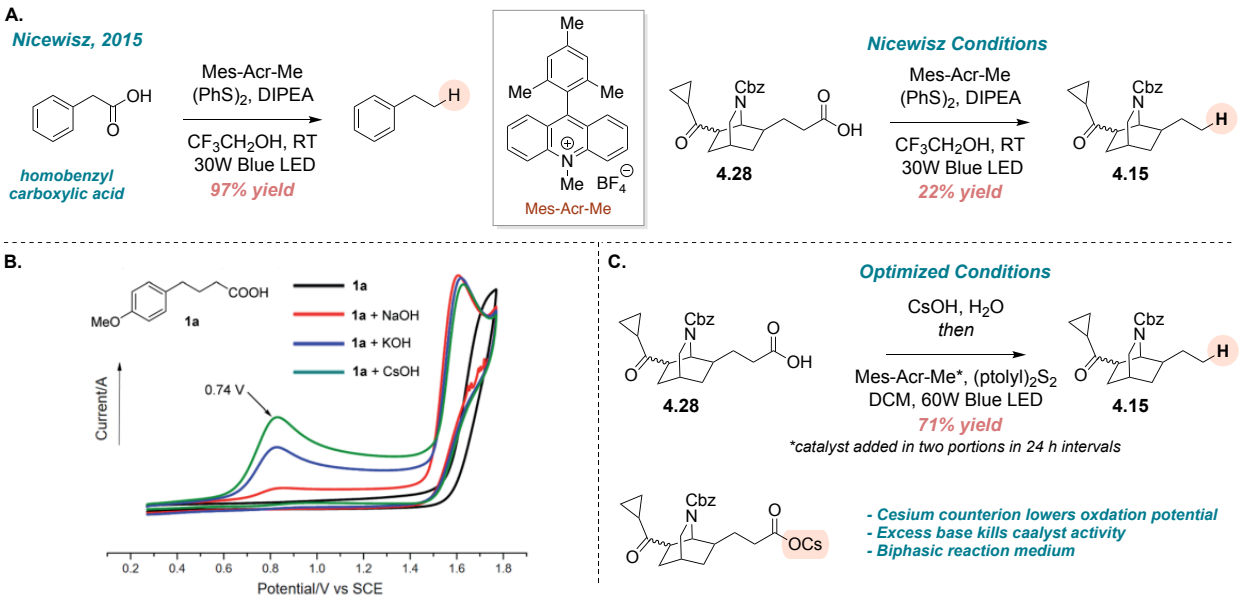

Figure 4.13. (A) Nicewicz photochemical hydrodecarboxylation of homobenzyl carboxylic acid; hydrodecarboxylation of **4.28** using Nicewicz conditions **(B)** Cyclic voltammetry of carboxylic acid and carboxylate salts **(C)** Optimized conditions for hydrodecarboxylation of **4.28**

This result was expected since **4.28** is a primary unactivated carboxylic acid with very different redox capability compared to Nicewicz's homobenzyl carboxylic acids. In 2021, Zhu and coworkers[132] performed cyclic voltammetry on 4-phenylbutanoic acid and noticed a significant peak at 0.74 V vs SCE for the oxidation potential when stoichiometric amount of base is added (**Figure 4.13B**). It appeared that addition of cesium hydroxide formed a cesium carboxylate that can undergo single electron oxidation with a photocatalyst. The oxidation potential of the cesium salt is more pronounced likely due to the weakened ion pairing compared to sodium or potassium salts. In situ generation of the cesium carboxylate salt followed by addition of photocatalyst and disulfide produced our desired product in 71% yield after 48 hours (**Figure 4.13C**).

Thorough optimization revealed that our hydrodecarboxylation performed best when ran using a biphasic solvent system (**Entries 6 and 14—17, Table 4.3**) and the cesium carboxylate was critical as yield diminished when using NaOH, KOH or Hunig's base (**Entry 3—5, Table 4.3**).

We found that $Ir(dF(CF_3)ppy_2(dtbpy)PF_6$ also produced decarboxylation but choose to use the organic acridinium photocatalyst for cost-efficiency on gram-scale. Initial decarboxylation screens were run with rigorous omission of oxygen but were later found to be compatible with air atmosphere.

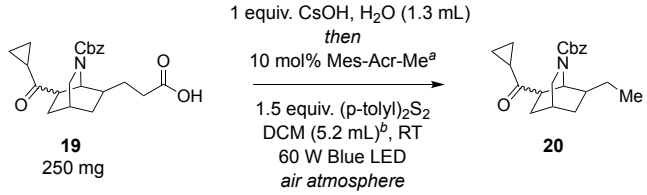

[a] Mes-Acr-Me added in 2 portions in 24 h intervals
[b] Reaction ran with 4:1 DCM/H2O (0.1 M) concentration

Entry	Deviation	**20**
1	None	71%
2	2 mol% $Ir(dF(CF_3)ppy_2(dtbpy)PF_6$	76%
3	1 equiv. KOH	<5%
4	1 equiv. NaOH	<5%
5	1 equiv. DIPEA, no H_2O	12%
6	No H_2O	21%
7	10 mol% Mes-Acr-Me in one portion	55%
8	10 mol% Mes-Acr-Ph in one portion	41%
9	5 mol% 4-CzIPN	trace
10	1.5 equiv. PhSH	62%
11	1.5 equiv. Ph_2S_2	69%
12	0.5 equiv. Ph_2S_2	34%
13	1.5 equiv. TRIP thiol	57%
14	CH_3CN (0.1M)	22%
15	4:1 CH_3CN/H_2O (0.1M)	31%
16	MeOH (0.1M)	trace
17	EtOAc (0.1M)	25%
18	Nitrogen atmosphere	70%

Table 4.3: Isolated yields shown. All reactions run at 250 mg scale for compound **19**. All reactions chromatographed using gradient elution 10:1→7:3 hexanes/EtOAc.

During our pilot experiments, we experienced numerous issues when performing the hydrodecarboxylation of **4.28** on gram scale. Initial reactions were run using phenyl disulfide and only 40% conversion was observed after 24 hours when adding 10 mol% acridinium catalyst at

the beginning of the reaction. As denoted in **Figure 4.14A**, our pilot experiments first involved stirring the carboxylic acid with cesium hydroxide in water before adding a solution of catalyst and disulfide in DCM to generate a biphasic reaction medium. The biphasic reaction mixture is then stirred vigorously between two 30W blue LED lamps with a cooling fan positioned above the flask. After 24 hours, we noticed that the reaction mixture was black and observed only 40% conversion via LCMS. Subjection to further blue LED irradiation had minimal effect and it appeared that reaction conversion had plateaued. An additional 10 mol% of catalyst can be added after 24 hours to increase the overall conversion to 65% after 48 hours. However, it was suspected that our acridinium catalyst had undergone decomposition to transition from a vibrant yellow to black colored solution. We hypothesize two modes of catalyst decomposition: nucleophilic attack on the

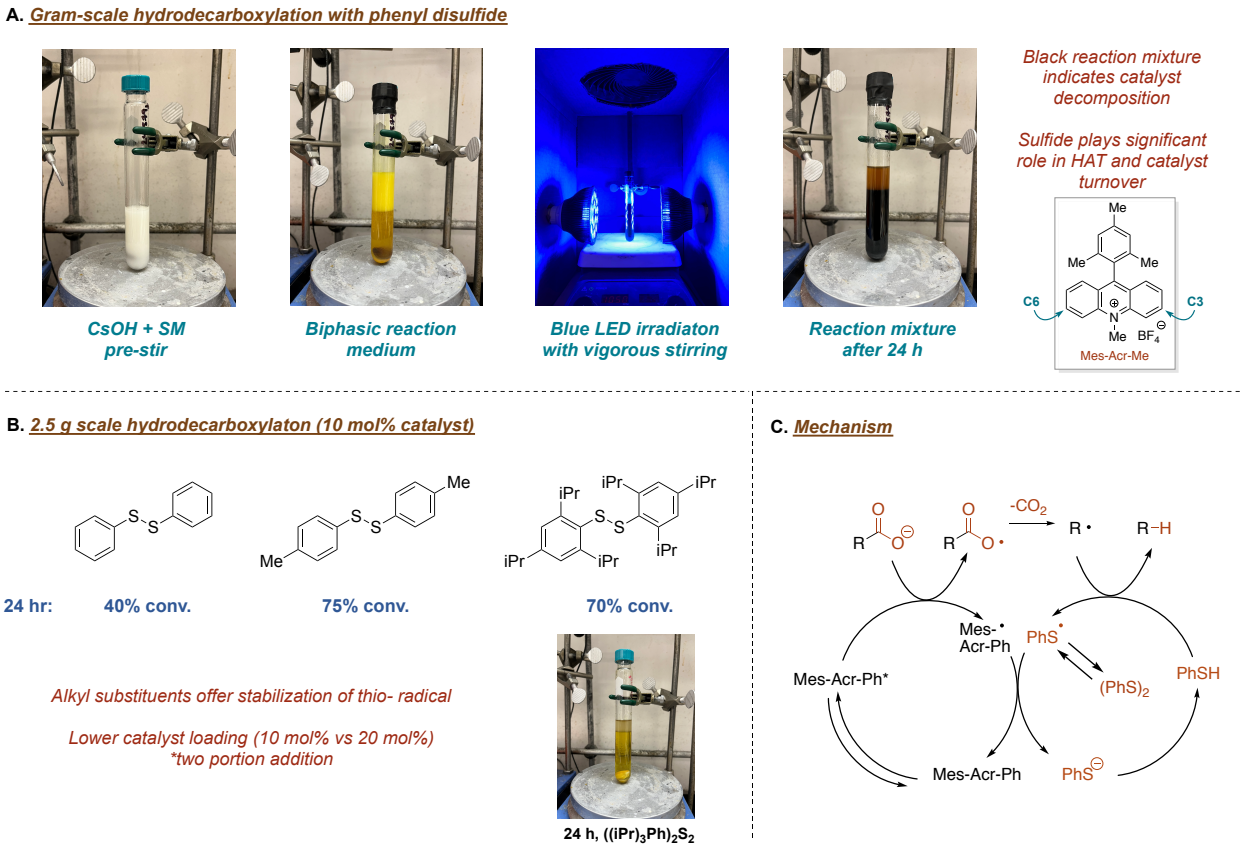

Figure 4.14. (A) Gram Scale hydrodecarboxylation using phenyl disulfide and 10 mol% acridinium – after 24 h reaction mixture has turned black; pathways for decomposition of acridinium catalyst **(B)** disulfide screen for hydrodecarboxylation **(C)** Mechanism of hydrodecarboxylation

C3/C6 carbons of the acridinium core or demethylation by the thiolate produced in the reaction.[133] Analysis of the mechanism reveals that the disulfide plays a critical role in hydrogen atom transfer and catalyst turnover. Blue LED irradiation of the disulfide generates a thiol radical that oxidizes the acridinium catalyst and gets converted to a thiol for hydrogen atom transfer. We postulated that reducing nucleophilicity and increasing thiyl- radical stability of our disulfide would minimize catalyst decomposition and facilitate higher catalyst turnover. To our delight, we noticed a significant increase in reaction conversion with *para*-tolyl disulfide and triisopropylphenyl disulfide when conducting our hydrodecarboxylation on gram scale (**Figure 4.14B**). The mixture had maintained its vibrant yellow color throughout the reaction and 70—75% conversion was observed. Furthermore, we also noticed that we could lower the overall catalyst loading to 10 mol% over two 24-hour intervals to achieve roughly 90% conversion and 71% yield of our product. Having devised an efficient two step (MHAT coupling, hydrodecarboxylation) protocol for ethyl group installation, we were now tasked with completing our total synthesis of ibogaine.

4.6 Completion of Ibogaine and Related Analogs

Our efforts thus far have culminated in an efficient 4 step protocol for the preparation of intermediate **4.15** in 46.3% overall yield (**Figure 4.15**). Each reaction can be run on gram-scale and is reproducible with a high degree of selectivity for the C20 ethyl group. Decarboxylated product **4.15** was subjected to the remaining iboga synthesis to afford ibogaine (**4.31**) in 7 steps starting from pyridine. We noticed that isolation of **4.30** via chromatography led to reduced yields and an unpurified mixture should be taken through the final three steps of the synthesis. On gram-scale there is a slight decrease in yield for the final three steps, but we suspect that this could be amended though rigorous temperature control of the ring closure.

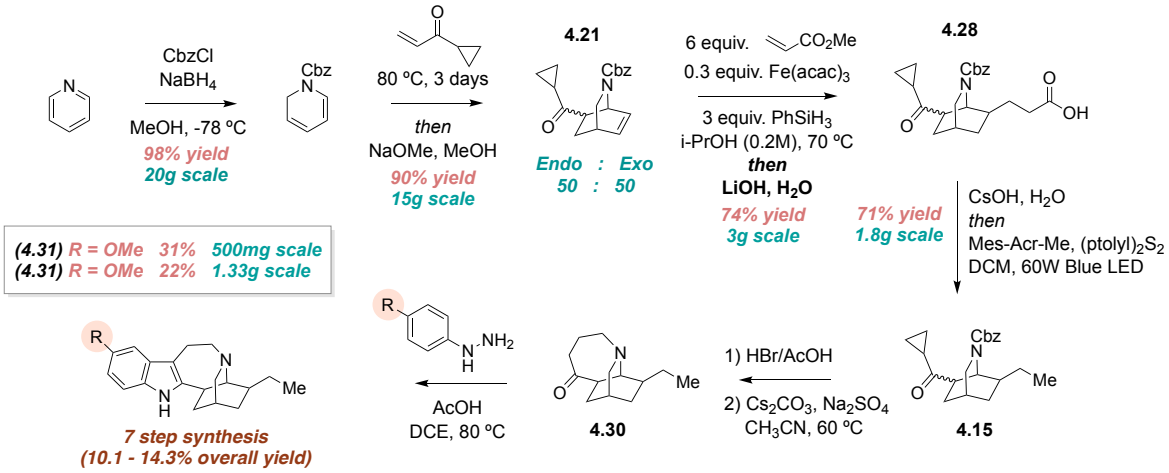

Figure 4.15 7 step total synthesis of ibogaine starting from pyridine

To fully showcase the modularity of our synthetic design, several structural derivatives of ibogaine were also prepared. Replacing para-methoxyphenylhydrazine with other substituted phenylhydrazines afforded several iboga natural products (**4.31—4.34, Figure 4.16A)** and related analogs (**4.35, 4.37, Figure 4.16A**). Our late-stage diversification approach grants unprecedented access to functionalizing the indole ring system of the iboga skeleton. Taken together, this completes the shortest and most efficient route to ibogaine (**Figure 4.16B**).

To better understand route modularity and synthetic efficiency, we analyzed the changes in molecular complexity (C_m) over the course of the synthesis (**Figure 4.16B**). Bottcher's complexity index (C_m)[134, 135] is a value calculated by assigning information content (mcbits) to each non-hydrogen atom to formalize the intrinsic information content of a molecule on a per-atom basis. Analysis of complexity changes throughout our synthesis reveals two distinct points of modularity for the preparation of analogs: diversification through olefin chemistry and diversification via carbonyl functionalization (i.e Fischer indole cyclization). Both modular points are at an intermediate with lower molecular complexity than their respective iboga derivatives; indicating that diversification can occur at a simplified intermediate that ultimately produces a greater-than-additive product.

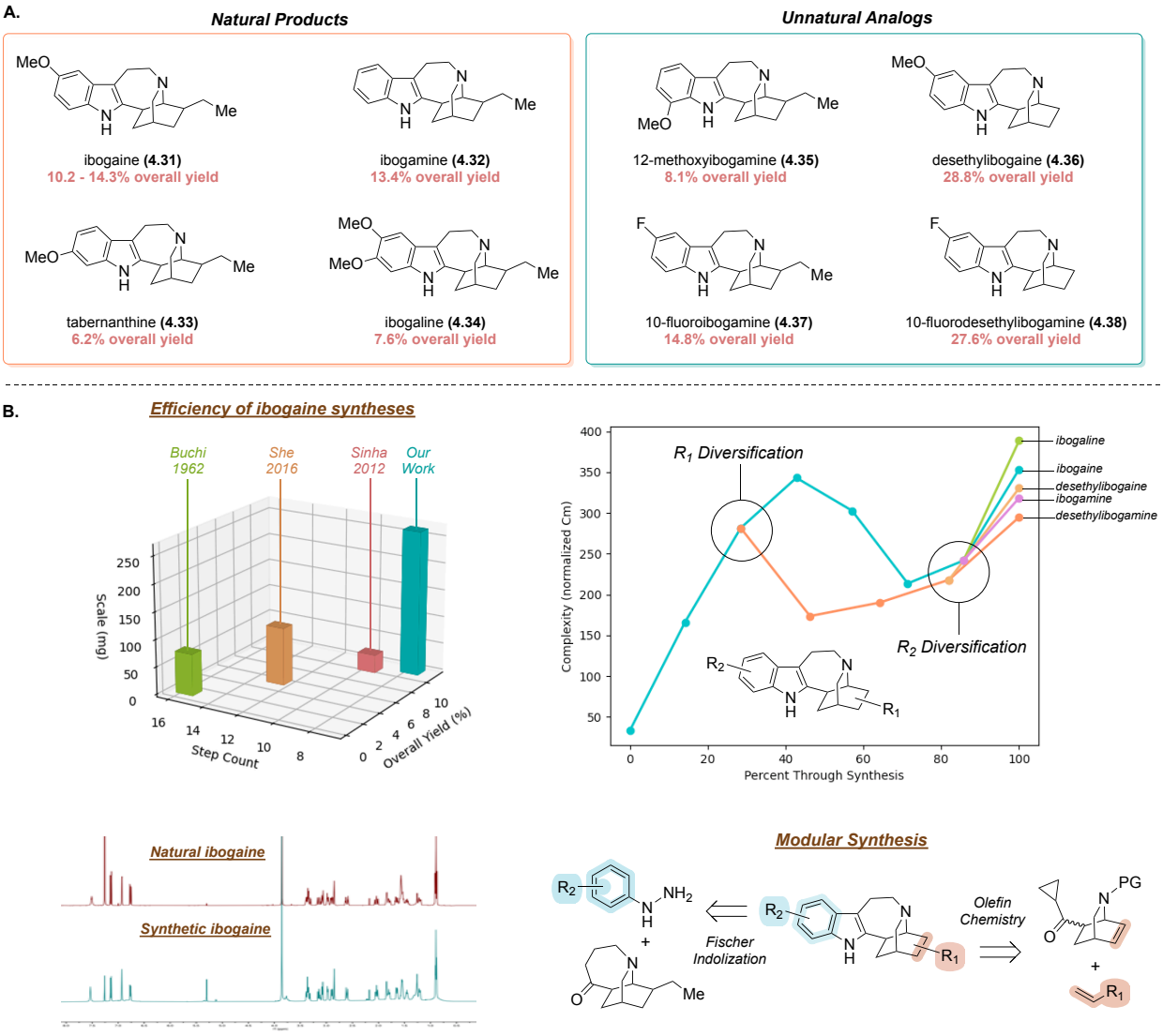

Figure 4.16. (A) Natural products and unnatural analogs synthesized from general ibogaine or desethylibogaine synthesis **(B)** Efficiency of our ibogaine synthesis; route modularity indicating two distinct points for diversification

The development of an efficient, scalable and modular total synthesis of racemic ibogaine is instrumental for the field of pharmacology and neurobiology. Though racemic ibogaine is highly sought after, (+)-ibogaine has never been accessed nor studied in biological experiments. Thus,

it was clear we needed to develop an asymmetric variant of our iboga alkaloid synthesis to fully showcase our synthetic tractability.

REFERENCES

105. Barton, D. H. R.; Robinson, C. H. The stereospecificity of carbanion reduction processes. *J. Am. Chem. Soc.* **1954**, 3045

106. Whitesides, G. M.; Ehmann, W. J. Reduction of olefins using sodium-hexamethylphosphoramide-tert-butyl alcohol. *J. Org. Chem.* **1970**, 35, 3565—3567

107. Iwasaki, K.; Wan, K. K.; Oppedisano, A.; Crossley, S. W. M.; Shenvi, R. A. Simple, Chemoselective Hydrogenation with Thermodynamic Stereocontrol. *J. Am. Chem. Soc.* **2014**, 136, 1300—1303

108. Yu, P.; Karmakar, A.; Sabbers, W. A.; Shajan, F.; Andrade, R. B. Asymmetric Total Synthesis of (+)-Epiibogamine Enabled by Three-Component Domino Michael/Michael/Mannich Annulation of N-Sulfinyl Metallosilylenamines. *Org. Lett.* **2023**, 25, 956—960

109. Hartwig, J. F. Organotransition Metal Chemistry, University Science Books, Sausalito, CA, 2010.

110. Holland, P. L. Distinctive Reaction Pathways at Base Metals in High-Spin Organometallic Catalysts *Acc. Chem. Res.* **2015**, 48, 1696—1702

111. Shigeru, I.; Mukaiyama, T. A New Method for Preparation of Alcohols from Olefins with Molecular Oxygen and Phenylsilane by the Use of Bis(acetylacetonato)cobalt(II). *Chem. Lett.* **1989**, 18, 1071—1074

112. Hamilton, D. E.; Drago, R. S. Mechanistic studies on the cobalt(II) Schiff base catalyzed oxidation of olefins by O2. *J. Am. Chem. Soc.* **1987**, 109, 374—379

113. Mukaiyama, T.; Yamada, T. Recent Advances in Aerobic Oxygenation. *Bull. Chem. Soc. Jpn.* **1995**, 68, 17—35

114. Kim, D.; Rahaman, S. M. W.; Mercado, B. Q.; Holland, P. L. Roles of Iron Complexes in Catalytic Radical Alkene Cross-Coupling: A Computational and Mechanistic Study. *J. Am. Chem. Soc.* **2019**, 141, 7473—7485

115. Shevick, S.; Wilson. C. V.; Kotesova, S.; Holland, P. L; Shenvi, R. A. Catalytic hydrogen atom transfer to alkenes: a roadmap for metal hydrides and radical. *Chem. Sci.* **2020**, 11, 12401—12422

116. Franck, J.; Rabinowitch, E. *Trans. Faraday Soc.*, **1934**, 30, 120—130

117. Touney, E. E.; Foy, N. J.; Pronin, S. V. Catalytic Radical–Polar Crossover Reactions of Allylic Alcohols. *J. Am. Chem. Soc.* **2018**, 140, 16982—16987

118. Discolo, C. A. ; Touney, E. E.; Pronin, S. V. Catalytic Asymmetric Radical–Polar Crossover Hydroalkoxylation. *J. Am. Chem. Soc.* **2019**, 141, 17527—17532

119. Lo, J. C.; Kim, D.; Pan, C.; Edwards, J. T.; Yabe, Y.; Holland, P. L.; Baran, P. S. Fe-Catalyzed C–C Bond Construction from Olefins via Radicals. *J. Am. Chem. Soc.* **2017**, 139, 2484—2503

120. Molander, G. A.; Alonso, C. A. Opening of cyclopropyl ketones with SmI2. Synthesis of spirocyclic and bicyclic ketones by intramolecular trapping of an electrophile. *Tetrahedron*. **1997**, 15, 8067—8084

121. Chen, Y.; McNamara, N.; May, O.; Blakemore, D. C. Ley, S. V. Photoredox Generation of Sulfonyl Radicals and Coupling with Electron Deficient Olefins. *Org. Lett.* **2020**, 22, 5746—5748

122. Bordwell, F. G.; Imes, R. H.; Steier, E. C. Acidities of sulfones. *J. Am. Chem. Soc.* **1967**, 89, 3905—3906

123. Laudadio, G.; Palkowitz, M. D.; Ewing, T. E.; Baran, P. S. Decarboxylative Cross-Coupling: A Radical Tool in Medicinal Chemistry. *ACS Med. Chem. Lett*. **2022**, 13, 1413—1420

124. Rodriguez, N.; Goossen, L. J. Decarboxylative coupling reactions: a modern strategy for C–C-bond formation. *Chem. Soc. Rev.* **2011**, 40, 5030—5048

125. Delahay, G. Fe-ZSM-5 Catalyst Prepared by Ion Exchange from Fe(acac)3: Application into NH3-SCR of NO. *Top. Catal.* **2016**, 59, 901—906

126. Button, R. G.; Taylor, P. G. The decarboxylation of some heterocyclic acetic acids. Part II. Direct and indirect evidence for the zwitterionic mechanism. *J. Chem. Soc., Perkin Trans.* **1973**, 2, 557—567

127. Barton, D. H. R. ; Crich, D.; Motherwell, W. B. New and improved methods for the radical decarboxylation of acids. *J. Chem. Soc. Chem. Commun.* **1983**, 939—941

128. Qin, T.; Malins, L. R.; Edwards, J. T.; Merchant, R. M.; Novak, J. E.; Mills, R. B.; Eastgate, M. D.; Baran, P. S. Nickel-Catalyzed Barton Decarboxylation and Giese Reactions: A Practical Take on Classic Transforms. *Angew. Chem. Int. Ed.* **2017**, 56, 260—265

129. Huihui, K. M.; Caputo, J. A.; Melchor, Z.; Olivares, A. M.; Ackerman, L. K. G.; Weix, D. J. Decarboxylative Cross-Electrophile Coupling of N-Hydroxyphthalimide Esters with Aryl Iodides. *J. Am. Chem. Soc.* **2016**, 138, 5016—5019

130. Zheng, C.; Wang, G.; Shang, R. Catalyst-free Decarboxylation and Decarboxylative Giese Additions of Alkyl Carboxylates through Photoactivation of Electron Donor-Acceptor Complex. *Adv. Synth. Catal.* **2019**, 361, 4500—4505

131. Griffin, J. D.; Zeller, M. A.; Nicewicz, D. A. Hydrodecarboxylation of Carboxylic and Malonic Acid Derivatives via Organic Photoredox Catalysis: Substrate Scope and Mechanistic Insight. *J. Am. Chem. Soc.* **2015**, 137, 11340—11348

132. Li, N.; Ning, Y.; Wu, X.; Xie, J.; Li, W.; Zhu, C. A highly selective decarboxylative deuteration of carboxylic acids. *Chem. Sci.* **2021**, 12, 5505—5510

133. Pangu, A.; Roth, H. G.; Oliver, S. F.; Campeau, L. C.; Nicewicz, D.; DiRocco, D. A. Acridinium-Based Photocatalysts: A Sustainable Option in Photoredox Catalysis. *J. Org. Chem*. **2016**, 81, 7244—7249

134. Bottcher, T. An Additive Definition of Molecular Complexity. *J. Chem. Inf. Model.* **2016**, 56, 462—470

135. Demoret, R. M.; Baker, M. A.; Ohtawa, M.; Chen, S.; Lam, C.; Khom, S.; Roberto, M.; Forli, S.; Houk, K. N.; Shenvi, R. A. Synthetic, Mechanistic, and Biological Interrogation of Ginkgo biloba Chemical Space En Route to (−)-Bilobalide. *J. Am. Chem. Soc.* **2020**, 142, 18599—18618

4.7 Methods

General Information for Chemical Synthesis

All reagents were obtained from commercial sources and reactions were performed using oven-dried glassware (120°C) under an inert N_2 atmosphere unless otherwise noted. Air- and moisture-sensitive liquids and solutions were transferred via syringe or stainless-steel cannula. Organic solutions were concentrated under reduced pressure (~5 Torr) by rotary evaporation. Solvents were purified by passage under 12 psi N_2 through activated alumina columns. Chromatography was performed using Fisher Chemical™ Silica Gel Sorbent (230–400 Mesh, Grade 60). Compounds purified by chromatography were typically applied to the adsorbent bed using the indicated solvent conditions with a minimum amount of added dichloromethane as needed for solubility. Thin layer chromatography (TLC) was performed on Merck silica gel 60 F254 plates (250 μm). Visualization of the developed chromatogram was accomplished by fluorescence quenching or by staining with iodine, butanolic ninhydrin, aqueous potassium permanganate, or aqueous ceric ammonium molybdate (CAM). Irradiation of photochemical reactions was carried out using 2 HIGROW LED Aquarium Light Blub, Wolezek 30W LED Plant Grow Light Bulb with 18x2W 450-460nm.

Nuclear magnetic resonance (NMR) spectra were acquired on either a Bruker 400 operating at 400 and 100 MHz, a Varian 600 operating at 600 and 150 MHz, or a Bruker 600 operating at 600 and 150 MHz for ^{1}H and ^{13}C, respectively, and are referenced internally according to residual solvent signals. Data for ^{1}H NMR are recorded as follows: chemical shift (δ, ppm), multiplicity (s, singlet; d, doublet; t, triplet; q, quartet; quint, quintet; m, multiplet), coupling constant (Hz), and integration. Data for ^{13}C NMR are reported in terms of chemical shift (δ, ppm). High-resolution mass spectra were obtained using a Thermo Fisher Scientific Q-Exactive HF Orbitrap.

Quantum Chemical Calculations

Structures were optimized at the M06-2X/6-31+G(d,p) level of theory, which is known to perform well for organic reactions. [refs:] Stationary points were characterized as minima via vibrational frequency analysis. Energies shown in the text are relative free energies at 298 K. All computations were carried out using Gaussian16.

[ref: Gaussian 16, M. J. Frisch, G. W. Trucks, H. B. Schlegel, G. E. Scuseria, M. A. Robb, J. R. Cheeseman, G. Scalmani, V. Barone, G. A. Petersson, H. Nakatsuji, X. Li, M. Caricato, A. V. Marenich, J. Bloino, B. G. Janesko, R. Gomperts, B. Mennucci, H. P. Hratchian, J. V. Ortiz, A. F. Izmaylov, J. L. Sonnenberg, D. Williams-Young, F. Ding, F. Lipparini, F. Egidi, J. Goings, B. Peng, A. Petrone, T. Henderson, D. Ranasinghe, V. G. Zakrzewski, J. Gao, N. Rega, G. Zheng, W. Liang, M. Hada, M. Ehara, K. Toyota, R. Fukuda, J. Hasegawa, M. Ishida, T. Nakajima, Y. Honda, O. Kitao, H. Nakai, T. Vreven, K. Throssell, J. A. Montgomery, Jr., J. E. Peralta, F. Ogliaro, M. J. Bearpark, J. J. Heyd, E. N. Brothers, K. N. Kudin, V. N. Staroverov, T. A. Keith, R. Kobayashi, J. Normand, K. Raghavachari, A. P. Rendell, J. C. Burant, S. S. Iyengar, J. Tomasi, M. Cossi, J. M. Millam, M. Klene, C. Adamo, R. Cammi, J. W. Ochterski, R. L. Martin, K. Morokuma, O. Farkas, J. B. Foresman, and D. J. Fox, Gaussian, Inc., Wallingford CT, 2019.]

Detailed Synthesis Procedures and Experimental Data

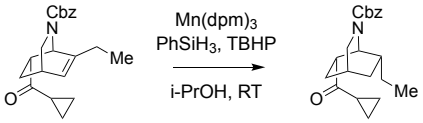

Benzyl(1*S*,4*R*,6*S*,7*R*)-6-(cyclopropanecarbonyl)-7-ethyl-2-azabicyclo[2.2.2]octane-2-carboxylate

To a stirring solution of the starting material (1.50 g, 4.42 mmol, 1 equv.) in anhydrous iPrOH (8.84 mL, 0.5M) was added phenylsilane (0.817 mL, 6.63 mmol, 1.5 equiv.) and a 5.5 M solution of tert-butyl hydroperoxide in decane (1.20 mL, 6.63 mmol, 1.5 equiv.). The resulting mixture was degassed by bubbling nitrogen through the solution for 10 mins. $Mn(dpm)_3$ (267 mg, 0.442 mmol, 0.1 equiv.) was added in one portion and the reaction was further degassed for an additional 30 seconds. The mixture was stirred at ambient temperature for 2 h after which it was concentrated under reduced pressure. The residue was purified via chromatography on silica gel (gradient elution 10:1→7:3 hexanes/EtOAc) to afford the product (1.26 g, 84%) as a clear oil.

R_f = 0.37 (7:3 hexanes/ethyl acetate)

^{1}H NMR (400 MHz, $CDCl_3$) δ (ppm) (rotamers observed) **=** 7.40 – 7.27 (m, 5H), 5.25 – 4.98 (m, 2H), 4.72 – 4.35 (m, 1H), 3.46 – 3.18 (m, 2H), 3.15 – 2.86 (m, 1H), 2.35 (d, 1H), 2.40 – 2.16 (m, 1H), 2.03 – 1.80 (m, 3H), 1.57 – 1.35 (m, 2H), 1.31 – 1.21 (m, 1H), 1.05 – 0.76 (m, 7H)

^{13}C NMR (101 MHz, $CDCl_3$) δ (ppm) = 210.06, 209.68, 155.15, 154.71, 137.27, 137.05, 128.64, 128.51, 128.09, 127.95, 127.84, 127.77, 127.56, 66.97, 51.62, 51.45, 50.11, 49.76, 48.06, 47.96, 46.38, 40.67, 40.54, 31.87, 31.85, 27.51, 27.48, 26.69, 26.55, 24.92, 24.77, 19.78, 19.57, 12.73, 12.63, 12.46, 12.26, 10.92

HRMS (ESI) = *m/z* $[M + Na]^+$ calcd. For $C_{21}H_{27}NO_3Na^+$, 364.1888; found, 364.1889

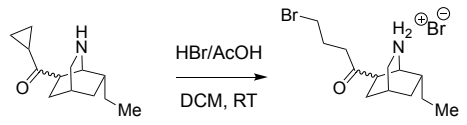

(1*S*,4*R*,7*R*)-6-(4-bromobutanoyl)-7-ethyl-2-azabicyclo[2.2.2]octan-2-ium bromide

To a stirring solution of the starting material (1.25 g, 6.03 mmol, 1 equiv.) in DCM (6.03 mL, 1.0M) was added 33 wt% HBr/AcOH (3.12 mL, 18.08 mmol, 3 equiv.) in one portion. The solution was stirred at ambient temperature for 2 h after which it was concentrated under reduced pressure. The residue was dried under high vacuum for 1 h and then stirred vigorously in diethyl ether (30 mL). The diethyl ether was decanted and the residue was dried under high vacuum. The product (2.18 g, 98%) was used isolated as an orange foam and was used in the next reaction without any further purification or characterization.

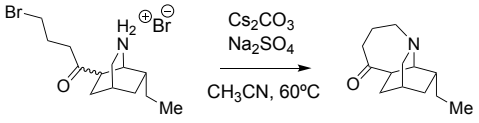

1-ethyloctahydro-3,10-methanopyrido[1,2-*a*]azepin-9(6*H*)-one

A flask was charged with the alkyl bromide (2.18 g, 5.90 mmol, 1 equiv.), anhydrous Cs_2CO_3 (2.88 g, 8.85 mmol, 1.5 equiv.), and anhydrous Na_2SO_3 (2.52 g, 17.71 mmol, 3 equiv.). The flask was evacuated and refilled with nitrogen 3 times after which anhydrous CH_3CN (59 mL, 0.1M) was added in one portion. The reaction mixture was heated to 60 °C and stirred for 6 h. The heterogeneous mixture was cooled to ambient temperature and filtered. The reaction vessel and filter cake were washed with DCM (2 x 30 mL). The filtrate was concentrated under reduced pressure and the residue was purified via chromatography on silica gel (20:1 DCM/MeOH) to afford the product (499 mg, 41%) as a light brown oil.

R_f = 0.43 (20:1 DCM/MeOH)

^{1}H NMR (400 MHz, $CDCl_3$) δ (ppm) = 3.18 – 2.92 (m, 3H), 2.80 (dd, *J* = 13.2, 2.7 Hz, 1H), 2.66 – 2.51 (m, 3H), 2.06 – 1.75 (m, 7H), 1.61 – 1.49 (m, 1H), 1.39 – 1.19 (m, 2H), 1.08 (dd, *J* = 12.7, 2.6 Hz, 1H), 0.90 (t, *J* = 7.4 Hz, 3H)

^{13}C NMR (101 MHz, $CDCl_3$) δ (ppm) = 216.98, 54.88, 53.83, 50.10, 46.87, 43.79, 41.70, 31.40, 30.54, 27.92, 26.77, 21.24, 12.31

HRMS (ESI) = *m/z* $[M + H]^+$ calcd. For $C_{14}H_{26}NO^+$, 208.1698; found, 208.1694

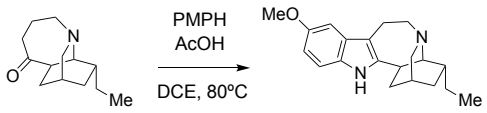

Epiibogaine

epiibogaine

A flask was charged with the starting material (200 mg, 0.964 mmol, 1 equiv.) and para-methoxy phenylhydrazine (252 mg, 1.44 mmol, 1.5 equiv.). The flask was evacuated and refilled with nitrogen 3 times after which anhydrous DCE (9.64 mL, 0.1M) and AcOH (0.827 mL, 14.47 mmol, 15 equiv.) was added. The resulting mixture was degassed by bubbling nitrogen through the solution for 10 mins. The flask was heated to 80 °C and stirred for 12 h after which it was cooled to ambient temperature and diluted with DCM (20 mL). Saturated aq. $NaHCO_3$ was added to the reaction mixture until the pH was adjusted to 7-8. The organic layer was separated, and the aqueous layer was further extracted with DCM (2 x 50 mL). The combined organic fractions were dried over sodium sulfate, filtered and concentrated under reduced pressure. Purification via chromatography on silica gel (gradient elution 20:1→10:1 DCM/MeOH, 0.25% NH_4OH) afforded **epiibogaine** (242 mg, 81%) as a colorless oil.

R_f = 0.33 (10:1 DCM/MeOH)

^{1}H NMR (400 MHz, MeOD) δ (ppm) = 7.16 (d, *J* = 8.7 Hz, 1H), 6.95 (d, *J* = 2.4 Hz, 1H), 6.73 (dd, *J* = 8.8, 2.4 Hz, 1H), 3.81 (s, 3H), 3.62–3.51 (m, 2H), 3.55 – 3.33 (m, 4H), 3.33 – 3.20 (m, 2H), 3.16 – 3.06 (m, 1H), 2.28 (d, *J* = 2.6 Hz, 1H), 2.22 – 2.01 (m, 3H), 1.75 – 1.63 (m, 1H), 1.56 (td, *J* = 7.3, 3.1 Hz, 2H), 1.38 – 1.19 (m, 1H), 1.01 (t, *J* = 7.4 Hz, 3H)

^{13}C NMR (101 MHz, MeOD) δ (ppm) = 154.01, 139.67, 130.07, 128.55, 111.18, 111.01, 107.34, 99.39, 59.08, 56.25, 54.92, 50.37, 48.27, 48.05, 47.91, 47.84, 47.70, 47.63, 47.41, 47.20, 46.99, 37.60, 32.16, 29.14, 28.18, 26.49, 24.11, 17.90, 10.58

HRMS (ESI) = *m/z* $[M + H]^+$ calcd. For $C_{20}H_{27}N_2O^+$, 311.2128; found, 311.2126

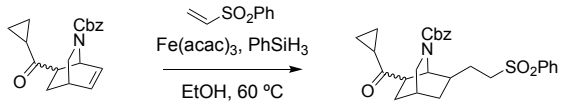

benzyl(1*S*,4*R*)-6-(cyclopropanecarbonyl)-7-(2-(phenylsulfonyl)ethyl)-2-azabicyclo [2.2.2] octane-2-carboxylate

A flask was sequentially charged with the starting material (3.3 g, 10.59 mmol, 1 equiv.), ethanol (53 mL, 0.2M), phenylvinyl sulfone (2.67 g, 15.88 mmol, 1.5 equiv.), and $Fe(acac)_3$ (1.12 g, 3.18 mmol, 0.3 equiv.). To this solution was added phenylsilane (3.91 mL, 31.79 mmol, 3 equiv.) in one portion. The mixture was stirred and heated at 60 °C under air atmosphere for 24 h, after which it was cooled to ambient temperature. The reaction mixture was concentrated under reduced pressure and the resulting residue was purified via chromatography on silica gel (gradient elution 10:1→1:1 hexanes/EtOAc) to afford the product (4.38g , 86%) as a clear foam.

R_f = 0.33 (10:1 hexanes/EtOAc)

^{1}H NMR (400 MHz, $CDCl_3$) δ (ppm) (rotamers observed) **=** 7.38 – 7.27 (m, 5H), 5.20 – 4.96 (m, 2H), 4.70 – 4.36 (m, 1H), 3.54 – 3.15 (m, 2H), 3.06 – 2.85 (m, 1H), 2.59 – 2.16 (m, 4H), 2.11 – 1.84 (m, 3H), 1.81 – 1.41 (m, 4H), 1.17 – 0.66 (m, 4H)

^{13}C NMR (101 MHz, $CDCl_3$) δ (ppm) = 210.17, 209.45, 178.74, 156.21, 137.09, 128.62, 128.56, 128.52, 128.33, 128.20, 127.92, 127.69, 127.66, 127.62, 67.23, 66.86, 52.14, 48.95, 48.74, 37.79, 37.68, 33.64, 32.26, 31.99, 31.53, 31.39, 30.02, 29.88, 29.69, 26.06, 25.96, 24.14, 24.03, 19.99, 19.88, 19.62, 12.55, 11.66, 11.36, 11.20

HRMS (ESI) = *m/z* $[M + H]^+$ calcd. For $C_{22}H_{28}NO_5^+$, 387.1968; found, 387.1962

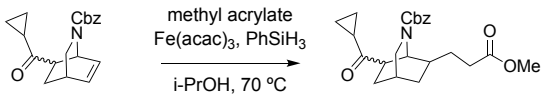

Benzyl(1*S*,4*R*)-6-(cyclopropanecarbonyl)-7-(3-methoxy-3-oxopropyl)-2 azabicyclo [2.2.2] octane-2-carboxylate

A flask was sequentially charged with the starting material (3.3 g, 10.59 mmol, 1 equiv.), isopropanol (53 mL, 0.2M), methyl acrylate (5.76 mL, 63.58 mmol, 6 equiv.), and $Fe(acac)_3$ (1.12 g, 3.18 mmol, 0.3 equiv.). To this solution was added phenylsilane (3.91 mL, 31.79 mmol, 3 equiv.) in one portion. The mixture was stirred and heated at 70 °C under air atmosphere for 24 h, after which it was cooled to ambient temperature. The reaction mixture was concentrated under reduced pressure and the resulting residue was purified via chromatography on silica gel (gradient elution 10:1→1:1 hexanes/EtOAc) to afford the product (3.25 g, 77%) as a clear foam.

R_f = 0.40 (7:3 hexanes/EtOAc)

^{1}H NMR (400 MHz, $CDCl_3$) δ (ppm) (rotamers observed) **=** 7.38 – 7.27 (m, 5H), 5.20 – 4.96 (m, 2H), 4.70 – 4.36 (m, 1H), 3.54 – 3.15 (m, 2H), 3.06 – 2.85 (m, 1H), 2.59 – 2.16 (m, 4H), 2.11 – 1.84 (m, 3H), 1.81 – 1.41 (m, 4H), 1.17 – 0.66 (m, 4H)

^{13}C NMR (101 MHz, $CDCl_3$) δ (ppm) = 210.17, 209.45, 178.74, 156.21, 137.09, 128.62, 128.56, 128.52, 128.33, 128.20, 127.92, 127.69, 127.66, 127.62, 67.23, 66.86, 52.14, 48.95, 48.74, 37.79,

37.68, 33.64, 32.26, 31.99, 31.53, 31.39, 30.02, 29.88, 29.69, 26.06, 25.96, 24.14, 24.03, 19.99, 19.88, 19.62, 12.55, 11.66, 11.36, 11.20

HRMS (ESI) = *m/z* $[M + H]^+$ calcd. For $C_{22}H_{28}NO_5^+$, 387.1968; found, 387.1962

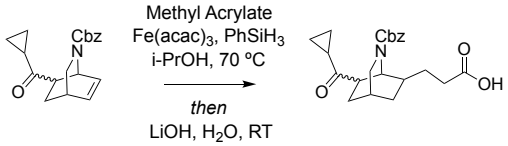

3-((1*S*,4*R*)-2-((benzyloxy)carbonyl)-7-(cyclopropanecarbonyl)-2-azabicyclo[2.2.2]octan-6-yl)propanoic acid

A flask was sequentially charged with the starting material (3.3 g, 10.59 mmol, 1 equiv.), isopropanol (53 mL, 0.2M), methyl acrylate (5.76 mL, 63.58 mmol, 6 equiv.), and $Fe(acac)_3$ (1.12 g, 3.18 mmol, 0.3 equiv.). To this solution was added phenylsilane (3.91 mL, 31.79 mmol, 3 equiv.) in one portion. The mixture was stirred and heated at 70 °C under air atmosphere for 24 h, after which it was cooled to ambient temperature. The reaction mixture was diluted in H_2O (100 mL) and LiOH (2.53 g, 105.97 mmol, 10 equiv.) was added in one portion. The solution was stirred at ambient temperature for 12 h after which it was acidified with 1M HCl (100 mL). The mixture was poured into DCM (200 mL) and the layers were separated. The aqueous layer was further extracted with DCM (2 x 100 mL) and the combined organic fractions were dried over sodium sulfate, filtered, and concentrated under reduced pressure. The residue was purified via chromatography on silica gel (gradient elution 10:1→1:1 hexanes/EtOAc) to afford the product (3.02 g, 74%) as a clear foam.

Note: Vigorous bubbling is observed upon 5 min of heating.

R_f = 0.15 (7:3 hexanes/EtOAc)

^{1}H NMR (400 MHz, $CDCl_3$) δ (ppm) (rotamers observed) **=** 7.38 – 7.27 (m, 5H), 5.20 – 4.96 (m, 2H), 4.70 – 4.36 (m, 1H), 3.54 – 3.15 (m, 2H), 3.06 – 2.85 (m, 1H), 2.59 – 2.16 (m, 4H), 2.11 – 1.84 (m, 3H), 1.81 – 1.41 (m, 4H), 1.17 – 0.66 (m, 4H)

^{13}C NMR (101 MHz, $CDCl_3$) δ (ppm) = 210.17, 209.45, 178.74, 156.21, 137.09, 128.62, 128.56, 128.52, 128.33, 128.20, 127.92, 127.69, 127.66, 127.62, 67.23, 66.86, 52.14, 48.95, 48.74, 37.79, 37.68, 33.64, 32.26, 31.99, 31.53, 31.39, 30.02, 29.88, 29.69, 26.06, 25.96, 24.14, 24.03, 19.99, 19.88, 19.62, 12.55, 11.66, 11.36, 11.20

HRMS (ESI) = *m/z* $[M + H]^+$ calcd. For $C_{22}H_{28}NO_5^+$, 387.1968; found, 387.1962

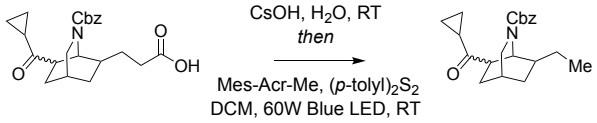

benzyl (1*S*,4*R*)-6-(cyclopropanecarbonyl)-7-ethyl-2-azabicyclo[2.2.2]octane-2-carboxylate

A glass reaction tube was charged with the starting material (1.85 g, 4.79 mmol, 1 equiv.). A solution of CsOH•H2O (806 mg, 4.79 mmol, 1 equiv.) in H_2O (9.6 mL) was added and the milky white heterogeneous mixture was stirred vigorously for 1 h. In a separate flask, 9-Mesityl-10-methylacridinium tetrafluoroborate (96 mg, 0.23 mmol, 0.05 equiv.) and p-tolyl disulfide (1.77 g, 7.19 mmol, 1.5 equiv.) was dissolved in DCM (38.4 mL). The acridinium/disulfide solution was added to the stating material in one portion. The biphasic solution was tightly capped under air atmosphere and stirred (1000 rpm) between two 30W blue LED lamps (8 cm distance between reaction vessel and lamp) for 24 h at ambient temperature. After 24 h, another portion of 9-Mesityl-10-methylacridinium tetrafluoroborate (96 mg, 0.23 mmol, 0.05 equiv.) was added to the reaction mixture and the resulting solution was placed in the photoreactor for an additional 24 h. Upon reaction completion, the reaction mixture was poured into water (50 mL) and the layers were separated. The aqueous layer was further extracted with DCM (2 x 50 mL) and the combined

organic fractions were dried over sodium sulfate, filtered and concentrated under reduced pressure. The residue was purified via chromatography on silica gel (7:3 hexanes/EtOAc) to afford the product as an orange oil. The product was further purified by dissolution in ethyl acetate and subsequent addition of activated charcoal (50 mg). Heating the stirred solution at 50 °C for 30 min, followed by filtration and concentration under reduced pressure afforded the product (1.21 g, 74%) as a light yellow oil.

Note: Conversion rate is highly dependent on the diameter of the reaction vessel. We have found best results when using a reaction vessel to reaction volume ratio of 1.5cm/15 mL. A fan was used to cool the reaction vessel during irradiation and it is advised to seal the reaction tube cap with electrical tape. It is essential that the biphasic reaction is stirred vigorously (>1000 rpm) so that the two layers mix properly. Inadequate mixing will result in poor transfer of the carboxylate salt into the organic layer and ultimately lead to poor reaction conversion. Heating the product in excess activated charcoal for longer than 30 minutes will lead to reduced yields.

R_f = 0.65 (7:3 hexanes/EtOAc)

^{1}H NMR (400 MHz, $CDCl_3$) δ (ppm) (rotamers observed) **=** 7.40 – 7.27 (m, 5H), 5.27 –4 .97 (m, 2H), 4.70 – 4.37 (m, 1H), 3.46 – 3.11 (m, 2H), 3.03 – 2.84 (m, 1H), 2.38 – 2.17 (m, 1H), 2.13 – 1.63 (m, 3H), 1.54 – 1.16 (m, 4H), 1.16 – 1.06 (m, 1H), 1.05 – 0.72 (m, 7H)

^{13}C NMR (101 MHz, $CDCl_3$) δ (ppm) = 210.37, 209.65, 156.00, 155.72, 137.35, 136.94, 128.48, 128.21, 127.80, 127.73, 66.95, 66.55, 52.44, 51.78, 51.08, 50.30, 49.35, 49.03, 46.88, 46.41, 46.31, 43.78, 40.78, 40.59, 36.50, 36.34, 36.03, 35.96, 35.40, 35.16, 34.87, 34.72, 32.38, 32.23, 29.53, 28.28, 28.14, 27.90, 26.58, 26.43, 26.15, 26.05, 24.26, 24.15, 19.88, 19.57, 12.41, 11.77, 11.75, 11.24, 11.09

HRMS (ESI) = *m/z* $[M + H]^+$ calcd. For $C_{21}H_{28}NO_3^+$, 342.2068; found, 342.2065

General procedure for preparation of iboga derivatives

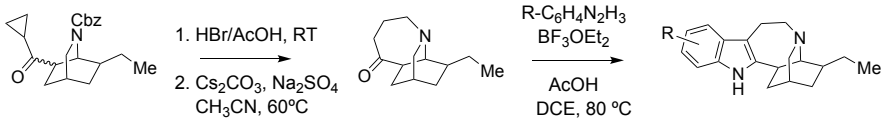

33 wt% HBr/AcOH (3 equiv.) was added in one portion to the starting material (1 equiv.) while stirring. The dark orange mixture was stirred at ambient temperature for 2 h after which it was concentrated under reduced pressure. The residue was dried under high vacuum for 1 h and then stirred vigorously in diethyl ether (30-50 mL). The diethyl ether was decanted, and the resulting alkyl bromide was dried under high vacuum. This process was repeated 3x to ensure all the benzyl bromide was removed. A flask was charged with alkyl bromide (1 equiv.), anhydrous Cs_2CO_3 (1.5 equiv.), and anhydrous Na_2SO_3 (3 equiv.). The flask was evacuated and refilled with nitrogen 3 times after which anhydrous CH_3CN (0.1M) was added in one portion. The reaction mixture was heated to 60 °C and stirred for 6 h. The heterogeneous mixture was cooled to ambient temperature and filtered. The reaction vessel and filter cake were washed with DCM (2 x 10 mL). The filtrate was concentrated under reduced pressure and the resulting residue was dissolved in DCM (10 mL) and washed with sat. $NaHCO_3$ (3 x 5 mL). The organic extract was dried over sodium sulfate, filtered and concentrated under reduced pressure to yield the tetrahydroazepine as a crude brown oil.

A flask was charged with crude tetrahydroazepine (1 equiv.) and substituted phenylhydrazine (1.5 equiv.). The flask was evacuated and refilled with nitrogen 3 times after which anhydrous DCE (0.1M) and AcOH (15 equiv.) was added. The resulting mixture was degassed by bubbling nitrogen through the solution for 10 mins. The flask was heated to 80 °C and stirred for 1 h after which it was cooled to ambient temperature and BF_3OEt_2 (1.2 equiv.) was added in one portion. The resulting mixture was heated at 80 °C for 12 h after which it was cooled to ambient

temperature and diluted with DCM (10 mL). Saturated aq. $NaHCO_3$ was added to the reaction mixture until the pH was adjusted to 7-8. The organic layer was separated, and the aqueous layer was further extracted with DCM (2 x 20 mL). The combined organic fractions were dried over sodium sulfate, filtered and concentrated under reduced pressure. Purification via chromatography on silica gel (gradient elution 20:1→10:1 DCM/MeOH, 0.25% NH_4OH) afforded iboga derivates.

Note: The solvent volume for extraction and dilution are representative of a 200 mg scale for intermediate the stating material. On larger scales, it was found that sonicating the alkyl bromide in diethyl ether allowed for more efficient benzyl bromide removal. We noticed a considerable decrease in yield (10-15%) when purifying the tetrahydroazepine via chromatography on silica gel (20:1 DCM/MeOH). Instead, the tetrahydroazepine was used as a crude mixture in the subsequent Fischer indole reactions. For obtaining biologically pure iboga alkaloids, a second purification via chromatography on silica gel was used with an 8:2 EtOAC/MeOH mobile phase.

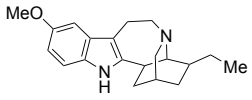

ibogaine

Ibogaine – 500 mg scale

Synthesized from the stating material (500 mg, 1.46 mmol, 1 equiv.) following the general procedure for iboga derivative preparation. Para-methoxyphenylhydrazine HCl (382 mg, 2.19 mmol, 1.5 equiv.) was used and BF_3OEt_2 was omitted from the Fischer indole reaction. **Ibogaine** (140 mg, 31% over three steps) was isolated as an orange foam.

Ibogaine – 1.33g scale

Synthesized from the stating material (1.33 g, 3.86 mmol, 1 equiv.) following the general procedure for iboga derivative preparation. Para-methoxyphenylhydrazine HCl (1.020 g, 5.84 mmol, 1.5 equiv.) was used and BF_3OEt_2 was omitted from the Fischer indole reaction. **Ibogaine** (263 mg, 22% over three steps) was isolated as an orange foam.

Note: Para-methoxyphenylhydrazine HCl (PMPH) is prone to decomposition and should be prepared fresh before use. Yields were diminished when using older bottles of PMPH.

R_f = 0.33 (10:1 DCM/MeOH)

^{1}H NMR (400 MHz, $CDCl_3$) δ (ppm) = 7.53 (s, 1H), 7.14 (d, *J* = 8.7 Hz, 1H), 6.93 (m, 1H), 6.77 (dd, *J* = 8.6, 2.4 Hz, 1H), 3.86 (s, 3H), 3.41 – 3.30 (m, 2H), 3.17–3.10 (m, 1H), 3.09 – 3.05 (m, 1H), 3.00 – 2.95 (m, 1H), 2.93 – 2.87 (m, 1H), 2.85 (s, 1H), 2.61 (dd, *J* = 17.3, 5.4 Hz, 1H), 2.09 – 2.00 (m, 1H), 1.85 (s, 1H), 1.83 – 1.77 (m, 1H), 1.65 (dq, *J* = 13.3, 3.5 Hz, 1H), 1.55 (q, *J* = 7.2 Hz, 2H), 1.48 – 1.43 (m, 1H), 1.24 – 1.18 (m, 1H), 0.90 (t, *J* = 7.1 Hz, 3H)

^{13}C NMR (101 MHz, $CDCl_3$) δ (ppm) = 153.98, 142.89, 130.13, 129.71, 110.75, 110.69, 109.17, 100.39, 57.48, 56.02, 54.19, 49.98, 41.97, 41.61, 34.22, 32.11, 27.84, 26.51, 20.71, 11.91

HRMS (ESI) = *m/z* $[M + H]^+$ calcd. For $C_{20}H_{27}N_2O^+$, 311.2128; found, 311.2127

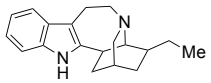

ibogamine

Ibogamine

Synthesized from the stating material (500 mg, 1.46 mmol, 1 equiv.) following the general procedure for iboga derivative preparation. Phenylhydrazine HCl (317 mg, 2.19 mmol, 1.5 equiv) was used in the Fischer indole reaction. **Ibogamine** (118 mg, 29% over 3 steps) was isolated as a yellow foam.

R_f = 0.37 (10:1 DCM/MeOH)

^{1}H NMR (400 MHz, $CDCl_3$) δ (ppm) = 7.69 (br. s., 1H), 7.48 – 7.44 (dd, *J* = 6.95 Hz, 1.61 Hz, 1H), 7.27 – 7.24 (m, 1H), 7.14 – 7.05 (m, 2H), 3.47 – 3.28 (m, 2H), 3.22 – 3.12 (dt, *J* = 13.61 Hz, 3.71 Hz), 3.10 – 3.02 (m, 2H), 2.99 – 2.86 (m, 3H), 2.76 – 2.68 (m, 1H), 2.11 – 2.01 (m, 1H), 1.90 – 1.78 (m, 2H), 1.69 – 1.48 (m, 4H), 1.26 – 1.20 (m, 1H), 0.90 (t, *J* = 7.10 Hz, 3H)

^{13}C NMR (101 MHz, $CDCl_3$) δ (ppm) = 141.37, 134.67, 129.55, 121.10, 119.18, 117.89, 110.12, 109.04, 57.83, 54.35, 49.95, 41.76, 40.95, 33.97, 31.79, 27.59, 26.23, 20.44, 11.90

HRMS (ESI) = *m/z* $[M + H]^+$ calcd. For $C_{19}H_{25}N_2^+$, 281.2018; found, 281.2026

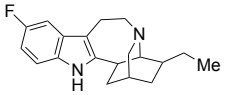

10-fluoroibogamine (24)

10-fluoroibogamine

Synthesized from the stating material (200 mg, 0.585 mmol, 1 equiv.) following the general procedure for iboga derivative preparation. 4-fluorophenylhydrazine HCl (143 mg, 0.876 mmol,

1.5 equiv.) was used in the Fischer indole reaction. **10-fluoroibogamine** (56 mg, 32% yield over 3 steps) was isolated as a clear orange oil.

R_f = 0.42 (10:1 DCM/MeOH)

^{1}H NMR (400 MHz, $CDCl_3$) δ (ppm) = 7.64 (s, 1H), 7.15 (dd, *J* = 8.7, 4.4 Hz, 1H), 7.10 (dd, *J* = 9.8, 2.5 Hz, 1H), 6.84 (td, *J* = 9.1, 2.5 Hz, 1H), 3.43 – 3.27 (m, 2H), 3.20 – 2.98 (m, 3H), 2.96 – 2.86 (m, 2H), 2.63 – 2.54 (m, 1H), 2.10 – 2.04 (m, 1H), 1.90 – 1.77 (m, 2H), 1.66 (m, 1H), 1.59 – 1.46 (m, 3H), 1.22 (m, 1H), 0.90 (t, *J* = 7.1 Hz, 3H)

^{13}C NMR (101 MHz, $CDCl_3$) δ (ppm) = 157.89 ($^1J_{CF}$ = 234.29 Hz), 143.72, 131.08, 130.11, 110.58 ($^1J_{CF}$ = 9.60 Hz), 109.53, 109.01 ($^1J_{CF}$ = 26.29 Hz), 103.03 ($^1J_{CF}$ = 22.72 Hz), 57.53, 54.19, 50.01, 41.89, 41.38, 34.08, 31.95, 27.77, 26.38, 20.59, 11.92

HRMS (ESI) = *m/z* $[M + H]^+$ calcd. For $C_{19}H_{24}N_2F^+$, 299.1928; found, 299.1925

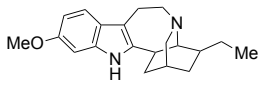

tabernanthine

Tabernanthine

Synthesized from the stating material (200 mg, 0.585 mmol, 1 equiv.) following the general procedure for iboga derivative preparation. 3-methoxyphenylhydrazine HCl (153 mg, 0.876 mmol, 1.5 equiv.) was used in the Fischer indole reaction. **Tabernanthine** (24 mg, 13.3% yield over 3 steps) was isolated as a clear orange oil.

R_f = 0.35

^{1}H NMR (400 MHz, $CDCl_3$) δ (ppm) = 7.54 (s, 1H), 7.35 (d, *J* = 8.5 Hz, 1H), 6.82 – 6.76 (m, 2H), 3.86 (s, 3H), 3.49 – 3.29 (m, 2H), 3.19 (td, *J* = 13.1, 3.7 Hz, 1H), 3.09 (d, *J* = 10.4 Hz, 2H),

3.02 – 2.85 (m, 2H), 2.69 (d, *J* = 16.3 Hz, 1H), 2.10 – 2.02 (m, 2H), 1.91 – 1.80 (m, 2H), 1.70 – 1.49 (m, 4H), 1.27 – 1.22 (m, 1H), 0.93 (t, *J* = 7.1 Hz, 3H)

^{13}C NMR (101 MHz, $CDCl_3$) δ (ppm) = 155.86, 140.47, 135.35, 124.19, 118.46, 108.83, 108.48, 94.37, 57.77, 55.84, 54.11, 49.82, 41.88, 41.28, 34.19, 32.06, 27.67, 26.45, 20.72, 11.89

HRMS (ESI) = *m/z* $[M + H]^+$ calcd. For $C_{20}H_{27}N_2O^+$, 311.2128; found, 311.2127

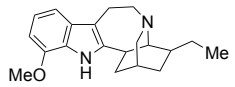

12-methoxyibogamine

12-methoxyibogamine

Synthesized from the stating material (200 mg, 0.585 mmol, 1 equiv.) following the general procedure for iboga derivative preparation. 2-methoxyphenylhydrazine HCl (153 mg, 0.876 mmol, 1.5 equiv.) was used in the Fischer indole reaction. **12-methoxyibogamine** (32 mg, 17.4% yield over 3 steps) was isolated as a clear yellow oil.

R_f = 0.31 (10:1 DCM/MeOH)

^{1}H NMR (400 MHz, $CDCl_3$) δ (ppm) = 7.85 (s, 1H), 7.09 (d, *J* = 7.9 Hz, 1H), 7.00 (t, *J* = 7.8 Hz, 1H), 6.59 (dd, *J* = 7.7, 0.9 Hz, 1H), 3.94 (s, 3H), 3.41 – 3.31 (m, 2H), 3.19 – 3.05 (m, 2H), 3.02 – 2.92 (m, 2H), 2.86 (d, *J* = 2.0 Hz, 1H), 2.69 – 2.62 (m, 1H), 2.08 – 2.00 (m, 1H), 1.86 – 1.78 (m, 2H), 1.67 – 1.47 (m, 4H), 1.21 – 1.17 (m, 1H), 0.90 (t, *J* = 7.1 Hz, 3H)

^{13}C NMR (101 MHz, $CDCl_3$) δ (ppm) = 145.49, 141.51, 131.02, 124.72, 119.47, 110.89, 109.74, 101.25, 57.55, 55.33, 54.21, 49.97, 41.94, 41.47, 34.23, 32.10, 27.81, 26.51, 20.84, 11.89

HRMS (ESI) = *m/z* $[M + H]^+$ calcd. For $C_{20}H_{27}N_2O^+$, 311.2128; found, 311.2127

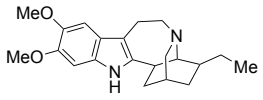

ibogaline

Ibogaline

Synthesized from the stating material (200 mg, 0.585 mmol, 1 equiv.) following the general procedure for iboga derivative preparation. 3,4-dimethoxyphenylhydrazine HCl (179 mg, 0.876 mmol, 1.5 equiv.) was used in the Fischer indole reaction. **Ibogaline** (32 mg, 16.4% yield over 3 steps) was isolated as a brown oil.

R_f = 0.22 (10:1 DCM/MeOH)

^{1}H NMR (400 MHz, $CDCl_3$) δ (ppm) = 6.86 (s, 1H), 6.84 (s, 1H), 3.91 (s, 3H), 3.86 (s, 3H), 3.47 – 3.27 (m, 2H), 3.26 – 2.94 (m, 4H), 2.09 – 1.87 (m, 4H), 1.83 – 1.57 (m, 4H), 1.56 – 1.37 (m, 3H), 0.96 – 0.82 (m, 3H)

^{13}C NMR (101 MHz, $CDCl_3$) δ (ppm) = 147.19, 145.45, 137.15, 128.90, 120.90, 108.05, 99.82, 94.93, 60.54, 56.62, 56.45, 56.38, 47.28, 34.20, 33.36, 27.91, 26.93, 21.19, 18.64, 14.33, 11.93

HRMS (ESI) = *m/z* $[M + H]^+$ calcd. For $C_{21}H_{29}N_2O_2^+$, 341.2228; found, 341.2231

Chapter 5 – Asymmetric Synthesis of Ibogaine

5.1 Efforts Towards Chiral Resolution of Ibogaine

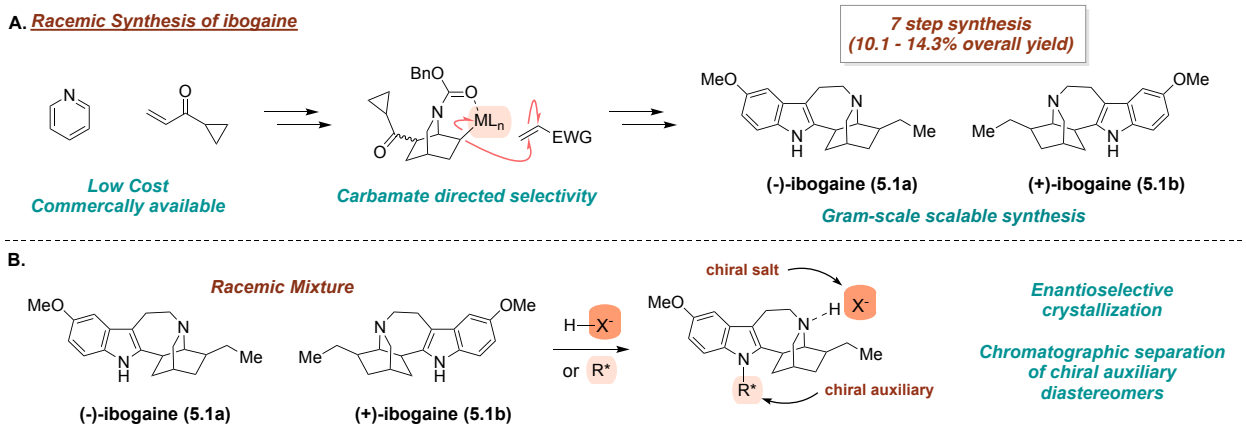

Figure 5.1. (A) Efficient and scalable racemic total synthesis of ibogaine (B) Chiral separation of racemic ibogaine; salt formation or chiral auxiliary placement

The biosynthesis of iboga alkaloids involves a late stage cycloaddition catalyzed by coronaridine synthase (CorS) to furnish the isoquinuclidine with precise enantioselectivity.[136] A thorough analysis of the literature reveals that only (-)-ibogaine has be isolated from nature and its antipode has never been synthesized nor studied. Furthermore, chiral HPLC analysis of a naturally sourced sample of (-)-ibogaine showed nearly 100:0 enantiopurity demonstrating the selectivity of the cycloaddition catalyzing enzyme. Having devised an efficient and scalable racemic synthesis of ibogaine (**Figure 5.1A**), we were intrigued by the possibility of performing a late-stage chiral separation of our natural product (**Figure 5.1B**). We postulated that enantiomer separation could most likely be achieved through either salt formation or chiral auxiliary placement. Racemic ibogaine is a semi-solid that can be converted into a pure crystalline solid upon acidification with hydrochloric acid. An alternative counterion for the ammonium salt could enable enantioselective crystallization in a specified solvent. In contrast, chiral auxiliary placement on the indole nitrogen of racemic ibogaine could produce two diastereomers separable by

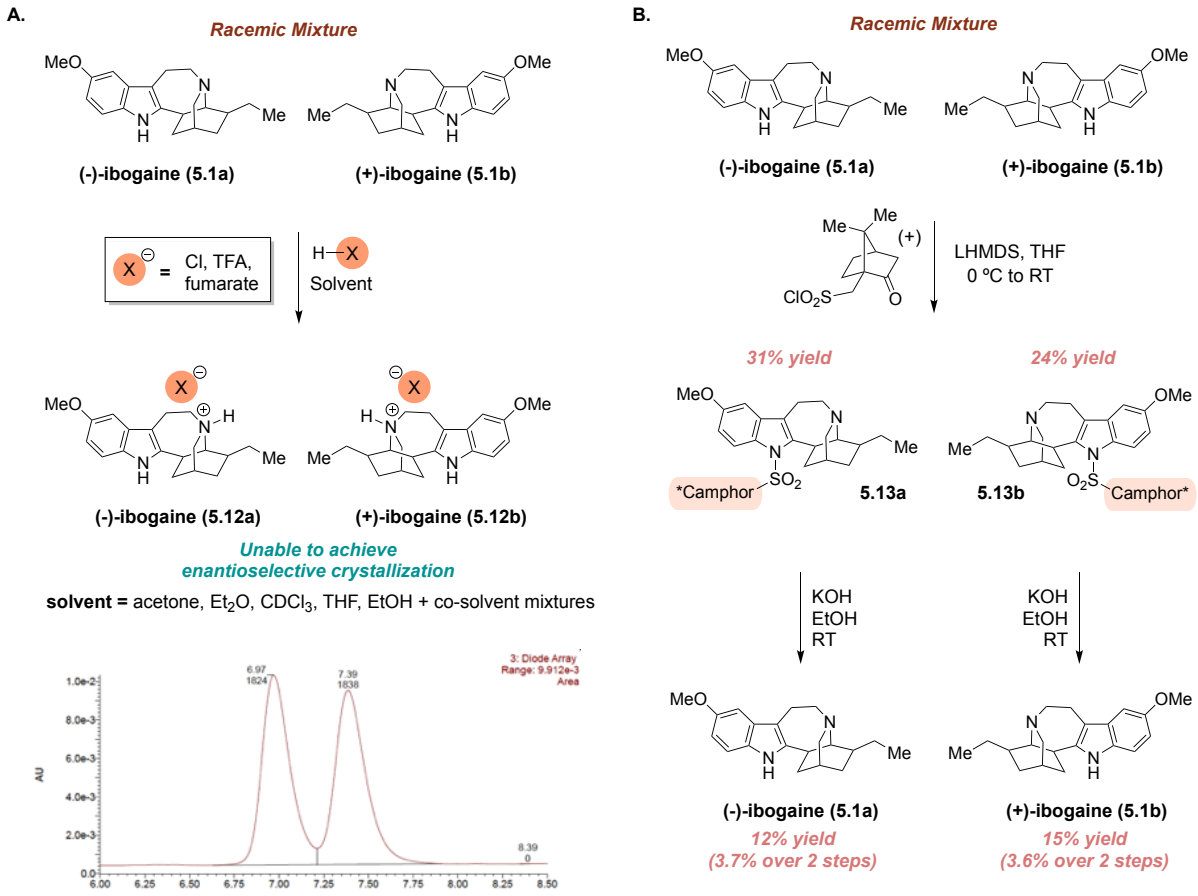

Figure 5.2. (A) Salt preparation of racemic ibogaine and enantioselective crystallization **(B)** Chiral auxiliary strategy for preparation of enantiopure ibogaine

chromatography. Separation of the diastereomers followed by removal of the auxiliary would ultimately afford enantiomerically pure ibogaine.

Several different salt forms of racemic ibogaine were prepared for a series of crystallization solvent screens (**Figure 5.2A**). We noticed that the hydrochloride and fumarate salts of racemic ibogaine produced fine crystals while the trifluoroacetate salt yielded an opaque oil. Numerous crystallization techniques (i.e recrystallization, solvent diffusion, evaporative crystallization) were examined; however, chiral LCMS analysis indicated minimal separation in all of our attempts. Having experienced such difficulty early on, we rendered this technique ineffective for separation.

Based on a report by Glick and co-workers[137], we elected to prepare a chiral sulfonamide for separation of racemic ibogaine (**Figure 5.2B**). Racemic ibogaine was treated with (+)-camphorsulfonyl chloride to afford a mono-sulfonylated mixture of diastereomers in 55% yield. The di-sulfonylated product was also observed in 36% yield as we were unable to prevent sulfonylation at the isoquinuclidine nitrogen during our optimization. Separation of the mono-sulfonylated diastereomers produced **5.13a** and **5.13b** in 31% and 24% yield, respectively. Removal of the sulfonamide with hydroxide was sluggish and enantiopure ibogaine was isolated in only 12-15% yield. Though this strategy can produce enantiomerically pure ibogaine, numerous issues with reproducibility and scalability indicated that this method was not ideal for large scale preparation. It was abundantly clear that we would need to develop an asymmetric total synthesis to ensure wide-spread access to enantiopure ibogaine.

5.2 Development of Asymmetric Diels-Alder Reaction

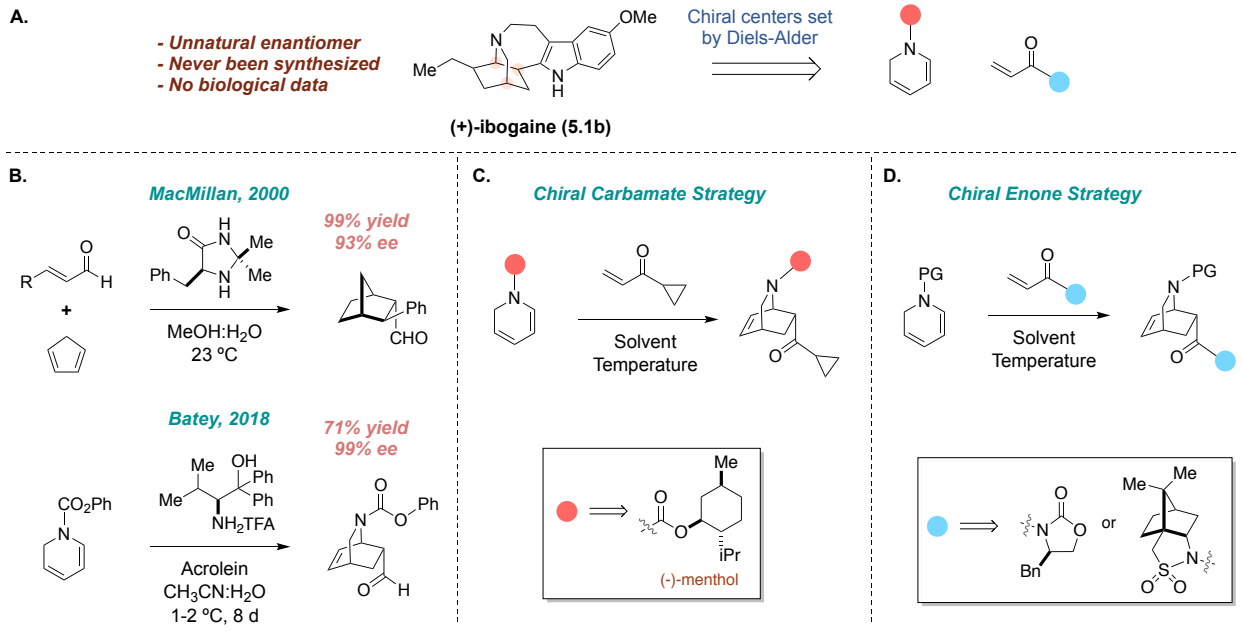

Figure 5.3. (A) Asymmetric synthesis of ibogaine from asymmetric Diels-Alder reaction **(B)** Chiral additive to induce asymmetry in Diels-Alder reaction **(C)** Chiral auxiliary placement on diene **(D)** Chiral auxiliary placement on dienophile

A key feature of our racemic ibogaine synthesis is an early stage construction of the isoquinuclidine ring system via Diels-Alder cycloaddition. It was clear that an asymmetric variant of our synthesis would be dependent on the development of an asymmetric Diels-Alder reaction to make the isoquinuclidine (**Figure 5.3A**). We postulated three possible strategies for achieving stereoselectivity in our cycloaddition: use of a chiral additive, chiral auxiliary placement on the diene, and chiral auxiliary placement on the dienophile. Pioneering work by MacMillan and co-workers[138] demonstrated an organocatalyzed Diels-Alder reaction with an α,β-unsaturated aldehyde and cyclopentadiene (**Figure 5.3B**). In this reaction, an imidazolidinone catalyst reacts with the aldehyde to form an intermediary iminium dienophile for subsequent cycloaddition. Seminal reports by Batey and co-workers[139] applied this strategy towards the preparation of the isoquinuclidine ring system by using a valine derived catalyst. In similar fashion, an intermediary iminium is formed to achieve high enantioselectivity in the Diels-Alder reaction.

Rather than using a chiral additive to achieve high enantioselectivity, we hypothesized that we could use a chiral auxiliary on the diene or dienophile to achieve high diastereoselectivity in our Diels-Alder reaction. Subsequent removal of the chiral auxiliary would then produce an enantiomerically pure intermediate for our ibogaine synthesis. We envisioned using a menthol derived carbamate for the diene since both enantiomers of the respective chloroformate precursor are readily available (**Figure 5.3C**). Alternatively, auxiliary placement on the enone in the form of an oxazolidinone or camphorsultam could also induce diastereoselectivity in our cycloaddition (**Figure 5.3D**).

When treating cyclopropyl enone **5.14** with a chiral amine catalyst, we noticed conjugate addition rather than imine formation (**Figure 5.4A**). This was observed with both MacMillan and Batey's organocatalyst and conjugate addition was favored irrespective to solvent and temperature. This phenomenon is attributed to the reduced electrophilicity of the carbonyl in **5.14** compared to acrolein. Conducting the subsequent Diels-Alder reaction with the conjugate addition product was unsuccessful, thus suggesting that regeneration of the dienophile via in situ

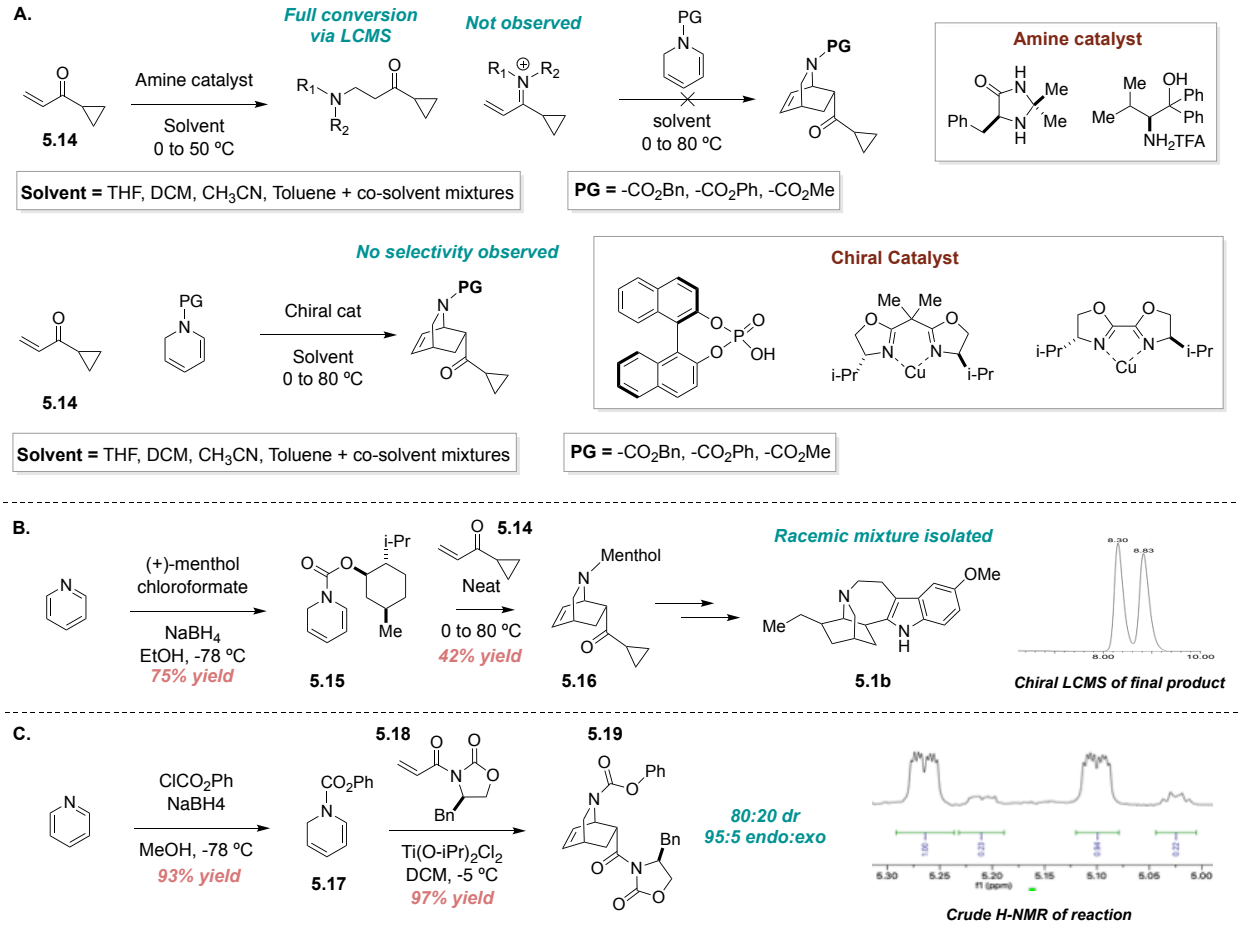

Figure 5.4. (A) Chiral additive strategy; amine organocatalysis and chiral catalyst **(B)** Chiral auxiliary strategy using menthol derived carbamate **(C)** Chiral auxiliary strategy using oxazolidinone dienophile

elimination was not possible. Several other chiral catalysts were screened,[140,141] and minimal product was observed in a variety of reaction conditions. We ascribe the difficulty in achieving selectivity to the marked difference in reactivity of the cyclopropyl ketone moiety compared to other commonly utilized ketones.

Having realized that the inclusion of a chiral additive was not a feasible strategy, we elected to make structural modifications to our reactants for the Diels-Alder reaction. Reduction of pyridine in the presence of (+)-menthol chloroformate afforded dihydropyridine **5.16** with a

tethered chiral auxiliary (**Figure 5.4B**). Diels-Alder cycloaddition of **5.15** with cyclopropyl enone **5.14** afforded product **5.16** in 42% yield after optimization. At first glance this reaction appeared diastereoselective; however, subjecting product **5.16** to the rest of the iboga synthesis produced a near racemic mixture of ibogaine. Unfortunately, chiral auxiliary placement on the diene did not exert any diastereoselectivity in our cycloaddition.

Inspired by the work of Evans and co-workers[142], we envisioned that a chiral oxazolidinone would be the ideal auxiliary for our dienophile (**Figure 5.4C**). Chiral oxazolidinone **5.18** was prepared from readily available S-phenylalanine on decagram quantities. Titanium catalyzed cycloaddition of **5.18** with dihydropyridine **5.17** afforded our desired product **5.19** in 97% yield.[143] Analysis of the crude 1H-NMR spectra revealed that our cycloaddition proceeded with an 80:20 diastereomeric ratio and greater than 95:5 for the endo epimer. Optimization revealed that $Ti(O\text{-}iPr)_2Cl_2$ was crucial for the reaction as the yield and dr decreased substantially in its absence or with other catalysts (**Entry 2—4, Table 5.1**). We noticed that the inclusion of a dioxolane ligand increased the diastereoselectivity in our reaction though slightly diminishing the yield (**Entry 5, Table 5.1**). For practical purposes, we opted to omit the ligand and separate our diastereomers

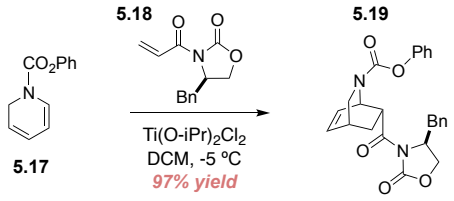

Entry	Deviation	Yield	dr
1	none	97%	80:20
2	No $Ti(O\text{-}iPr)_2Cl_2$	31%	50:50
3	$TiCl_4$ for $Ti(O\text{-}iPr)_2Cl_2$	88%	65:45
4	$Cu(OTf)_2$ for $Ti(O\text{-}iPr)_2Cl_2$	38%	50:50
5	1 equiv. TADDOL additive	83%	95:5
6	Camphorsultam auxiliary	63%	50:50
7	Cbz fr Ph Carbamate	44%	60:40

Table 5.1: Isolated yields shown. All reactions run on 1.0 mmol scale for **17** (312 mg). All reactions chromatographed using gradient elution 10:1→7:3 hexanes/EtOAc.

manually via chromatography. A key element to ensuring high diastereoselectivity is the choice of carbamate for the dihydropyridine. When conducting the Diels-Alder reaction with a benzyl carbamate, we observed a significant reduction in yield and selectivity (**Entry 7, Table 5.1**). We suspect that the acid labile benzyl carbamate is prone to cleavage during the reaction, thus reducing the amount of available diene for cycloaddition. Furthermore, free rotation about the methylene bridge in the benzyl carbamate could also be a factor for diminished selectivity. Having developed a strategy to inducing asymmetry, **5.19** was separated via chromatography with nearly full recovery of each diastereomer. With diastereomerically pure **5.19** in hand, we were now tasked with completing the remaining steps of our ibogaine synthesis.

5.3 Asymmetric Synthesis of Ibogaine

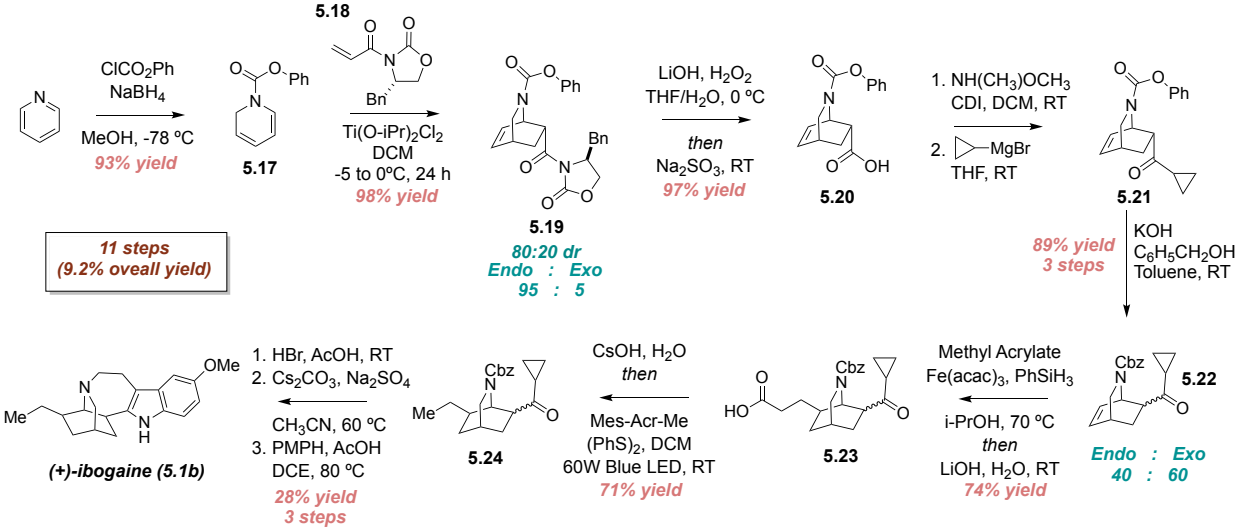

Figure 5.5. Asymmetric Total synthesis of (+)-ibogaine

Upon diastereomeric separation of **5.19**, subsequent hydrolysis of the chiral oxazolidinone[144] was conducted using LiOOH and Na_2SO_3 to give the parent carboxylic acid (**5.20**) in near quantitative yield (**Figure 5.5**). Conversion to the Weinreb amide followed by addition of cyclopropyl magnesium bromide proceeded smoothly to furnish cyclopropyl ketone **32**

in 86% yield over two steps. To verify enantiopurity, chiral LCMS analysis was conducted on **5.21** to reveal a 98:2 enantiomeric ratio. Initial attempts to deprotect the carbamate were met with difficulty as the phenyl carbamate was resistant to acidic conditions and base mediated removal resulted in decomposition. However, a carbamate swap performed with KOH and benzyl alcohol allowed us to intercept isoquinuclidine **5.22** from our racemic route. Isoquinuclidine **5.22** was subjected through the remaining synthesis to ultimately afford (+)-ibogaine (**5.1b**) in 11 steps and 9.2% overall yield. Taken together, these strategic decisions complete the first asymmetric synthesis of ibogaine and the first ever synthesis of the unnatural enantiomer (**5.1b**). When using the R enantiomer of oxazolidinone **5.18**, iboga alkaloids of the opposite optical series can also be obtained with similar selectivity.

5.4 Conclusion

The development of an asymmetric route to ibogaine and related analogs has the ability to change the landscape of neurobiology and pharmacology. Our strategic decisions have enabled access to a wide array of analogs for structure-activity-relationship (SAR) studies accessed from readily available pyridine in only 7-11 steps. Current efforts are underway to synthesize a library of enantiomerically pure analogs and alkaloids for various assays relating to plasticity and addiction. We hope that the work presented in this dissertation can aid in the discovery of a novel and efficacious therapeutic for combating substance use disorders.

REFERENCES

136. Farrow, S. C.; Kamileen, M. O.; Caputi, L.; Bussey, K.; Mundy, J. E. A.; Mcatee, R. C.; Stephenson, C. R. J.; O'Connor, S. E. Biosynthesis of an Anti-Addiction Agent from the Iboga Plant, *J. Am. Chem. Soc.* **2019**, 141, 12979—12983

137. King, C. R.; Meckler, H.; Trova, M. P; Glick, S. D. Synthesis of enantiomerically pure (+)- and (−)-18-methoxycoronaridine hydrochloride and Their preliminary assessment as anti-addictive agents. *Bioorg. Med. Chem*. **2000**, 10, 473—476

138. Ahrendt, K. A.; Borths, C. J.; MacMillan, D. W. C. New Strategies for Organic Catalysis: The First Highly Enantioselective Organocatalytic Diels-Alder Reaction. *J. Am. Chem. Soc.* **2000**, 122, 4243—4244

139. Kim, S. J.; Batey, R. A. Enantioselective Isoquinuclidine Synthesis via Sequential Diels–Alder/Visible-Light Photoredox C–C Bond Cleavage: A Formal Synthesis of the Indole Alkaloid Catharanthine. *Org. Chem. Front.* **2018**, 5, 2934—2939

140. Takenaka, N.; Huang, Y.; Rawal, V. H. The first catalytic enantioselective Diels–Alder reactions of 1,2-dihydropyridine: efficient syntheses of optically active 2-azabicyclo[2.2.2]octanes with chiral BINAM derived Cr(III) salen complexes. *Tetrahedron*. **2002**, 58, 8299—8305

141. Nakano, H.; Tsugawa, N.; Takahashi, K.; Okuyama, Y.; Fujita, R. An efficient synthetic methodology of chiral isoquinuclidines by the enantioselective Diels–Alder reaction of 1,2-dihydropyridines using chiral cationic palladium–phosphinooxazolidine catalyst. *Tetrahedron*. **2006**, 62 10879—10887

142. Evans, D. A.; Champman, K. T.; Bisaha, J. Asymmetric Diels-Alder cycloaddition reactions with chiral .alpha.,.beta.-unsaturated N-acyloxazolidinones. *J. Am. Chm. Soc.* **1988**, 110, 1238—1256

143. Seki, C.; Hirama, M.; Hutabarat, R.; Takada, J.; Suttibut, C.; Takahashi, H.; Takaguchi, T.; Kohari, Y.; Nakano, H.; Uwai, K.; Takano, N.; Yasui, M.; Okuyama, Y.; Takeshita, M.; Matsuyama, H. Asymmetric synthesis of isoquinuclidines by Diels–Alder reaction of 1,2-dihydropyridine utilizing a chiral Lewis acid catalyst. *Tetrahedron*. **2012**, 68, 1774—178

144. Buetner, G. L.; Cohen, B. M.; DelMonte, A. J.; Dixon, D. D.; Fraunhoffer, K. J.; Glace, A. W.; Lo, E.; Stevens, J. M.; Vanyo, D.; Wilbert, C. Revisiting the Cleavage of Evans Oxazolidinones with LiOH/H2O2. *Org. Process Res. Dev*. **2019**, 23, 1378—1385

5.4 Methods

General Information for Chemical Synthesis

All reagents were obtained from commercial sources and reactions were performed using oven-dried glassware (120°C) under an inert N_2 atmosphere unless otherwise noted. Air- and moisture-sensitive liquids and solutions were transferred via syringe or stainless-steel cannula. Organic solutions were concentrated under reduced pressure (~5 Torr) by rotary evaporation. Solvents were purified by passage under 12 psi N_2 through activated alumina columns. Chromatography was performed using Fisher Chemical™ Silica Gel Sorbent (230–400 Mesh, Grade 60). Compounds purified by chromatography were typically applied to the adsorbent bed using the indicated solvent conditions with a minimum amount of added dichloromethane as needed for solubility. Thin layer chromatography (TLC) was performed on Merck silica gel 60 F254 plates (250 μm). Visualization of the developed chromatogram was accomplished by fluorescence quenching or by staining with iodine, butanolic ninhydrin, aqueous potassium permanganate, or aqueous ceric ammonium molybdate (CAM). Irradiation of photochemical reactions was carried out using 2 HIGROW LED Aquarium Light Blub, Wolezek 30W LED Plant Grow Light Bulb with 18x2W 450-460nm.

Nuclear magnetic resonance (NMR) spectra were acquired on either a Bruker 400 operating at 400 and 100 MHz, a Varian 600 operating at 600 and 150 MHz, or a Bruker 600 operating at 600 and 150 MHz for ^{1}H and ^{13}C, respectively, and are referenced internally according to residual solvent signals. Data for ^{1}H NMR are recorded as follows: chemical shift (δ, ppm), multiplicity (s, singlet; d, doublet; t, triplet; q, quartet; quint, quintet; m, multiplet), coupling constant (Hz), and integration. Data for ^{13}C NMR are reported in terms of chemical shift (δ, ppm). High-resolution mass spectra were obtained using a Thermo Fisher Scientific Q-Exactive HF Orbitrap.

Detailed Synthesis Procedures and Experimental Data

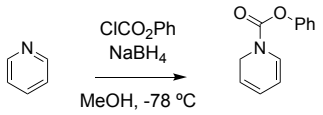

phenyl pyridine-1(2*H*)-carboxylate

A flask was charged with methanol (200 mL, 0.5M) and pyridine (8.05 mL, 100 mmol, 1 equiv.) and cooled to -78 °C after which sodium borohydride (4.54 g, 120 mL, 120 mmol) was added in one portion. Phenyl chloroformate (15.05 mL, 120 mmol, 1.2 equiv.) was added dropwise over 1 h to the reaction mixture. The reaction mixture was stirred at -78°C for an additional 3 h after which it was diluted in Et_2O (100 mL), poured into 1M HCl (200 mL) and the layers were separated. The aqueous layer was extracted with Et_2O (2 x 100 mL) and the combined organic extracts were washed with 1M NaOH (50 mL) followed by brine (50 mL). The organic extracts were dried over sodium sulfate, filtered and concentrated under reduced pressure. The residue was recrystallized from ethanol to afford the product (18.71 g, 93%) as a crystalline white solid.

^{1}H NMR (400 MHz, $CDCl_3$) δ (ppm) (rotamers observed) **=** 7.39 (t, *J* = 7.9 Hz, 2H), 7.28 – 7.21 (m, 1H), 7.20 – 7.12 (m, 2H), 6.95 – 6.79 (m, 1H), 5.91 (m, 1H), 5.66 – 5.53 (m, 1H), 5.33 – 5.21 (m, 1H), 4.60 (dd, *J* = 4.1, 2.1 Hz, 1H), 4.47 (dd, *J* = 4.1, 2.1 Hz, 1H)

^{13}C NMR (101 MHz, $CDCl_3$) δ (ppm) = 152.46, 151.43, 150.88, 150.70 (d, *J* = 10.0 Hz), 129.29, 125.99, 125.61 (d, *J* = 4.5 Hz), 125.29, 122.16, 121.77, 121.48, 119.39, 118.84, 105.94, 105.75, 44.21, 43.73

HRMS (ESI) = *m/z* $[M + H]^+$ calcd. For $C_{12}H_{13}NO_2^+$, 202.0868; found, 202.0866

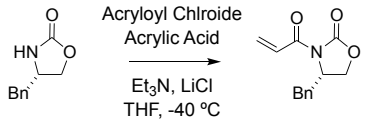

(*S*)-3-acryloyl-4-benzyloxazolidin-2-one

A flask was sequentially charged with THF (250 mL, ~0.2M), acrylic acid (4.44 mL, 64.77 mmol, 1.3 equiv.) and triethylamine (17.36 mL, 124.57 mmol, 2.5 equiv.) under nitrogen atmosphere and cooled to -40 °C using a dry ice/acetonitrile cooling bath. Acryloyl chloride (4.83 mL, 59.78 mmol, 1.2 equiv.) was added dropwise to the reaction mixture and the resulting milky yellow solution was stirred at -40 °C for 1 h. Lithium chloride (2.64 g, 62.27 mmol, 1.25 equiv.) followed by (*S*)-4-benzyloxazolidin-2-one (8.83 g, 49.82 mmol, 1 equiv.) was added in one portion to the reaction mixture and the solution was slowly warmed to ambient temperature over the course of 24 h. The reaction mixture was then concentrated under reduced pressure and the resulting residue was dissolved in DCM (200 mL) and poured into a solution of 2M HCl (100 mL). The layers were separated and the aqueous layer was washed with DCM (2 x 100 mL). The organic extracts were combined, dried over sodium sulfate, filtered and concentrated under reduced pressure. The residue was purified via chromatography on silica gel (gradient elution hexanes→7:3 hexanes/EtOAc) to afford the product (7.83 g, 68%) as a white solid.

R_f = 0.6 (7:3 hexanes/EtOAc)

^{1}H NMR (400 MHz, $CDCl_3$) δ (ppm) = 7.51 (dd, *J* = 17.0, 10.4 Hz, 1H), 7.40 – 7.17 (m, 5H), 6.61 (dd, *J* = 17.0, 1.8 Hz, 1H), 5.94 (dd, *J* = 10.4, 1.8 Hz, 1H), 4.74 (ddt, *J* = 9.5, 7.0, 3.4 Hz, 1H), 4.30 – 4.14 (m, 2H), 3.35 (dd, *J* = 13.4, 3.3 Hz, 1H), 2.81 (dd, *J* = 13.4, 9.5 Hz, 1H).

^{13}C NMR (101 MHz, $CDCl_3$) δ (ppm) = 164.91, 153.34, 135.23, 131.94, 129.46, 129.01, 127.41, 127.38, 66.29, 55.32, 37.82

HRMS (ESI) = *m/z* $[M + H]^+$ calcd. For $C_{13}H_{14}NO_3^+$, 232.0978; found, 232.0971

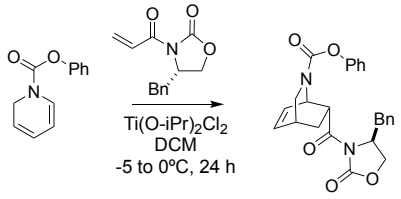

Phenyl (1*R*,4*R*,7*R*)-7-((*S*)-4-benzyl-2-oxooxazolidine-3-carbonyl)-2-azabicyclo[2.2.2]oct-5-ene-2-carboxylate

A flask was sequentially charged with activated 4A molecular sieves (16 g), dihydropyridine (6.5 g, 28.10 mmol, 1 equiv.), and $Ti(O\text{-}iPr)_2Cl_2$ (13.31 g, 56.20 mmol, 2 equiv.). The flask was evacuated and refilled with nitrogen 3 times after which DCM (175 mL) was added and the resulting milky solution was stirred at ambient temperature for 1 h. The flask was then cooled to 0 °C in an ice bath and a solution of dienophile (11.31 mmol, 56.20 mmol, 2 equiv.) in DCM (175 mL) was added dropwise over 30 min. The reaction mixture was stirred at -10 °C to 0 °C for 48 h after which it was quenched with saturated aq. $NaHCO_3$ (200 mL). The organic layer was separated and the aqueous layer was washed with DCM (2 x 200 mL). The combined organic extracts were dried over sodium sulfate, filtered and concentrated under reduced pressure. The reside was purified via chromatography on silica gel (gradient elution 10:1→7:3 hexanes/EtOAc) to afford the product (11.91 g, 98%, 77:23) as a white foam. The diastereomeric ratio of the crude residue is 77:23 (^{1}H-NMR) and the major diastereomer (9.17 g, 75%) can be separated via chromatography.

Note: The reaction was performed in a NaCl/ice bath placed in a cold room (~5 °C). Cooling bath temperatures ranged from -10 °C to 0 °C over the course of 48 hours. On larger scales, it is advised to filter the quenched reaction mixture over a bed of celite to remove the molecular sieves.

R_f = 0.25 (7:3 hexanes/EtOAc)

^{1}H NMR (400 MHz, MeOD) δ (ppm) = 7.46 – 7.10 (m, 10H), 6.65 – 6.43 (m, 2H), 5.28 (ddd, *J* = 6.1, 2.8, 1.3 Hz, 0.5H), 5.12 (ddd, *J* = 5.8, 2.7, 1.5 Hz, 0.5H), 4.73 – 4.58 (m, 1H), 4.34 – 4.13 (m, 3H), 3.59 (dd, *J* = 10.3, 2.0 Hz, 0.5H), 3.38 (dd, *J* = 10.5, 2.0 Hz, 0.5H), 3.28 – 3.20 (m, 0.5H), 3.14 (dd, *J* = 13.5, 3.3 Hz, 1H), 3.07 – 3.01 (m, 0.5H), 2.92 (dtd, *J* = 15.0, 7.8, 4.1 Hz, 2H), 2.24 – 2.14 (m, 0.5H), 2.10 – 1.99 (m, 0.5H), 1.97 – 1.87 (m, 0.5H), 1.82 – 1.71 (m, 0.5H)

^{13}C NMR (101 MHz, MeOD) δ (ppm) = 173.93, 173.53, 155.26, 154.85, 154.71, 152.72, 152.68, 137.01, 136.95, 136.69, 135.83, 132.05, 130.84, 130.59, 130.57, 130.31, 130.29, 129.83, 129.78, 128.20, 126.46, 123.02, 122.92, 67.88, 67.81, 56.64, 56.56, 45.81, 45.39, 38.48, 38.33, 32.20, 31.95, 28.34, 27.44.

HRMS (ESI) = *m/z* $[M + H]^+$ calcd. For $C_{25}H_{25}N_2O_5^+$, 433.1768; found, 433.1760

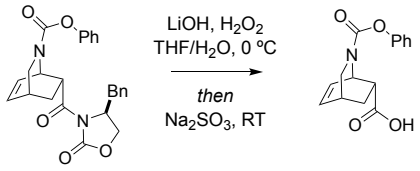

(1*R*,4*R*,6*R*)-2-(phenoxycarbonyl)-2-azabicyclo[2.2.2]oct-7-ene-6-carboxylic acid

A flask was sequentially charged with the starting material (8.50 g, 19.65 mmol, 1 equiv.), THF (260 mL) and 30% aq. H_2O_2 (9.23 mL, 90.39 mmol , 4.6 equiv.) and cooled to 0 °C in an ice bath. A solution of LiOH (753 mg, 31.44 mmol, 1.6 equiv.) in H_2O (130 mL) was added via syringe pump (30 mL/hr) to the reaction and the resulting solution was slowly warmed to ambient temperature over 5 h. A solution of Na_2SO_3 (12.35 g, 98.05 mmol, 4.98 equiv.) in H_2O (50 mL) was added and the reaction mixture was stirred at ambient temperature for 1 h. A 5M solution of aq. NaOH (75 mL) was added and the resulting mixture was poured into DCM (100 mL) and the layers were separated. The aqueous layer was washed with DCM (2 x 50 mL) and then acidified to pH 3 with 4M HCl (100 mL). The acidic aqueous layer was then extracted with DCM (3 x 150 mL) and the

organic extracts were combined, dried over sodium sulfate, filtered and concentrated under reduced pressure to afford the product (5.21 g, 97%) as a white solid.

^{1}H NMR (400 MHz, MeOD) δ (ppm) (rotamers observed) **=** 7.44 – 7.30 (m, 2H), 7.25 – 7.06 (m, 3H), 6.55 (ddd, *J* = 8.2, 6.6, 1.5 Hz, 1H), 6.43 (tdd, *J* = 8.0, 5.9, 1.5 Hz, 1H), 5.24 (ddd, *J* = 5.9, 3.3, 1.3 Hz, 0.4H), 5.11 (ddd, *J* = 5.9, 3.3, 1.4 Hz, 0.6H), 3.54 (dd, *J* = 10.3, 2.2 Hz, 0.6H), 3.35 – 3.32 (m, 0.4H), 3.29 – 3.10 (m, 1.6H), 3.03 – 2.88 (m, 1.4H), 2.06 – 1.80 (m, 2H)

^{13}C NMR (101 MHz, MeOD) δ (ppm) = 175.85, 155.52, 154.90, 152.68, 137.08, 137.00, 131.23, 131.10, 130.39, 130.33, 126.55, 126.51, 122.89, 44.89, 44.59, 32.09, 31.80, 26.95, 26.83

HRMS (ESI) = *m/z* $[M + H]^+$ calcd. For $C_{15}H_{16}NO_4^+$, 274.1078; found, 274.1071

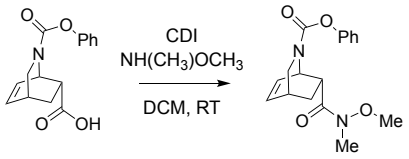

Phenyl(1*R*,4*R*,7*R*)-7-(methoxy(methyl)carbamoyl)-2-azabicyclo[2.2.2]oct-5-ene-2-carboxylate

To a stirring solution of the starting material (4.85 g, 17.74 mmol, 1 equiv.) in DCM (88 mL, 0.2M) was added CDI (3.74 g, 23.06 mmol, 1.3 equiv.) in one portion. The resulting clear solution was stirred at ambient temperature for 1 h after which N,O-dimethylhydroxylamine hydrochloride (3.46 g, 35.48 mmol, 2 equiv.) was added in one portion. The mixture was stirred at ambient temperature for 12 h after which 4M HCl (100 mL) was added and the layers were separated. The aqueous layer was further washed with DCM (2 x 100 mL) and the combined organic extracts were dried over sodium sulfate, filtered and concentrated under reduced pressure to afford the product (5.55 g, 99%) as a white solid.

^{1}H NMR (400 MHz, $CDCl_3$) δ (ppm) (rotamers observed) **=** 7.32 (ddd, *J* = 8.2, 7.2, 2.3 Hz, 2H), 7.19 – 7.07 (m, 3H), 6.54 – 6.38 (m, 2H), 5.20 – 5.03 (m, 1H), 3.70 (d, *J* = 4.4 Hz, 3H), 3.53 – 3.32 (m, 2H), 3.22 – 3.03 (m, 4H), 2.87 (dq, *J* = 5.1, 2.6 Hz, 1H), 1.97 (dddd, *J* = 12.5, 9.6, 5.6, 2.6 Hz, 1H), 1.77 (dddd, *J* = 12.3, 9.3, 4.7, 2.9 Hz, 1H)

^{13}C NMR (101 MHz, $CDCl_3$) δ (ppm) = 153.50, 152.92, 151.34, 134.66, 134.18, 130.96, 130.50, 129.28, 129.23, 125.19, 121.74, 121.63, 61.41, 61.30, 47.76, 47.36, 47.32, 47.05, 42.38, 41.82, 30.87, 30.60, 27.56, 27.34

HRMS (ESI) = *m/z* $[M + H]^+$ calcd. For $C_{17}H_{21}N_2O_4^+$, 317.1498; found, 317.1499

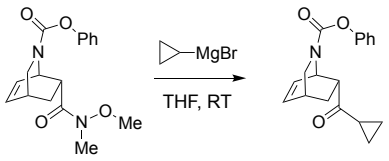

phenyl(1*R*,4*R*,7*R*)-7-(cyclopropanecarbonyl)-2-azabicyclo[2.2.2]oct-5-ene-2-carboxylate

A flask was charged with the starting material (5.55 g, 17.56 mmol, 1 equiv.) after which THF (175 mL, 0.1M) was added under a stream of nitrogen. A solution of 1.0M cyclopropyl magnesium bromide (52.68 mL, 52.68 mmol, 3 equiv.) was added dropwise over 2 h to the reaction mixture at ambient temperature. The resulting solution was stirred at ambient temperature for 1 h after which it was quenched with saturated aq. NH_4Cl (100 mL). The mixture was diluted in DCM (200 mL) and poured into water (100 mL). The layers were separated and the aqueous layer was further washed with DCM (2 x 100 mL). The organic fractions were collected, dried over sodium sulfate, filtered and concentrated under reduced pressure. The resulting residue was purified via chromatography on silica gel (7:3 hexanes/EtOAc) to afford the product (5.01 g, 96%) as a white solid.

R_f = 0.45 (7:3 hexanes/EtOAc)

^{1}H NMR (400 MHz, $CDCl_3$) δ (ppm) (rotamers observed) **=** 7.36 (tt, *J* = 6.9, 2.1 Hz, 2H), 7.19 (td, *J* = 7.2, 1.3 Hz, 1H), 7.16 – 7.09 (m, 2H), 6.50 – 6.27 (m, 2H), 5.32 (dq, *J* = 3.0, 1.3 Hz, 1H), 3.56 – 3.36 (m, 2H), 3.23 – 3.06 (m, 1H), 2.92 (s, 1H), 2.10 – 1.77 (m, 3H), 1.08 – 0.84 (m, 4H)

^{13}C NMR (101 MHz, $CDCl_3$) δ (ppm) = 208.72, 208.37, 151.33, 135.03, 130.13, 129.29, 129.25, 125.28, 121.73, 52.69, 52.17, 47.67, 47.17, 30.83, 30.54, 25.12, 24.32, 19.45, 19.34, 11.52, 11.39, 10.97, 10.71

HRMS (ESI) = *m/z* $[M + H]^+$ calcd. For $C_{18}H_{20}NO_3^+$, 298.1438; found, 298.1433

Specific Rotation = $[\alpha]_D^{20}$ = 12.5 (c = 0.15 in MeOH)

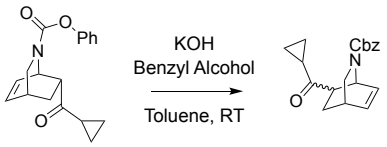

benzyl (1*S*,4*S*)-7-(cyclopropanecarbonyl)-2-azabicyclo[2.2.2]oct-5-ene-2-carboxylate

A flask was sequentially charged with the starting material (5 g, 16.81 mmol, 1 equiv.), toluene (84 mL, 0.2M) and benzyl alcohol (2.09 mL, 20.17 mmol, 1.2 equiv.). Powdered KOH (1.13 g, 20.17, 1.2 equiv.) was added to the reaction mixture in one portion and the resulting solution was stirred at ambient temperature for 12 h. The reaction was diluted in DCM (100 mL), poured into water (50 mL) and the layers were separated. The aqueous layer was washed with DCM (2 x 50 mL) and the combined organic extracts were dried over sodium sulfate, filtered and concentrated under reduced pressure. The resulting residue was purified via chromatography on silica gel (7:3 hexanes/EtOAc) to afford the product (4.92 g, 94%) as a light yellow oil.

R_f = 0.42 (7:3 hexanes:EtOAc)

^{1}H NMR (400 MHz, $CDCl_3$) δ (ppm) (rotamers observed) **=** 7.38 – 7.30 (m, 10H), 6.58 – 6.44 (m, 2H), 6.43 – 6.34 (m, 1H), 6.30 – 6.24 (m, 1H), 5.23 (d, *J* = 6.1 Hz, 1H), 5.18 – 5.02 (m, 4H), 4.70 (d, *J* = 5.7 Hz, 1H), 3.38 – 3.25 (m, 3H), 3.05 – 2.71 (m, 5H), 2.27–2.16 (m, 1H), 2.14 – 2.02 (m, 1H), 2.03 – 1.81 (m, 2H), 1.77 – 1.67 (1H), 1.48 – 1.41 (m, 1H), 1.06 – 0.81 (m, 8H)

^{13}C NMR (101 MHz, $CDCl_3$) δ (ppm) = 209.36, 208.75, 208.49, 155.26, 154.76, 137.04, 136.85, 136.78, 135.52, 135.35, 134.90, 134.72, 132.28, 131.88, 130.42, 130.15, 128.53, 128.50, 128.43, 128.36, 128.18, 128.09, 127.99,127.84, 127.72, 127.57, 127.49, 66.93, 66.59, 52.49, 52.32, 52.29, 47.91, 47.62, 47.50, 47.19, 47.00, 30.78, 30.55, 30.31, 30.13, 24.28, 23.62, 23.50, 20.05, 19.73, 19.43, 19.27, 12.50, 11.82, 11.50, 11.36, 11.21, 10.86, 10.64

HRMS (ESI) = *m/z* $[M + H]^+$ calcd. For $C_{19}H_{22}NO_3^+$, 312.1598; found, 312.1599

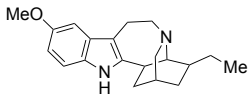

ibogaine

Ibogaine

R_f = 0.33 (10:1 DCM/MeOH)

^{1}H NMR (400 MHz, $CDCl_3$) δ (ppm) = 7.53 (s, 1H), 7.14 (d, *J* = 8.7 Hz, 1H), 6.93 (m, 1H), 6.77 (dd, *J* = 8.6, 2.4 Hz, 1H), 3.86 (s, 3H), 3.41 – 3.30 (m, 2H), 3.17–3.10 (m, 1H), 3.09 – 3.05 (m, 1H), 3.00 – 2.95 (m, 1H), 2.93 – 2.87 (m, 1H), 2.85 (s, 1H), 2.61 (dd, *J* = 17.3, 5.4 Hz, 1H), 2.09 – 2.00 (m, 1H), 1.85 (s, 1H), 1.83 – 1.77 (m, 1H), 1.65 (dq, *J* = 13.3, 3.5 Hz, 1H), 1.55 (q, *J* = 7.2 Hz, 2H), 1.48 – 1.43 (m, 1H), 1.24 – 1.18 (m, 1H), 0.90 (t, *J* = 7.1 Hz, 3H)

^{13}C NMR (101 MHz, $CDCl_3$) δ (ppm) = 153.98, 142.89, 130.13, 129.71, 110.75, 110.69, 109.17, 100.39, 57.48, 56.02, 54.19, 49.98, 41.97, 41.61, 34.22, 32.11, 27.84, 26.51, 20.71, 11.91

HRMS (ESI) = *m/z* $[M + H]^+$ calcd. For $C_{20}H_{27}N_2O^+$, 311.2128; found, 311.2128

Note: Enantiopurity determined by HPLC

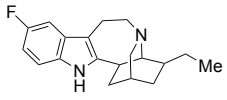

10-fluoroibogamine

10-fluoroibogamine

R_f = 0.42 (10:1 DCM/MeOH)

^{1}H NMR (400 MHz, $CDCl_3$) δ (ppm) = 7.64 (s, 1H), 7.15 (dd, *J* = 8.7, 4.4 Hz, 1H), 7.10 (dd, *J* = 9.8, 2.5 Hz, 1H), 6.84 (td, *J* = 9.1, 2.5 Hz, 1H), 3.43 – 3.27 (m, 2H), 3.20 – 2.98 (m, 3H), 2.96 – 2.86 (m, 2H), 2.63 – 2.54 (m, 1H), 2.10 – 2.04 (m, 1H), 1.90 – 1.77 (m, 2H), 1.66 (m, 1H), 1.59 – 1.46 (m, 3H), 1.22 (m, 1H), 0.90 (t, *J* = 7.1 Hz, 3H)

^{13}C NMR (101 MHz, $CDCl_3$) δ (ppm) = 157.89 ($^1J_{CF}$ = 234.29 Hz), 143.72, 131.08, 130.11, 110.58 ($^1J_{CF}$ = 9.60 Hz), 109.53, 109.01 ($^1J_{CF}$ = 26.29 Hz), 103.03 ($^1J_{CF}$ = 22.72 Hz), 57.53, 54.19, 50.01, 41.89, 41.38, 34.08, 31.95, 27.77, 26.38, 20.59, 11.92

HRMS (ESI) = *m/z* $[M + H]^+$ calcd. For $C_{19}H_{24}N_2F^+$, 299.1928; found, 299.1925

Specific Rotation for (-)-fluoroibogamine = $[\alpha]_D^{20}$ = -35.3 (c = 0.01 in MeOH)

Specific Rotation for (+)-fluoroibogamine = $[\alpha]_D^{20}$ = 34.6 (c = 0.01 in MeOH)

Chiral HPLC Chromatograms

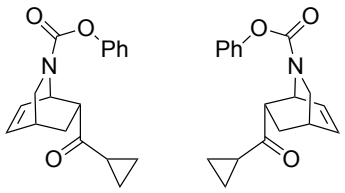

(±)-32
(Chiralpak IA 90:10 Hexanes/i-PrOH, 1 mL/min, λ 254nm)
t_{R1} = 9.49 min, t_{R2} = 12.16 min

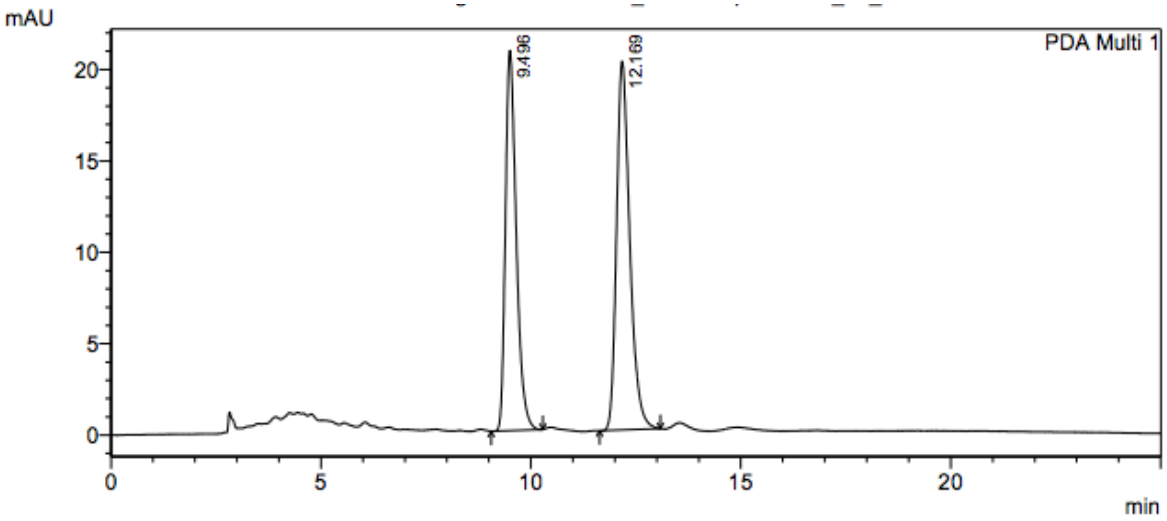

1 PDA Multi 1/254nm 4nm

< Peak Table >

PeakTable C:\LabSolutions\Training1107\Rishab\OD_PhCarbCp-racemic_90_10.lcd

PDA Ch1 254nm 4nm

Peak#	Ret. Time	Area	Height	Area %	Height %
1	9.496	372120	20782	45.708	50.748
2	12.169	442011	20169	54.292	49.252
Total		814130	40951	100.000	100.000

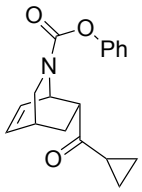

(+)-32
(Chiralpak IA 90:10 Hexanes/i-PrOH, 1 mL/min, λ 254nm)
t_{Rmajor} = 9.48 min, t_{Rminor} = 12.23 min

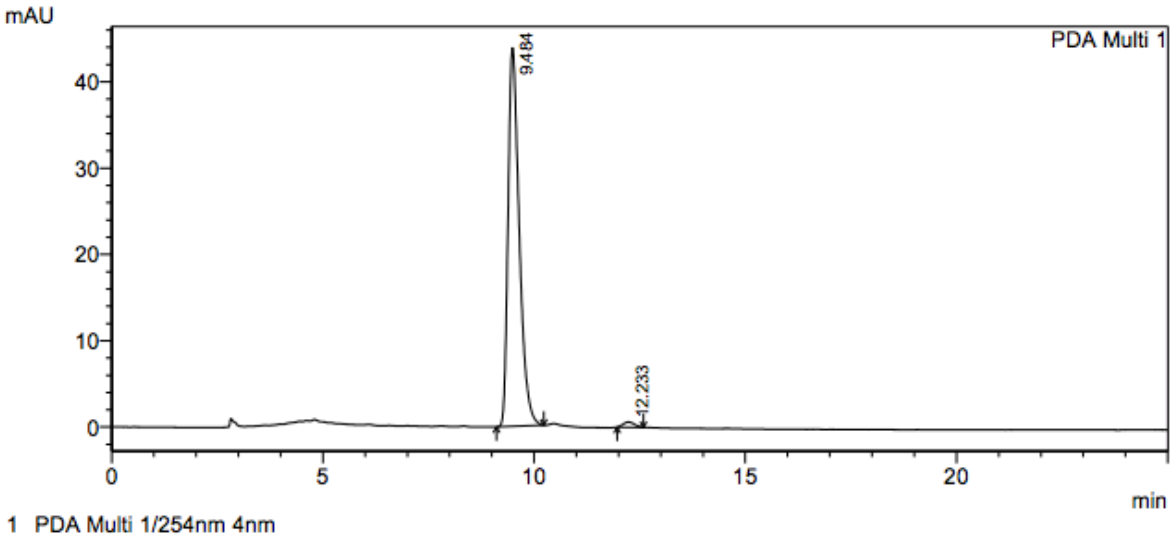

1 PDA Multi 1/254nm 4nm

< Peak Table >

PeakTable C:\LabSolutions\Training1107\Rishab\OD_PhCarbCp-enantiomer2_90_10.lcd
PDA Ch1 254nm 4nm

Peak#	Ret. Time	Area	Height	Area %	Height %
1	9.484	807319	43854	98.657	98.645
2	12.233	10990	602	1.343	1.355
Total		818309	44456	100.000	100.000

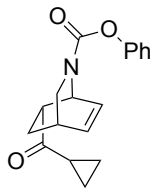

(-)-32
(Chiralpak IA 90:10 Hexanes/i-PrOH, 1 mL/min, λ 254nm)
t_{Rminor} = 9.53 min, t_{Rmajor} = 12.18 min

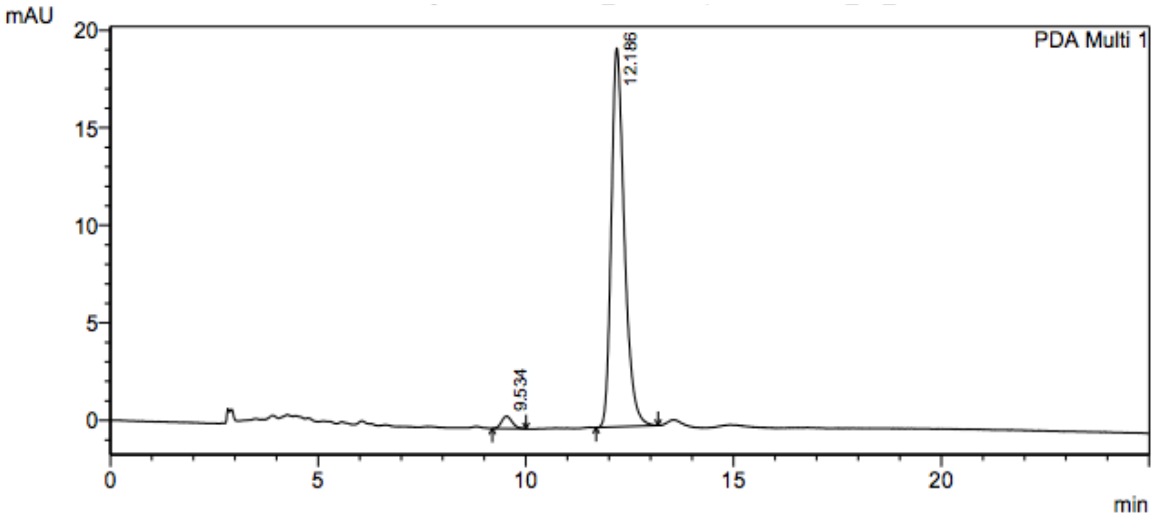

1 PDA Multi 1/254nm 4nm

< Peak Table >

PeakTable C:\LabSolutions\Training1107\Rishab\OD_PhCarbCp-enantiomer1_90_10.lcd
PDA Ch1 254nm 4nm

Peak#	Ret. Time	Area	Height	Area %	Height %
1	9.534	10892	633	2.502	3.157
2	12.186	424404	19418	97.498	96.843
Total		435296	20051	100.000	100.000

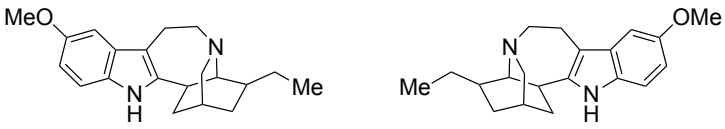

(±)-ibogaine
(Poroshell 120 Chiral-V MeOH/15mM NH_4HCO_2, 0.8 mL/min, 40 °C, λ 254nm)
Concentration: 0.9 mg/mL
t_{R1} = 6.97min, t_{R2} = 7.39 min

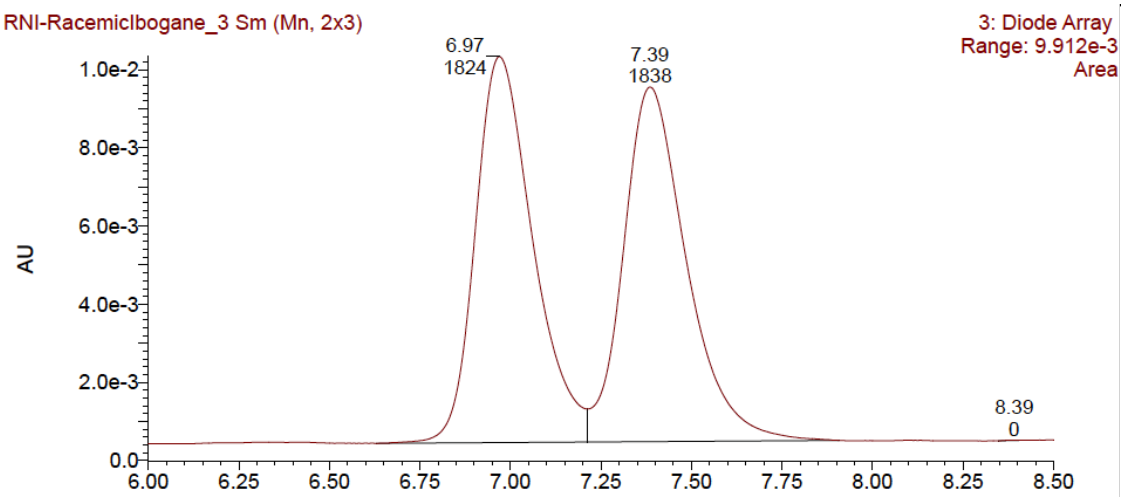

Peak	Ret. Time	Area	Area%
1	6.97	1824	49.808
2	7.39	1838	50.192
Total		3662	100.000

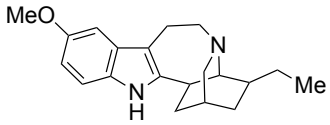

(-)-ibogaine
(Poroshell 120 Chiral-V MeOH/15mM NH_4HCO_2, 0.8 mL/min, 40 °C, λ 254nm)
Concentration: 0.5 mg/mL
t_{Rmajor} = 7.34min, t_{Rminor} = N/A

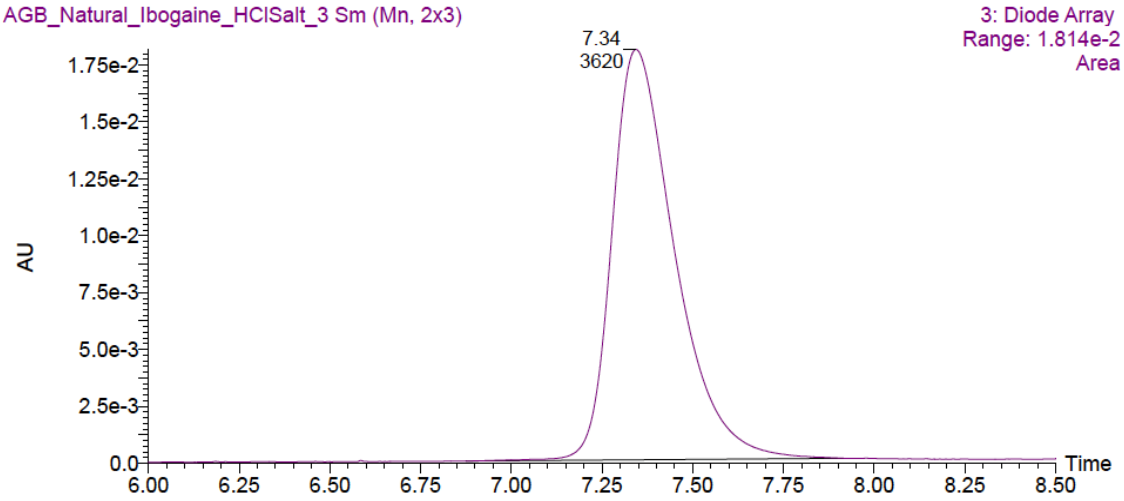

Peak	Ret. Time	Area	Area%
1	-	0	0
2	7.39	3620	100.000
Total		3620	100.000

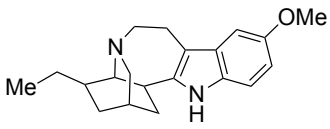

(+)-ibogaine
(Poroshell 120 Chiral-V MeOH/15mM NH_4HCO_2, 0.8 mL/min, 40 °C, λ 254nm)
Concentration: 0.5 mg/mL
t_{Rmajor} = 7.34min, t_{Rminor} = N/A

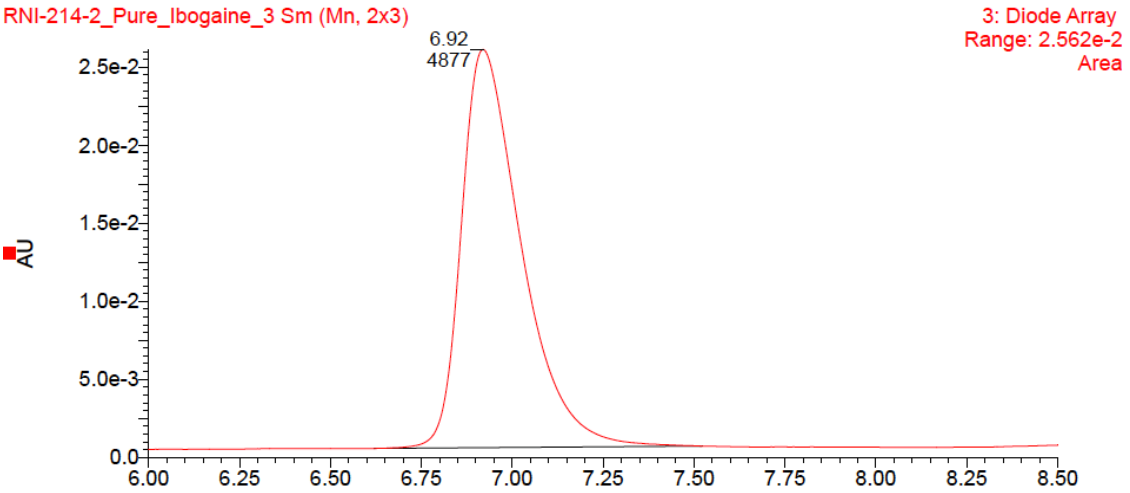

Peak	Ret. Time	Area	Area%
1	6.92	4877	100.00
2	-	0	0
Total		4877	100.000